

THE UNIVERSITY OF MICHIGAN
INDUSTRY PROGRAM OF THE COLLEGE OF ENGINEERING

THERMAL LOADING AND WALL TEMPERATURES AS
FUNCTIONS OF PERFORMANCE OF TURBOCHARGED
COMPRESSION IGNITION ENGINES

Naeim Abdou Henein

This dissertation was submitted in partial
fulfillment of the requirements for the degree of
Doctor of Philosophy in the University of Michigan,
1957.

July, 1957

IP-229

ACKNOWLEDGEMENTS

It is a pleasure to acknowledge all those who have offered assistance and encouragement during the course of this investigation.

The author is particularly indebted to Professor E. T. Vincent, the Chairman of the Doctoral Committee, for his continued active interest and suggestions which were a major factor in the completion of this work. Professor J. A. Bolt and W. H. Graves were important in helping with the experimental portions of the work. The author wishes to thank Professor R. B. Morrison and Professor R. A. Wolfe for their cooperation.

Help in preparation of this report by the Industry Program of the University of Michigan is gratefully acknowledged. The author also wishes to express his appreciation to the men of the Automotive Laboratory shop who, despite the pressure of other duties in the new building, were of help in building the experimental equipment.

TABLE OF CONTENTS

	Page
ACKNOWLEDGEMENTS.....	i
LIST OF TABLES.....	iii
LIST OF FIGURES.....	v
NOMENCLATURE.....	ix
I. INTRODUCTION.....	1
II. THEORY OF HEAT TRANSFER IN THE ENGINE-CYLINDER.....	3
III. EXPERIMENTAL SET-UP.....	15
IV. EXPERIMENTAL PROCEDURE.....	37
V. EXPERIMENTAL RESULTS.....	45
VI. DISCUSSION OF THE EXPERIMENTAL RESULTS.....	61
VII. HEAT TRANSFER ANALYSIS OF THE EXPERIMENTAL RESULTS.....	66
VIII. INVESTIGATION ON THE EFFECT OF AFTERCOOLING.....	76
IX. CONCLUSIONS AND RECOMMENDATIONS.....	92
X. APPENDICES:	
A. Sample Calculations.....	95
B. Calculation of Constant "C" of Equation [2.11].....	111
C. Calculation of Combustion Chamber Wall Temperature.....	113
D. Calculation of Intensity of Thermal Load on the Combustion Chamber Walls.....	116
E. Calculation of Mean Wall-Temperatures.....	131
F. Scavenging Air Flow-Rate.....	140
G. Sample Calculations for the Effect of Aftercooling.....	143
H. Correction Factor for the B.M.E.P.....	155
I. Engine Specifications.....	157
BIBLIOGRAPHY.....	158

LIST OF TABLES

<u>Table</u>	<u>Page</u>
I. Heat Transfer Analysis for the Cycle, (Run #95).....	106
II. Heat Transfer Analysis for the Cycle, (Run #95).....	107
III. Engine Test Results, for: Pm: 30" Hg, Tm: 80°F & N: 800 R.P.M.....	117
IV. Engine Test Results, for: Pm: 33" Hg, Tm: 80°F & N: 800 R.P.M.....	118
V. Engine Test Results, for: Pm: 36" Hg, Tm: 80°F & N: 800 R.P.M.....	119
VI. Engine Test Results, for: Pm: 39" Hg, Tm: 80°F & N: 800 R.P.M.....	120
VII. Engine Test Results, for: Pm: 42" Hg, Tm: 80°F & N: 800 R.P.M.....	121
VIII. Engine Test Results, for: Pm: 45" Hg, Tm: 80°F & N: 800 R.P.M.....	122
IX. Engine Test Results, for: Pm: 36" Hg, Tm: 80°F & N: 1200 R.P.M.....	123
X. Engine Test Results, for: Pm: 36" Hg, Tm: 140°F & N: 1200 R.P.M.....	124
XI. Engine Test Results, for: Pm: 36" Hg, Tm: 200°F & N: 1200 R.P.M.....	125
XII. Engine Test Results, for: Pm: 36" Hg, Tm: 80°F & N: Variable.....	126
XIII. Engine Test Results, for: Extra runs referred to in calculations.....	127
XIV. Calculation of Constant "C" in Equation [2.11].....	128
XV. Calculation of Constant "C" in Equation [2.11].....	129
XVI. Mean Coefficients of Heat Transfer and Mean Effective Temperatures.....	134
XVII. Mean Coefficients of Heat Transfer and Mean Effective Temperatures.....	135
XVIII. Combustion Chamber Wall Temperatures: Calculated and Measured.....	136

LIST OF TABLES (CONT'D)

<u>Table</u>	<u>Page</u>
XIX. Combustion Chamber Wall Temperature: Calculated and Measured.....	137
XX. Calculated Thermal Loadings and Measured Heat Losses to Cooling Water.....	138
XXI. Calculated Thermal Loading and Measured Heat Losses to Cooling Water.....	139
XXII. Piston-crown Temperatures and Intensity of Thermal Loads, for $\epsilon = 0\%$	145
XXIII. Piston-crown Temperatures and Intensity of Thermal Loads, for $\epsilon = 50\%$	146
XXIV. Piston-crown Temperatures and Intensity of Thermal Loads, for $\epsilon = 100\%$	147

LIST OF FIGURES

<u>Figure</u>		<u>Page</u>
1	Gas and Cylinder Wall Temperatures.....	7
2	Areas of Heat Transfer.....	7
3	Graphical Construction for the Imaginary Walls.....	10
4	Graphical Construction and Temperature Fields for the Piston.....	12
5	General Layout of Experimental Set-Up.....	16
6	Side View Showing the Air Flow Meter and the Intake System.....	17
7	Instrumentation.....	18
8	General View of the Oscilloscope and Amplifiers.....	19
9	Diagram of Intake System.....	20
10	Cooling Water System.....	23
11	Automatic Fuel Weighing and Revolutions Counting Devices	25
12	The Degree Marking Unit.....	27
13	Layout of Electrical Circuits for Pressure and Temperature Recording.....	28
14	"Tyni-Couple" Assembly.....	30
15	The Basic "Tyni-Couple" Unit.....	31
16	Sectional Plan of the Cylinder Head.....	32
17	Sectional Elevation of the Cylinder Head.....	33
18	Calibration Curve for the Combustion Chamber Thermocouple.....	34
19	Thermocouples Positions on the Cylinder-Liner Walls.....	35
20	Gas Pressure During the Cycle.....	41
21	Combustion Chamber Surface Transient-Temperature.....	42

LIST OF FIGURES (CONT'D)

<u>Figure</u>		<u>Page</u>
22	Combustion Chamber Surface Transient-Temperature.....	43
23	Pressure and Temperature Calibration Traces.....	44
24	Effect of F/A Ratio on B.M.E.P. for Various Manifold Pressures.....	46
25	Effect of F/A Ratio on I.M.E.P. for Various Manifold Pressures.....	47
26	$\left[\text{I.M.E.P.} \times \frac{14.7}{P_m} \times \frac{T_m}{540} \right]$ vs $\frac{F}{A}$ Ratio for Various Manifold Pressures.....	48
27	B.S.F.C. vs $\frac{F}{A}$ Ratio for Various Manifold Pressures...	49
28	Mechanical Efficiency vs $\frac{F}{A}$ Ratio for Various Manifold Pressures.....	50
29	Heat Losses to Cooling Water vs $\frac{F}{A}$ Ratio for Various Manifold Pressures.....	51
30	Heat Losses to Cooling Water vs I.M.E.P. for Various Manifold Pressures.....	52
31	Exhaust Gas Temperature vs $\frac{F}{A}$ for Various Manifold Pressures.....	53
32	$\eta_{I.Th.}$ vs I.M.E.P. for Various Manifold Pressures.....	54
33	B.M.E.P. vs $\frac{F}{A}$ Ratio for Various Intake Air Temps.....	55
34	I.M.E.P. vs $\frac{F}{A}$ Ratio for Various Intake Air Temps.....	56
35	$\left[\text{I.M.E.P.} \times \frac{T_m}{540} \right]$ vs $\frac{F}{A}$ Ratio for Various Intake Air Temperatures.....	57
36	B.S.F.C. vs $\frac{F}{A}$ Ratio for Various Intake Air Temps.....	58
37	Heat Losses to Cooling Water vs I.M.E.P. for Various Air Temperatures.....	59
38	Exhaust Gas Temperature vs $\frac{F}{A}$ Ratio for Various Intake Air Temperatures.....	60

LIST OF FIGURES (CONT'D)

<u>Figure</u>		<u>Page</u>
39	$\frac{\alpha_M}{\sqrt[3]{S}} \cdot \frac{1}{\sqrt[3]{P_m T_m}}$ vs I.M.E.P.....	68
40	$\frac{\alpha_M}{\sqrt[3]{S}} \cdot \frac{T_{M.E.}}{T_m}$ vs I.M.E.P.....	69
41	Check on $T_{M.E.}$ and α_M	70
42	Diagram of assumed Turbocharged C.I. Engine.....	77
43	Performance with 100% aftercooler Effectiveness.....	80
44	Performance with 50% aftercooler Effectiveness.....	81
45	Performance without aftercooling.....	82
46	Effect of Aftercooler Effectiveness for $P_m = 45''$ Hg.....	85
47	Effect of Aftercooler Effectiveness for $P_m = 45''$ Hg.....	86
48	Effect of Aftercooling on Intensity of Thermal Loading and Piston Maximum Temperature	89
49	Effect of Aftercooling on Power Output.....	90
50	Effect of Aftercooling on Reduction of Thermal Loading and Piston Maximum Temperature.....	91
51	(P-V) Diagram for Run Number 95.....	101
52	Coefficient of Heat Transfer from Gas to Walls for the Cycle of Run No. 95.....	108
53	$(\alpha_g T_g)$ for the Cycle of Run No. 95.....	109
54	Surface Area Variation vs Crank Angles.....	110
55	Calculation of the Average Wall Temperature for Run No. 95.....	112
56	Calculation of T_{wg} and T_{pg}	115
57	Calculation of Constant "C" in Equation [2.11].....	130
58	Calculation of Cylinder Walls Mean Temperature for Run No. 95.....	133

LIST OF FIGURES (CONT'D)

<u>Figure</u>		<u>Page</u>
59	Scavenging Air Flow Rate Diagram.....	142
60	Tp.g. vs I.M.E.P. for Different Manifold Pressures $\epsilon = 100\%$	148
61	q. vs I.M.E.P. for Different Manifold Pressures $\epsilon = 100\%$	149
62	Tp.g. vs I.M.E.P. for Different Manifold Pressures, $\epsilon = 50\%$	150
63	q. vs I.M.E.P. for Different Manifold Pressures, $\epsilon = 50\%$	151
64	Tp.g. vs I.M.E.P. for Different Manifold Pressures, $\epsilon = 0\%$	152
65	q. vs I.M.E.P. for Different Manifold Pressures, $\epsilon = 0\%$	153
66	q. vs I.M.E.P. for Different Effectiveness.....	154
67	Correction factor for the B.M.E.P.	156

NOMENCLATURE

a_c	=	Area factor for the coolant side of wall = $\frac{A_g}{A_c}$	
a_m	=	Area factor for the mean area of wall = $\frac{A_g}{A_m}$	
A_a	=	Area of piston-crown on the crank-case side (sq. ins. or sq. ft.)	
A_{bore}	=	Area of cylinder bore. (sq. ins. or sq. ft.)	
A_c	=	Area of wall on the coolant side. (sq. ins. or sq. ft.)	
$A_{c.ch.}$	=	Area of combustion chamber. (sq. ins. or sq. ft.)	
$A_{exh. man.}$	=	Area of the exhaust manifold enclosed in the cylinder head (sq. ins. or sq. ft.)	
A_g	=	Area of wall on the gas side. (sq. ins. or sq. ft.)	
$A_{int. man.}$	=	Area of the intake manifold enclosed in the cylinder head (sq. ins. or sq. ft.)	
A_m	=	Mean area of wall. (sq. ins. or sq. ft.)	
A_M	=	Mean effective area of heat transfer. (sq. ins. or sq. ft.)	
$A_{P.T.}$	=	Area of piston top. (sq. ins. or sq. ft.)	
c	=	Specific heat. $\frac{B.T.U.}{lb. \text{ } ^\circ F}$	
C and C_1	=	Constants.	
c_p	=	Specific heat at constant pressure. $\frac{B.T.U.}{lb. \text{ } ^\circ F}$	
D	=	Diameter ins. or ft.	
E	=	Area multiplier for thermal expansion.	
G	=	Flow rate $\frac{lbs.}{hr. \text{ sq. ft.}}$	
h_1	=	Enthalpy of air at compressor inlet $\frac{B.T.U.}{lb.}$	
h_2	=	Enthalpy of air at compressor outlet $\frac{B.T.U.}{lb.}$	
h_2'	=	Enthalpy of air after isentropic compression $\frac{B.T.U.}{lb.}$	
h_a	=	Enthalpy of air $\frac{B.T.U.}{lb.}$	
$h_{exh.}$	=	Enthalpy of exhaust gases $\frac{B.T.U.}{lb.}$	

NOMENCLATURE (CONT'D)

h_{mix}	=	Enthalpy of mixture of air and exhaust gases. $\frac{\text{B.T.U.}}{\text{lb.}}$
k	=	Thermal conductivity of water. $\frac{\text{B.T.U.}}{\text{hr. sq. ft. } (\frac{^{\circ}\text{F}}{\text{ft}})}$
k_w	=	Thermal conductivity of the wall metal. $\frac{\text{B.T.U.}}{\text{hr. sq. ft. } (\frac{^{\circ}\text{F}}{\text{ft}})}$
K	=	Flow coefficient.
m, n	=	Exponents.
N	=	Revolutions per minute.
N_{t_F}	=	Revolutions of crank shaft for the time period t_F .
P_1	=	Air pressure at compressor inlet $\frac{\text{lbs}}{\text{sq. in.}}$ or ins. Hg.
P_a	=	Air pressure at inlet tap of orifice meter $\frac{\text{lbs}}{\text{sq. in.}}$ or ins. Hg.
P_b	=	Barometric pressure $\frac{\text{lbs}}{\text{sq. in.}}$ or ins. Hg.
P_m	=	Manifold Air pressure $\frac{\text{lbs}}{\text{sq. in.}}$ or ins. Hg.
P_{r_1}, P_{r_2}	=	Relative Air pressures $\frac{\text{lbs}}{\text{sq. in.}}$ or ins. Hg.
Q	=	Quantity of heat transfer $\frac{\text{B.T.U.}}{\text{hr.}}$
q	=	Intensity of thermal load $\frac{\text{B.T.U.}}{\text{hr. sq. ft.}}$
r_m	=	Mean radius
R	=	Universal gas constant $\frac{\text{ft. lb.}}{\text{lb. } ^{\circ}\text{R}}$
Re	=	Reynold's number
S	=	Mean piston speed $\frac{\text{ft.}}{\text{sec.}}$
t	=	Time
t_F	=	Average time for consumption of 0.1 lb of fuel --- minutes.
T_a	=	Air temperature at orifice meter $^{\circ}\text{F}$ or $^{\circ}\text{R}$
T_1	=	Air temperature at compressor inlet, or atmospheric $^{\circ}\text{F}$ or $^{\circ}\text{R}$
T_2	=	Air temperature at compressor outlet, or atmospheric $^{\circ}\text{F}$ or $^{\circ}\text{R}$

NOMENCLATURE (CONT'D)

T_{c1}	=	Cooling water temperature at inlet to barrel	°F or °R
T_{c2}	=	Cooling water temperature at inlet to cylinder head	°F or °R
T_{c3}	=	Cooling water temperature at exit from cylinder head	°F or °R
T_E	=	Mean effective temperature over the suction stroke	°F or °R
$T_{exh.}$	=	Exhaust gas temperature	°F or °R
T_g	=	Gas temperature	°F or °R
T_{l1}	=	Liner wall outside surface temperature at T.D.C.	°F
T_{l2}	=	Liner wall outside surface temperature between T.D.C. and B.D.C.	°F
T_{l3}	=	Liner wall outside surface temperature at B.D.C.	°F
T_m	=	Air temperature in intake manifold.	°F or °R
$T_{M.E.}$	=	Gas mean effective temperature over the whole cycle.	°F or °R
$T_{mix.}$	=	Temperature of mixture of air and clearance exhaust gases	°F or °R
T_o	=	Oil temperature in crank case.	°F or °R
$T_{p.a.}$	=	Temperature of piston-crown on the crank-case side.	°F or °R
$T_{p.g.}$	=	Temperature of piston-crown on the gas side.	°F or °R
T_s	=	Average temperature of the engine outside wall.	°F or °R
$T_{w.c.}$	=	Wall temperature on the coolant side.	°F or °R
$T_{w.ex.}$	=	Wall temperature of the exhaust manifold (coolant side)	°F or °R
$T_{w.g.}$	=	Wall temperature on the gas side	°F or °R
U	=	Overall coefficient of heat transfer	$\frac{\text{B.T.U.}}{\text{hr. sq. ft. °F}}$
v	=	Velocity of flow	$\frac{\text{ft.}}{\text{sec.}}$
V	=	Volume	cu. ins. or cu. ft.
V_s	=	Engine swept volume	cu. ins.
ω_a	=	Weight of air per cycle	

ω_{exh}	=	Weight of residual exhaust gases per cycle
W_a	=	Air flow rate $\frac{\text{lbs}}{\text{hr}}$
W_B	=	Brake load lbs.
W_C	=	Cooling water flow rate $\frac{\text{lbs}}{\text{hr}}$
W_F	=	Friction load lbs.
W_I	=	Indicated load lbs.
x	=	Wall thickness ins.
x_p	=	Piston-crown thickness ins.
Y	=	Constant = $x_p + \frac{k_w}{\alpha_a}$
Z	=	Constant = $a_m x + a_c \frac{k_w}{\alpha_c}$

α_a	=	Coefficient of heat transfer from wall to air	$\frac{\text{B.T.U.}}{\text{hr. sq. ft. } ^\circ\text{F}}$
α_c	=	Coefficient of heat transfer from wall to coolant	$\frac{\text{B.T.U.}}{\text{hr. sq. ft. } ^\circ\text{F}}$
α_g	=	Coefficient of heat transfer from gas to wall	$\frac{\text{B.T.U.}}{\text{hr. sq. ft. } ^\circ\text{F}}$
α_M	=	Mean coefficient of heat transfer over the whole cycle	$\frac{\text{B.T.U.}}{\text{hr. sq. ft. } ^\circ\text{F}}$
ρ_a	=	Density of air	$\frac{\text{lb.}}{\text{cu. ft.}}$
ρ_c	=	Density of coolant	$\frac{\text{lb.}}{\text{cu. ft.}}$
ϵ	=	Aftercooler effectiveness	$= \frac{T_2 - T_m}{T_2 - T_1}$
μ	=	Dynamic viscosity	$\frac{\text{lb.}}{\text{ft. hr.}}$
$\eta_{\text{comp}E}$	=	Compressor Isentropic efficiency	
$\eta_{\text{B.Th.}}$	=	Brake thermal efficiency	
$\eta_{\text{I.Th.}}$	=	Indicated thermal efficiency	
η_m	=	Mechanical efficiency	

NOMENCLATURE (CONT'D)

List of Abbreviations and Definitions:

B.D.C. = Bottom dead center.

T.D.C. = Top dead center.

$\frac{F}{A}$ = Fuel air ratio.

B.M.E.P. = Brake mean effective pressure. $\frac{\text{lbs.}}{\text{sq. in.}}$

I.M.E.P. = Indicated **mean** effective pressure. $\frac{\text{lbs.}}{\text{sq. in.}}$

B.S.F.C. = Brake specific fuel consumption $\frac{\text{lbs.}}{\text{B.H.P. hr.}}$

I.S.F.C. = Indicated specific fuel consumption $\frac{\text{lbs.}}{\text{I.H.P. hr.}}$

B.H.P. = Brake horse power.

I.H.P. = Indicated horse power.

H.V. = Heating value of fuel $\frac{\text{B.T.U.}}{\text{lb.}}$

C.I. Engine: Compression ignition engine.

Thermal loading equals the direct heat transfer from the gas to
the enclosing walls per hour.

I. INTRODUCTION

The purpose of this investigation was to study the performance of the turbocharged compression ignition engines with emphasis on the fuel economy and the heat problem.

The main idea of turbocharging is to compress air into the engine cylinder to increase its ability to burn more fuel; thus increasing its power output. The energy in the exhaust gases is used to drive a turbine which, in turn, drives the compressor. Due to compression, the air temperature rises to values higher than atmospheric. In some turbocharged units an after-cooler cools the air after it leaves the compressor to get more power from the engine.

Besides increasing the engine power output, turbocharging improves its efficiency; however, higher gas pressures and temperatures are reached in the cylinder. These tend to increase the mechanical loads on the engine parts and the thermal loads on the cooling system while the temperatures of the engine parts go up. These temperatures are a major factor in the engine operation because:

- a. High local temperatures in some hot spots in the combustion chamber or piston-top, causing excessive heat-stresses, might end with cracking.
- b. The temperatures of the piston and cylinder walls might get high enough to cause rapid evaporation of the piston lubricating oil film, thus injuring the piston and cylinder surfaces.
- c. **The piston ring-temperatures might get high enough** to cause them to stick or loose their springy action.

The above conditions pointed out the need to study the factors affecting the thermal loads and the wall temperatures, as well as investigating the way engine performance and fuel economy are improved.

For this purpose a new single cylinder C.I. Engine at the Automotive Laboratory was chosen to be supercharged. Since applying a turbocharger to this engine was impossible; it was decided to investigate, individually, the effect of the different variables on the engine operation. Air from a compressed-air line was delivered to the engine, while an electric heater served to heat the air before it entry into the intake manifold.

Besides the measurements necessary to study the engine performance; it was of interest to measure the transient surface temperature of the combustion chamber. A thermocouple manufactured to measure the bore temperature of gun barrels was used for this purpose. Pictures for the surface transient-temperature and the gas pressure during the cycle were taken for each run.

As a result of this study some formulae were derived to calculate the power output, wall inside surface temperature, and intensity of thermal loads of the turbocharged engine. The combustion chamber temperatures and the heat losses calculated from the derived formulae were compared with those measured.

Applying these formulae an investigation was made of the effect of aftercooling on the turbocharged engine power output, thermal loading and wall temperatures.

II. THEORY OF HEAT-TRANSFER IN THE ENGINE-CYLINDER

The heat transfer in the engine-cylinder occurs in three steps:

- A. Heat transfer from the gases to the walls.
- B. Heat transfer through the walls.
- C. Heat transfer from the walls to the cooling medium.

In this chapter, the process of heat transfer in each of these steps will be discussed separately. The final equation for the overall heat transfer will be used to find the combustion chamber wall temperature.

Other equations will be given for the maximum temperature of the piston top, the intensity of thermal loading on the combustion chamber walls, and the thermal loading on the cylinder walls.

A. Heat-Transfer from the Gases to the Wall:

The rate of heat transfer from a gas to a surrounding surface is, in general, a function of many factors such as: the surface area, the temperature difference between the gas and the surface, and a coefficient of heat transfer. For any internal combustion engine, these factors change from instant to instant throughout the cycle.

a. Surface Area Variations:

The surface exposed to the gases in the cylinder varies from a minimum at top dead center to a maximum at bottom dead center. When the piston is at the top dead center, the surface exposed to the gases consists of that of the combustion chamber plus the piston top. As the piston moves toward the bottom dead center, the cylinder bore is exposed to the gases.

The surface area variation of the engine, used in tests, is given in figures (2) and (54). The area during the intake and exhaust strokes includes the portions of the intake and exhaust manifolds enclosed in the cylinder head respectively. These manifold walls transfer heat between the gases and the cooling water during the corresponding strokes.

b. Gas Temperature Variations:

The temperature of the gases in the cylinder varies appreciably during the different strokes. At the beginning of the intake stroke, the temperature is that of the clearance gases, but falls rapidly as the fresh air is brought in. It rises during the compression stroke, reaches its maximum at the end of the combustion process, then decreases with expansion and drops rapidly after the exhaust valve opens. There is a small drop in the temperature during the exhaust stroke.

c. Wall Temperature Variations:

The temperature of the inside surface of the cylinder wall fluctuates during the cycle following the variation of the gas temperature. The wall temperature goes to its maximum at the end of the combustion process, then drops continually during the exhaust and intake strokes, and reaches its minimum during the early part of the compression stroke.

Figure (21) shows a picture of the wall temperature variations for the whole cycle of the engine during run No. 95,

whose conditions are given in Appendix A.

d. Coefficient of Heat Transfer Variations:

The change in the coefficient of heat transfer, during the cycle, follows the variations in the gas temperature and pressure. At any instant of the cycle this coefficient is a function of the instantaneous pressure and temperature of the gas. This function was given by G. Eichelberg^{(9)*}:

$$\alpha_g = 2.1 \sqrt[3]{S} \sqrt{PT_g} \quad \frac{\text{K. cal.}}{\text{hr. m}^2 \cdot \text{°C.}}$$

where S is in meters per sec.

P in atmospheres.

T_g in degrees Kelvin.

This equation was put in B.T.U.s as follows:

$$\alpha_g = 0.0564 \sqrt[3]{S} \sqrt{PT_g} \quad \frac{\text{B.T.U.}}{\text{hr. sq. ft. °F.}}$$

[2.1]

where S is in feet per sec.

P in lbs. per sq. in.

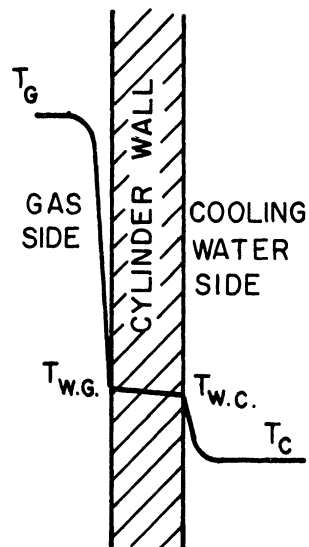
T_g in degrees Rankine.

Equation of Heat Transfer:

The heat transfer from the gas to the cylinder walls is given by,

$$Q = \int_0^{t_4} \alpha_g \cdot A \cdot (T_g - T_{w.g.}) dt$$

Writing this equation for each stroke:



* References are given in Bibliography.

(i) Intake Stroke:

$$Q = [A_{c.ch.} + A_{P.T.} + A_{Int.Man.}] \int_0^{t_1} \alpha_g (T_g - T_{w.g.}) dt + \int_0^{t_1} A_{bore} \alpha_g (T_g - T_{w.g.}) dt \quad [2.2]$$

(ii) Compression Stroke:

$$Q = [A_{c.ch.} + A_{P.T.}] \int_{t_1}^{t_2} \alpha_g (T_g - T_{w.g.}) dt + \int_{t_1}^{t_2} A_{bore} \alpha_g (T_g - T_{w.g.}) dt \quad [2.3]$$

(iii) Expansion Stroke:

$$Q = [A_{c.ch.} + A_{P.T.}] \int_t^{t_3} \alpha_g (T_g - T_{w.g.}) dt + \int_{t_2}^{t_3} A_{bore} \alpha_g (T_g - T_{w.g.}) dt \quad [2.4]$$

(iv) Exhaust Stroke:

$$Q = [A_{c.ch.} + A_{P.T.} + A_{Exh.Man.}] \int_{t_3}^{t_4} \alpha_g (T_g - T_{w.g.}) dt + \int_{t_3}^{t_4} A_{bore} \alpha_g (T_g - T_{w.g.}) dt \quad [2.5]$$

Since heat transferred during the cycle = the sum of heat transferred during the four strokes, then by adding equations [2.2], [2.3], [2.4] and [2.5] we get:

Equation of Heat Transfer to the Combustion Chamber Walls:

$$Q_{c.ch.} = A_{c.ch.} \int_0^{t_4} \alpha_g (T_g - T_{w.g.}) dt \quad [2.6]$$

and the mean heat transferred

$$= \frac{A_{c.ch.}}{t_4} \int_0^{t_4} \alpha_g (T_g - T_{w.g.}) dt$$

In this integral the wall temperature $T_{w.g.}$ can be considered as constant, and the equation becomes:

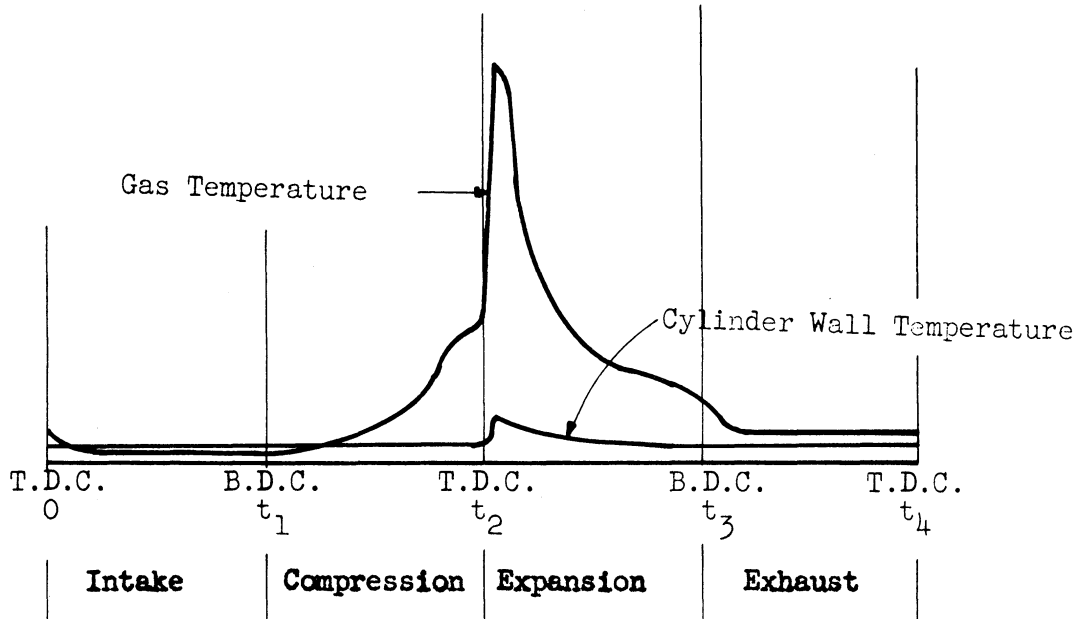


Figure 1. Gas and Cylinder Wall Temperatures.

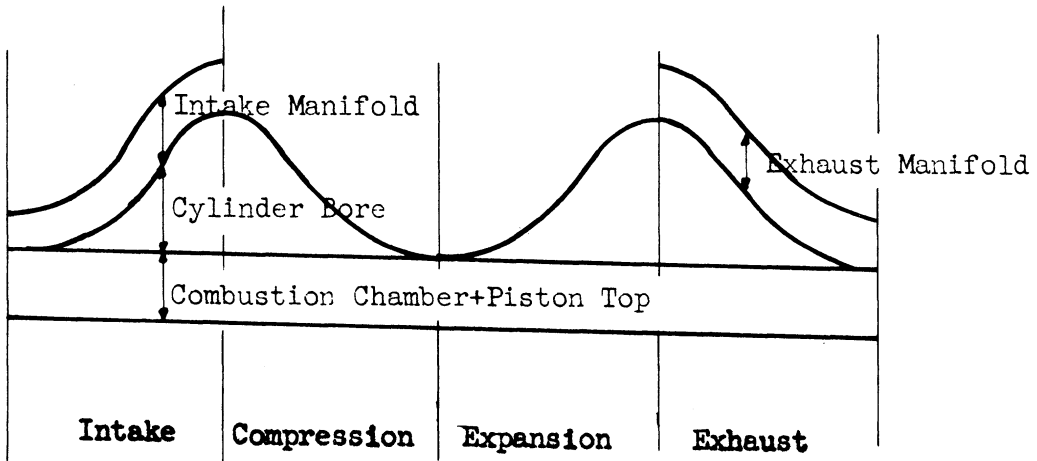


Figure 2. Area of Heat Transfer.

$$\begin{aligned} Q_{c.ch.} &= A_{c.ch.} [(\alpha_g T_g)_M - \alpha_M T_{w.g.}] \\ &= A_{c.ch.} \alpha_M [T_{M.E.} - T_{w.g.}] \end{aligned} \quad [2.7]$$

where

$$T_{M.E.} = \text{the mean effective temperature} = \frac{(\alpha_g T_g)_M}{\alpha_M} \quad [2.8]$$

α_M = the mean coefficient of heat transfer from the gases to the walls.

B. Heat Transfer Through the Walls:

The net heat given by the gases to the surrounding surface is transferred by conduction through the walls.

The equation of heat transfer by conduction is,

$$Q = A_m \frac{k_w}{x} (T_{w.g.} - T_{w.c.}) \quad [2.9]$$

and $T_{w.g.}$ can be considered constant as in equation [2.6].

C. Heat Transfer to the Cooling Medium:

The heat conducted through the walls is transferred to the cooling medium, mainly, by convection. The equation of heat transfer by convection is,

$$Q = \alpha_c A_c (T_{w.c.} - T_c) \quad [2.10]$$

where α_c is a function of: the rates of flow of the cooling medium; its physical properties, and the mechanism of cooling. For an engine

cooled with water, α_c can be calculated by using the Nusselt's equation:

$$\frac{\alpha_c D}{K} = C_1 \left(\frac{vD\rho}{\mu} \right)^m \left(\frac{c\mu}{K} \right)^n$$

For any engine: D , is constant; and $v\rho$, is proportional to the rate of flow of the cooling water. If the cooling water temperature is thermostatically controlled; K will be constant, and Nusselt's equation will take the form:

$$\alpha_c = C \left(\frac{W_c}{\mu} \right)^m \left(\frac{c\mu}{K} \right)^n \quad [2.11]$$

The values of the exponents m and n were given by B. Pinkel⁽³¹⁾:

$m = 0.6$, $n = 0.4$ and C is a constant of each engine.

Equation for the Combustion Chamber Wall Temperature:

Equating for Q from equations [2.7], [2.9] and [2.10] we get:

$$\begin{aligned} A_g & \cdot \alpha_M [T_{M.E.} - T_{w.g.}] \\ &= A_m \cdot \frac{k_w}{x} [T_{w.g.} - T_{w.c.}] \\ &= A_c \cdot \alpha_c [T_{w.c.} - T_c] \end{aligned}$$

These equations can be arranged in the following form,

$$\frac{k_w}{\alpha_M [T_{M.E.} - T_{w.g.}]} = \left(\frac{A_g}{A_m} \right) \times \frac{x}{(T_{w.g.} - T_{w.c.})} = \left(\frac{A_g}{A_c} \right) \times \frac{k_w}{\alpha_c [T_{w.c.} - T_c]} \quad [2.12]$$

Equation [2.12] is represented graphically in figure (3), by the slope of the straight line between $T_{M.E.}$ and T_c .

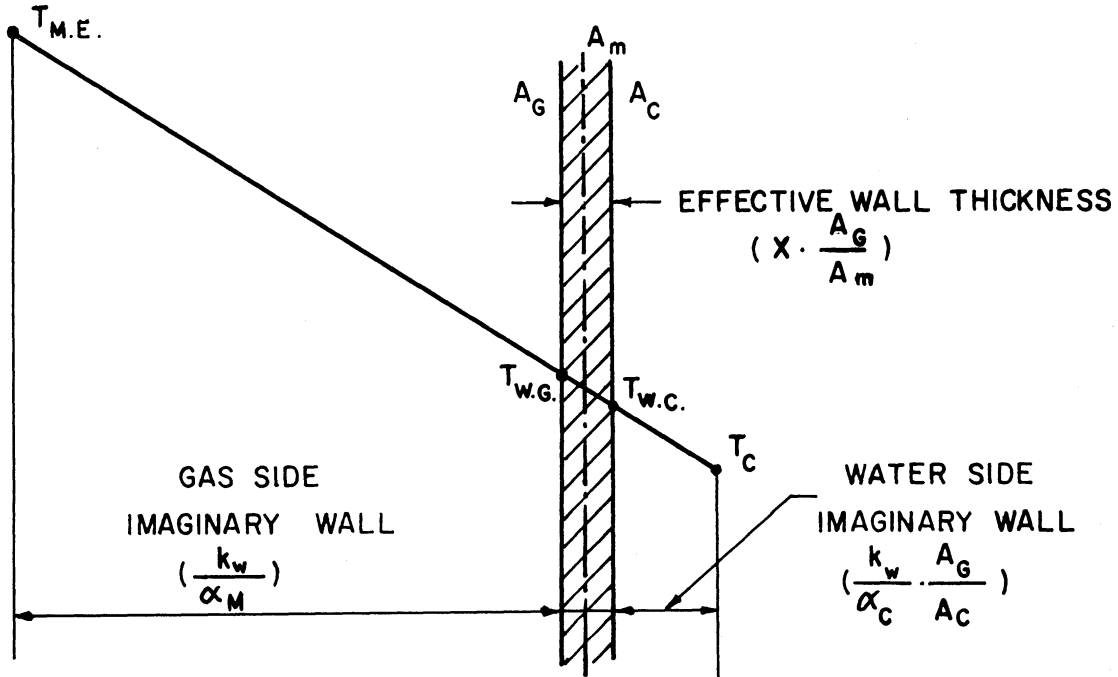


Figure 3 Graphical Construction for the Imaginary Walls

Using the following area factors: $a_m = \frac{A_g}{A_m}$

and $a_c = \frac{A_g}{A_c}$

the following equation can be derived from figure (3):

$$\frac{\frac{T_{M.E.} - T_c}{\frac{k_w}{\alpha_M}}}{\left[a_m x + a_c \frac{k_w}{\alpha_C} \right]} = \frac{\frac{T_{w.g.} - T_c}{\frac{k_w}{\alpha_C}}}{\left[a_m x + a_c \frac{k_w}{\alpha_C} \right]} \quad [2.13]$$

Let $Z = \left[a_m x + a_c \frac{k_w}{\alpha_C} \right]$

$$\therefore \left[\frac{T_{w.g.} - T_c}{T_{M.E.} - T_c} \right] = \frac{Z}{Z + \frac{k_w}{\alpha_M}}$$

and the equation of combustion-chamber-wall inside-surface temperature will be:

$$T_{w.g.} = T_{M.E.} \left[\frac{Z}{Z + \frac{k_w}{\alpha_M}} \right] + T_c \left[\frac{\frac{k_w}{\alpha_M}}{k_w + Z} \right] \quad [2.14]$$

Intensity of the Thermal Loading on the Combustion Chamber Walls:

This is given by the amount of heat transferred to the walls per unit area per unit time.

$$q = U (T_{M.E.} - T_c) \quad [2.15]$$

where U is the overall coefficient of heat transfer between the gases and the cooling medium, and can be calculated from equations [2.7], [2.9] and [2.10] as,

$$\frac{1}{U} = \frac{1}{\alpha_M} + a_m \cdot \frac{x}{k_w} + a_c \cdot \frac{1}{\alpha_c} \quad [2.16]$$

Thermal Load on the Cylinder Walls:

This is given by the heat transferred per unit time to the engine walls surrounding the gases.

$$Q = A_M U [T_{M.E.} - T_c] \quad [2.17]$$

where A_M is the mean effective area for heat transfer, and is given by:

$$A_M = \frac{\int_0^{t_4} \alpha_g A (T_g - T_{w.g.}) dt}{\int_0^{t_4} \alpha_g (T_g - T_{w.g.}) dt} \quad [2.18]$$

and U is the same as that in equation [2.16].

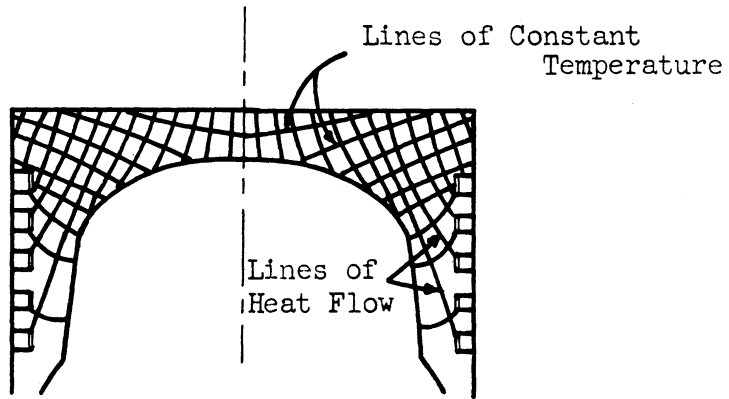


Figure (4,a) Temperature Field in the Piston-Crown.

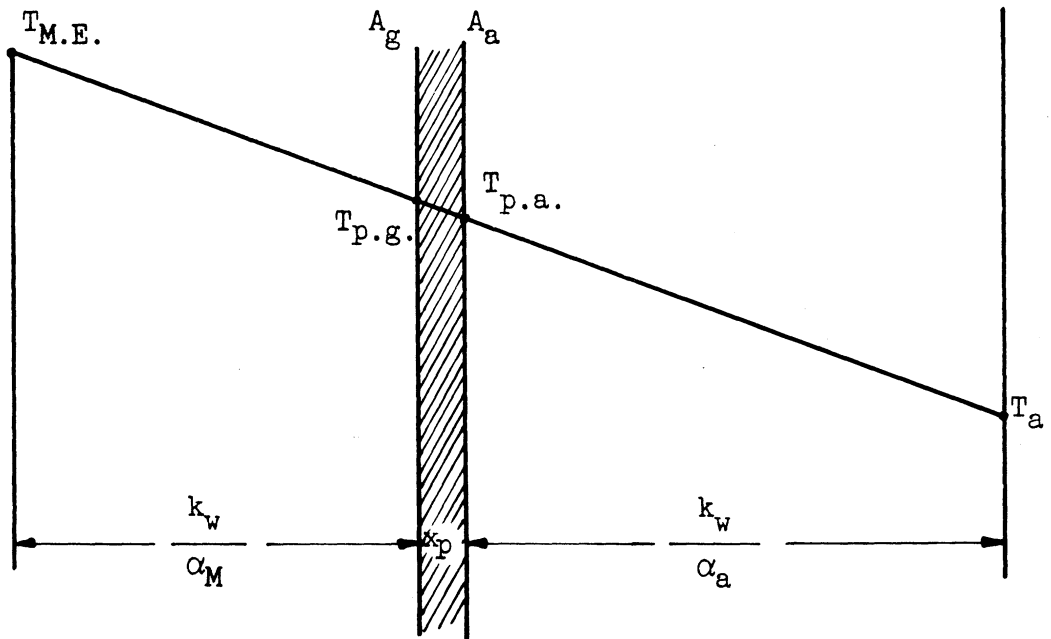


Figure (4,b) Graphical Construction of the Imaginary Walls for the Piston Crown.

Equation for Piston Top Maximum Temperature:

Part of the heat transferred from the hot combustion gases to the piston top, goes to the mixture of the hot air and oil vapor on the other side of the crown. The rest goes to the cylinder liner, through the piston rings and the lubricating oil film. This is illustrated in figure (4,a) by the temperature fields calculated for similar types of pistons. (9) The maximum piston temperature occurs at the center of the piston-crown, as it is the point farthest from the cylinder liner.

Applying equation [2.13] to a small area at the center, with α_a in place of α_c , we get:

$$\frac{T_{M.E.} - T_a}{\frac{k_w}{\alpha_M} + \left[x_p \frac{A_g}{A_m} + \frac{k_w}{\alpha_a} \frac{A_g}{A_a} \right]} = \frac{T_{p.g.} - T_a}{\left[x_p \frac{A_g}{A_m} + \frac{k_w}{\alpha_a} \frac{A_g}{A_a} \right]} \quad [2.19]$$

To get $\frac{A_g}{A_m}$ and $\frac{A_g}{A_a}$, the temperature field in the crown has to be calculated. Since the surface temperature is changing for each cycle, these calculations will turn out to be very complicated. Yet for the purpose of comparison between the piston temperatures at the different turbocharging conditions, the following assumptions will be made:

$$\frac{A_g}{A_m} = 1 \quad \text{and} \quad \frac{A_g}{A_a} = 1$$

Then equation [2.19] becomes:

$$\frac{T_{M.E.} - T_a}{\left(\frac{k_w}{\alpha_M} \right) + \left[x_p + \frac{k_w}{\alpha_a} \right]} = \frac{T_{p.g.} - T_a}{\left[x_p + \frac{k_w}{\alpha_a} \right]} \quad [2.20]$$

where x_p and k_w are constants for any engine, and α_a is constant for constant crank oil temperatures

$$\text{Let } Y = \left[\frac{k_w}{\alpha_a} + x_p \right]$$

$$\therefore \left[\frac{T_{M.E.} - T_a}{\frac{k_w}{\alpha_M} + Y} \right] = \left[\frac{T_{p.g.} - T_a}{Y} \right]$$

And the equation for the maximum temperature of the piston-crown will be:

$$T_{p.g.} = T_{M.E.} \left[\frac{Y}{Y + \frac{k_w}{\alpha_M}} \right] + T_a \frac{\frac{k_w}{\alpha_M}}{\left[\frac{k_w}{\alpha_M} + Y \right]} \quad [2.21]$$

The wall temperatures of other parts of the cylinder can be evaluated by a similar analysis if their cooling mechanism is known.

For the above analysis the gas mean effective temperature and the gas mean coefficient of heat transfer were evaluated, from the cycle analysis, as functions of the following performance conditions:

- a - The indicated mean effective pressure.
- b - The intake manifold pressure.
- c - The intake manifold temperature.
- d - The mean piston speed.

The thermal loading and wall temperatures were then calculated and compared with the experimental results, as shown in the following chapters.

III. EXPERIMENTAL SETUP

A single-cylinder, 4-stroke cycle, liquid-cooled Nordberg Diesel Engine was used in the experimental work. The cylinder had a bore of $4 \frac{1}{2}$ inches, a stroke of $5 \frac{1}{4}$ inches, and a compression ratio of 14.5, (Other engine specifications are given in Appendix I.). The general test setup is shown in figures (5), (6), (7) and (8). The various systems are described in the following paragraphs.

A. Air Intake System:

The air intake system is shown schematically in figure (9). Air under pressure entered the system through a filter to eliminate entrained solids, and then passed through an automatic pressure-regulating valve before entering the air flowmeter. This consisted of an A.S.M.E. sharp-edged orifice in a flange mounting, figure (6). The orifice disc was of stainless steel and the orifice was 0.7018 inch diameter. The conduits on both sides of the orifice disc were of stainless steel tubing of 2.0052 inches inside diameter. The length of the straight tube ahead of the orifice was 36 inches and was used to secure a fairly uniform velocity profile in the approaching stream.

Air leaving the flow meter passed through an electric-heater to be heated to the required temperature. The heater shown in Figures (5), (6) and (8) has a capacity of 3000 watts. It had 3 coils connected in parallel through a switch, which allowed reduced power outputs of 1500 or 750 watts.

A copper-wool chamber and a surge tank were placed between the heater and the engine intake manifold, to reduce pulsation to a

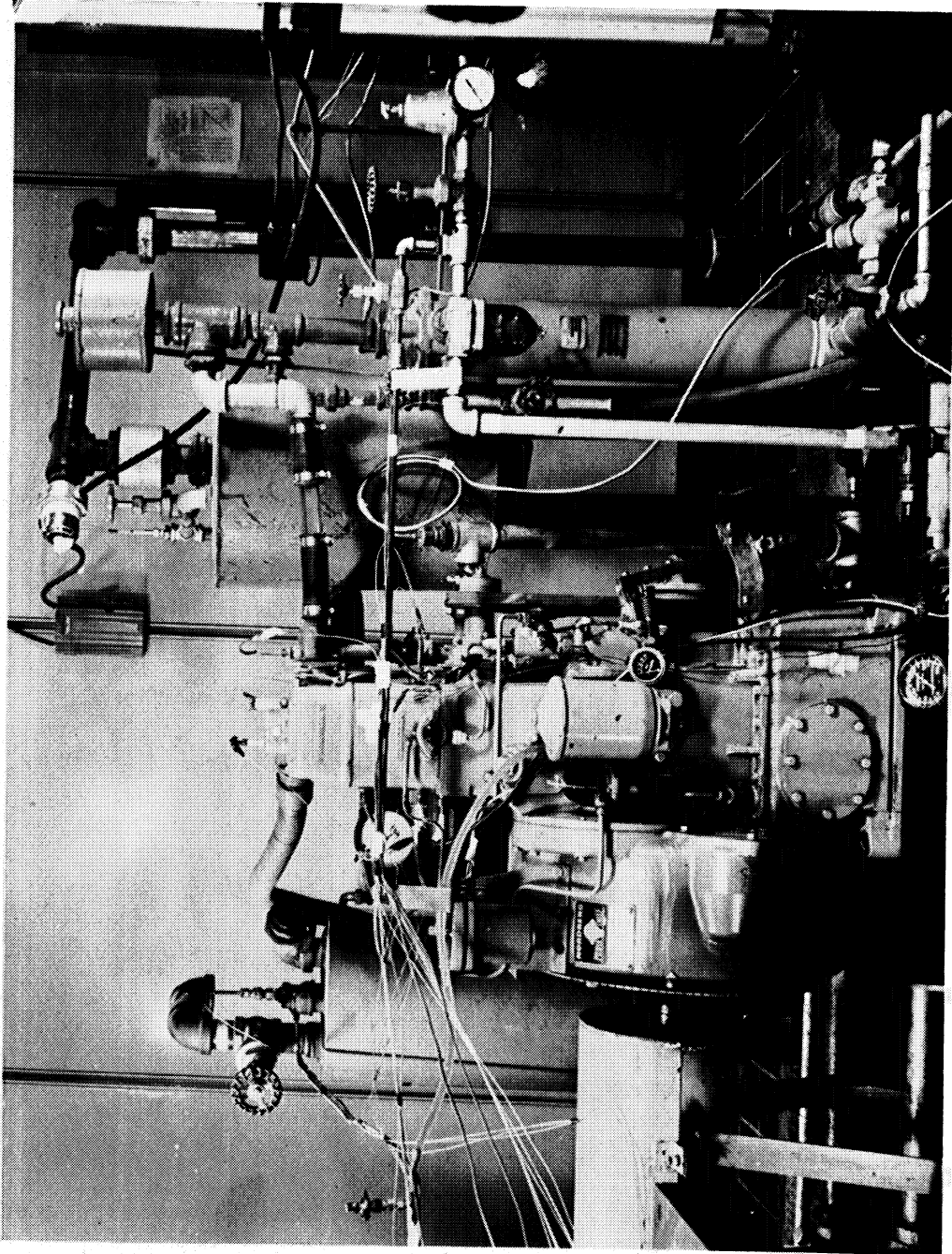


Figure 5. General Layout of the Experimental Setup

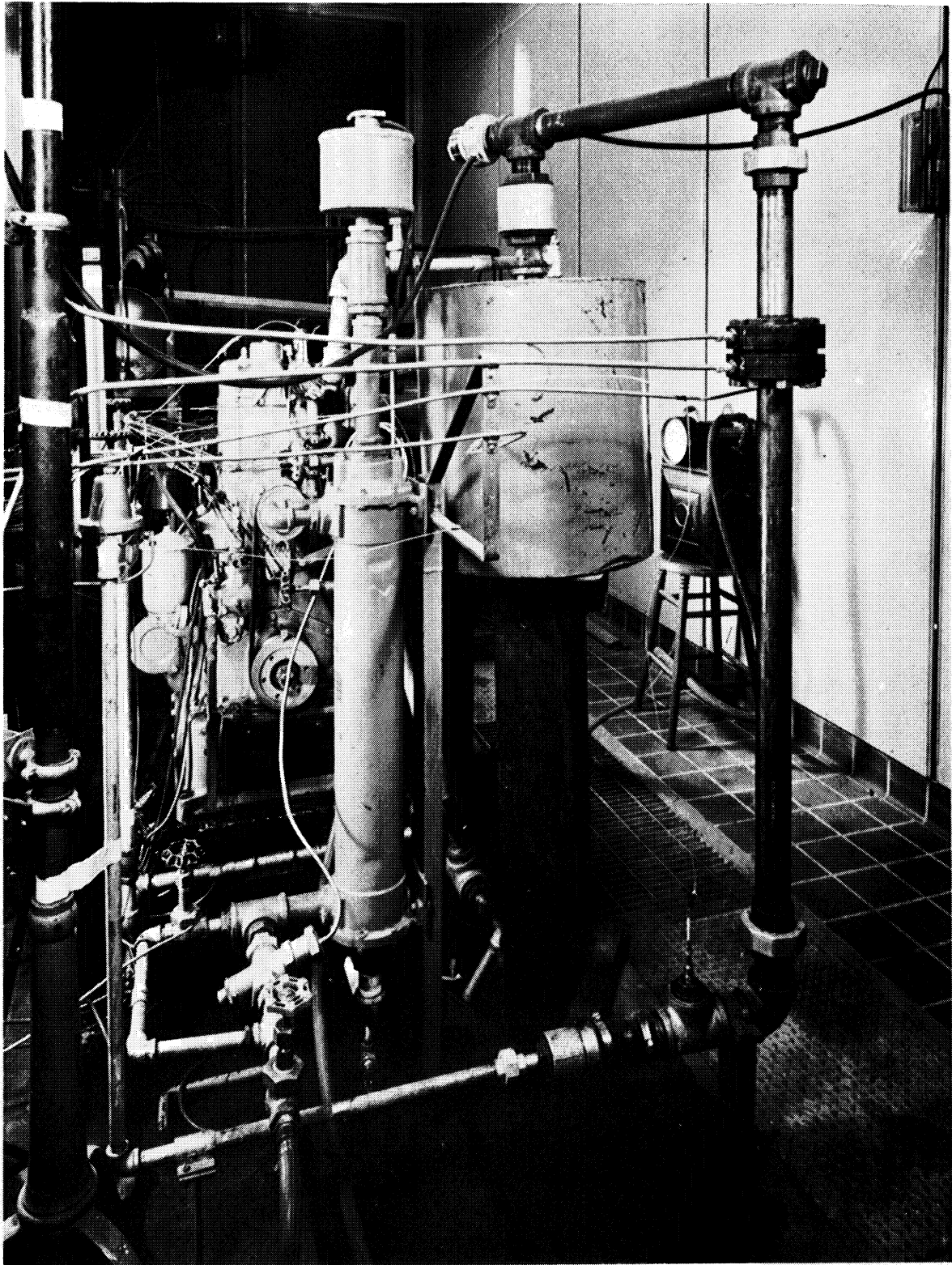


Figure 6. Side View Showing the Air Flowmeter and the Air Intake System.

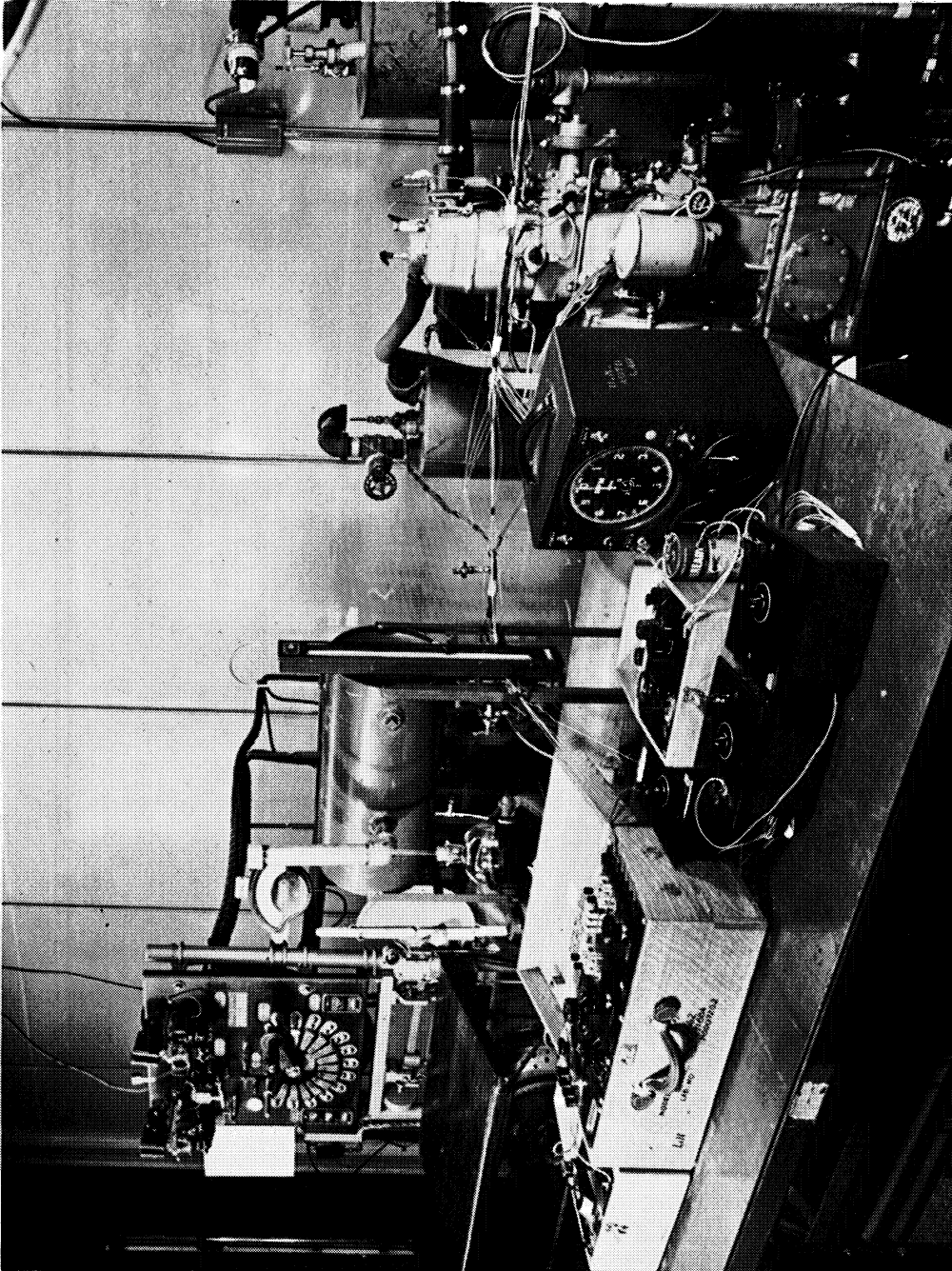
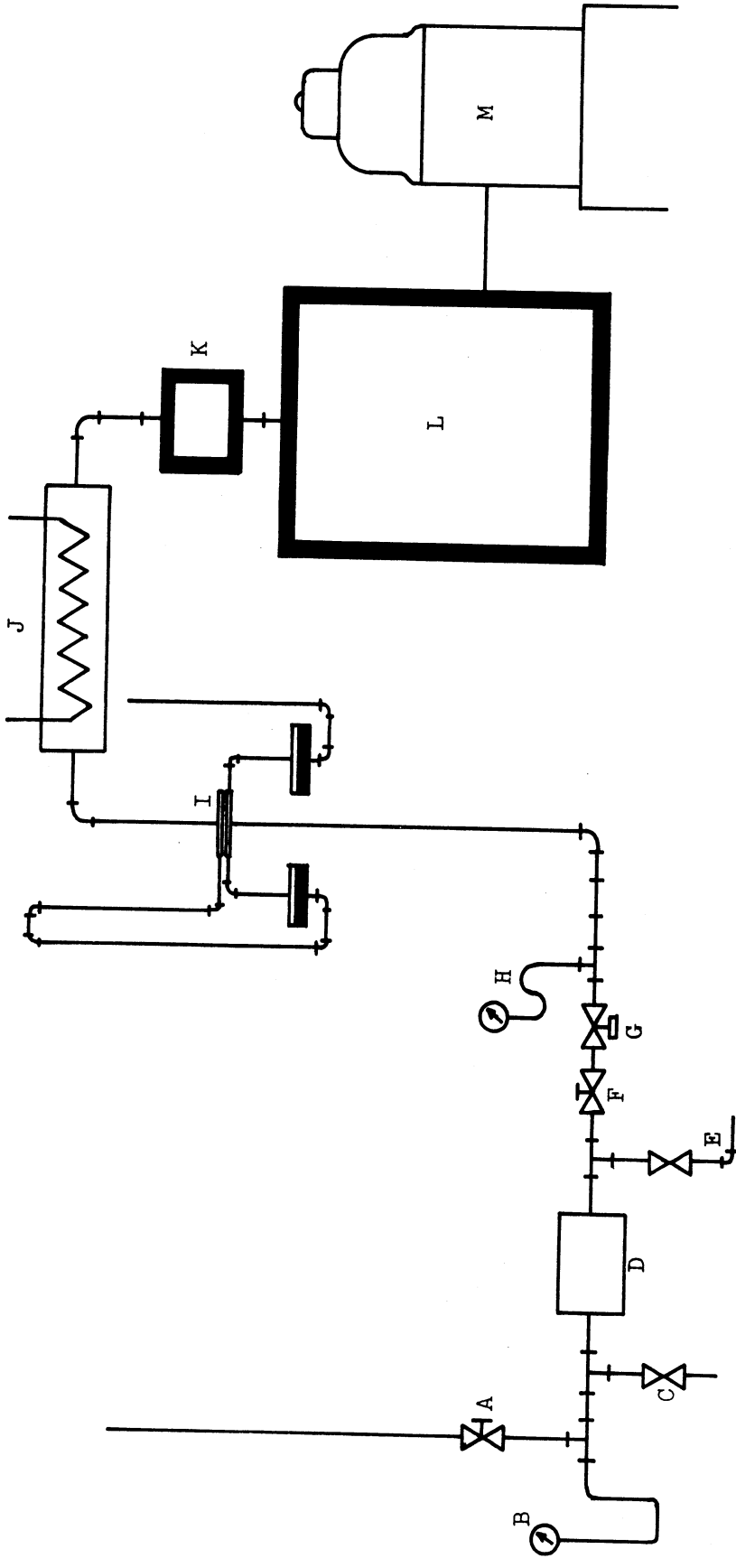


Figure 7. Instrumentation



Figure 8. General View of the Oscilloscope and Amplifiers.



- A. Main Air Supply Valve
- B. Main Air Pressure Gage
- C. Condensate Bleed Valve
- D. Air Filter
- E. Air Line to Pressure Pick Up
- F. Air Supply Valve
- G. Air Supply Control Valve
- H. Air Pressure Gage
- I. Air Flowmeter and Manometers
- J. Electric Heater
- K. Copper-Wool Chamber
- L. Surge Tank
- M. Engine

Figure 9. DIAGRAM OF INTAKE SYSTEM.

minimum. The copper wool chamber was 4 inches in diameter and 4 inches long. The surge tank was 15 inches in diameter and 19 inches long; with a volume 40.5 times the engine swept volume.

The air pressure was measured before the flowmeter and in the surge tank by a mercury manometer. The pressure drop across the orifice was measured from two flange **taps** connected to a water manometer. The air temperature was measured by iron-constantan thermocouples, placed at the flowmeter and in the intake manifold of the engine.

B. Exhaust System:

For most of the runs a flexible exhaust pipe was connected between the engine exhaust manifold and the main exhaust underground conduit. For runs requiring back pressures, a surge tank was connected between the engine and the main conduit. The discharge pipe from the surge tank had a 2 inch gate valve to throttle the exhaust gases flow; thus building the required gas pressure.

The pressure in the surge tank was measured by a mercury manometer. The gas temperature was measured by a chromel-alumel thermocouple placed in the exhaust manifold just after it leaves the cylinder head block.

C. Cooling System:

A cooling water closed system, equipped with a heat exchanger, was used to cool the engine. It is shown schematically in figure (10). It consisted of a pump driven by the engine, a heat exchanger, an automatic thermostatic control with a manual temperature control, and a water flow meter.

The manual temperature control was set to keep the water temperature at about 160°F, as it entered the engine. A 2 inch A.S.M.E. sharp edged orifice, similar to that used in the air inlet system, was used to measure the water flow rate. The temperature of the water was measured before entering and after leaving the engine, and in three passages leading from the cylinder barrel to the cylinder head to separate barrel and head losses.

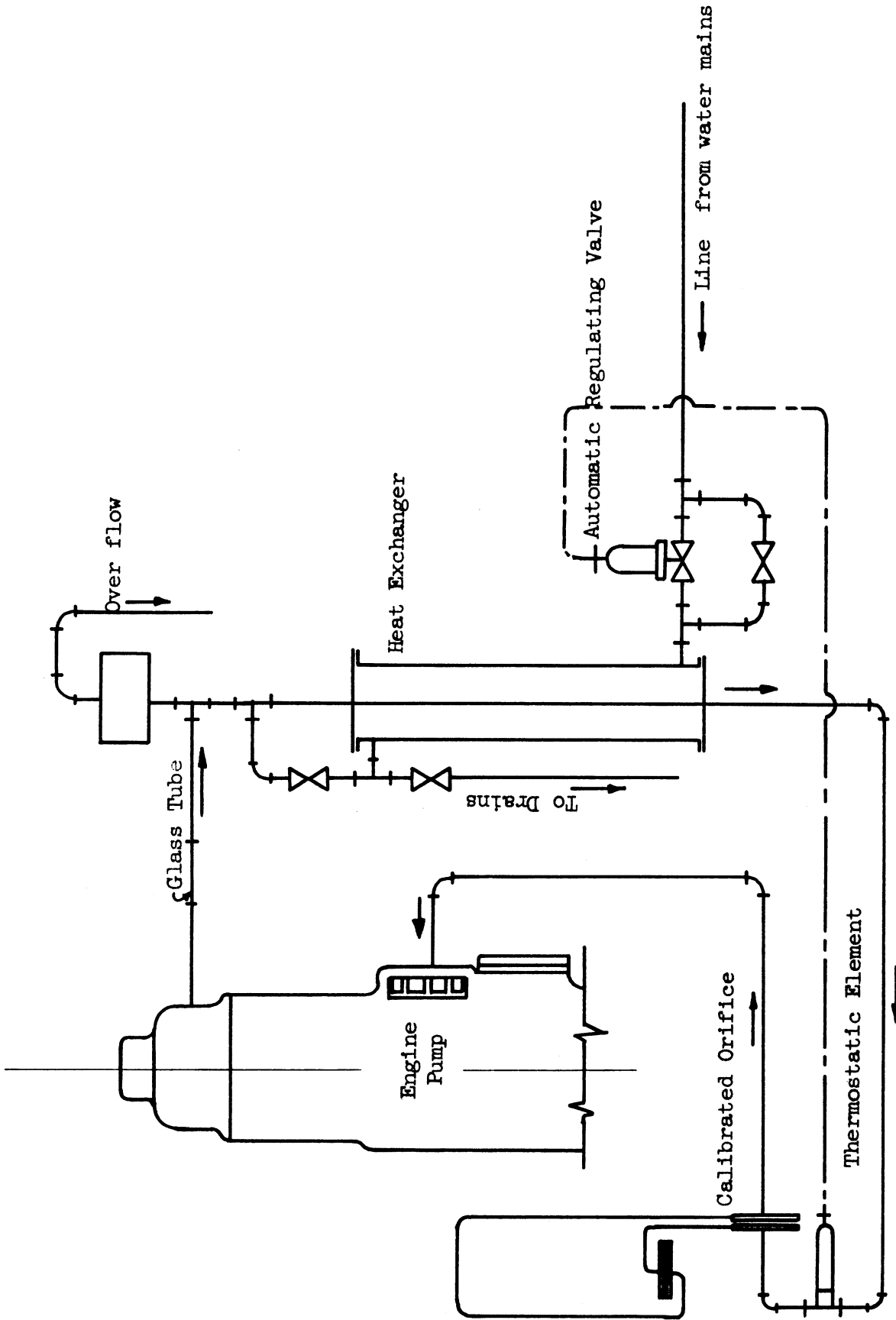


Figure 10. Cooling Water System.

Fuel Weighing System:

The fuel weighing system measured the time required for the engine to consume definite weights of fuel. The system, figure (11), consisted of a scale which was equipped with a mercoid contactor. This operated electrical circuits which started and stopped an elapsed-time electric clock, and a revolution counter. The scale, clock, and counter measured the time required for the engine to consume a pre-determined weight of fuel, and the number of revolutions of the crank shaft during the same period of time. This system had been used at the Automotive Laboratory, University of Michigan.

Power Absorbing Unit:

A cradle type direct current dynamometer, was used to start the engine and absorb the power developed. When operated as a generator it measured the power input and turned it into electrical energy, which was converted into heat in loading resistance grids. The power was measured by the pull exerted on the dynamometer scale beam and the engine speed.

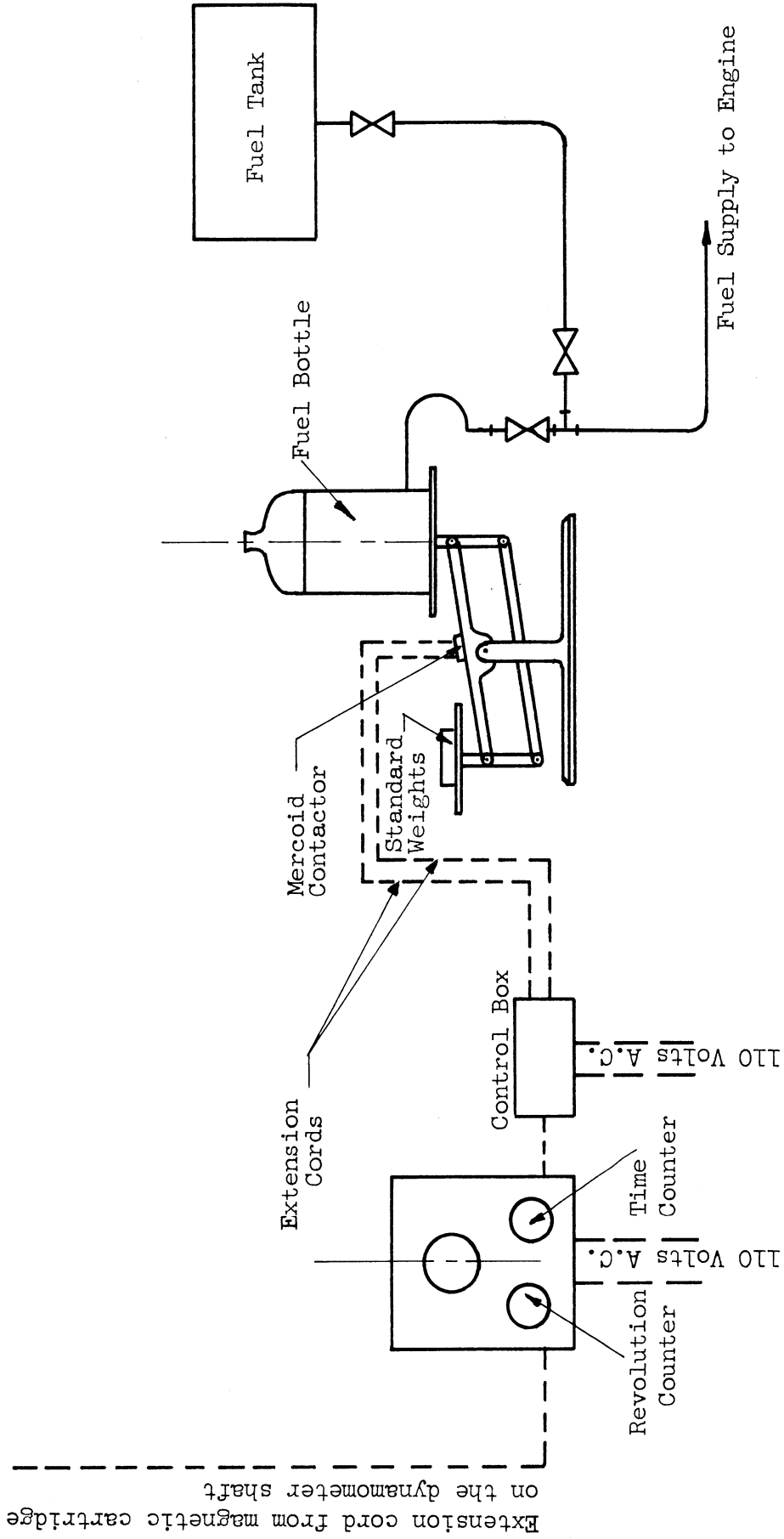


Figure 11. Automatic Fuel Weighing and Revolution Counting Devices

Gas Pressure Indicator:

A cathode ray indicator was used to obtain a pressure-time diagram of the gas pressure in the cylinder. The electrical circuit consisted of:

1. The pressure pick-up unit.
2. The degree marking unit.

1. The Pressure Pick-Up Unit:

This was of the two catenary shaped diaphragm type. Its function was to convert the cylinder pressure variations into corresponding voltage variations which were applied to the input of a bridge-amplifier. The output of the amplifier was fed, through a switch, to channel A of a dual beam oscilloscope, figure (13). The trace obtained on the screen was photographed by a polaroid camera attached to the oscilloscope.

2. The Degree Marking Unit:

The degree marks were produced by a steel disc, 20 inches diameter, 1/8 inch thick, mounted on the engine flywheel. The rim of the disc was slotted at 3° intervals, with deeper slots at 45° intervals, figure (12). A magnetic pick-up was mounted on the flywheel casing, with its pole close to the rim. The alternating voltage generated by the rotation of the disc was applied to channel B of the dual beam oscilloscope of item 1. The corresponding figure obtained on the screen consisted of a serrated line across the horizontal diameter of the screen. Every three and forty five degrees were thereby marked, and one of the deep 45° slots in the disc was aligned at the top dead-center, then the crank **angle** positions along the indicator diagram were directly determined.

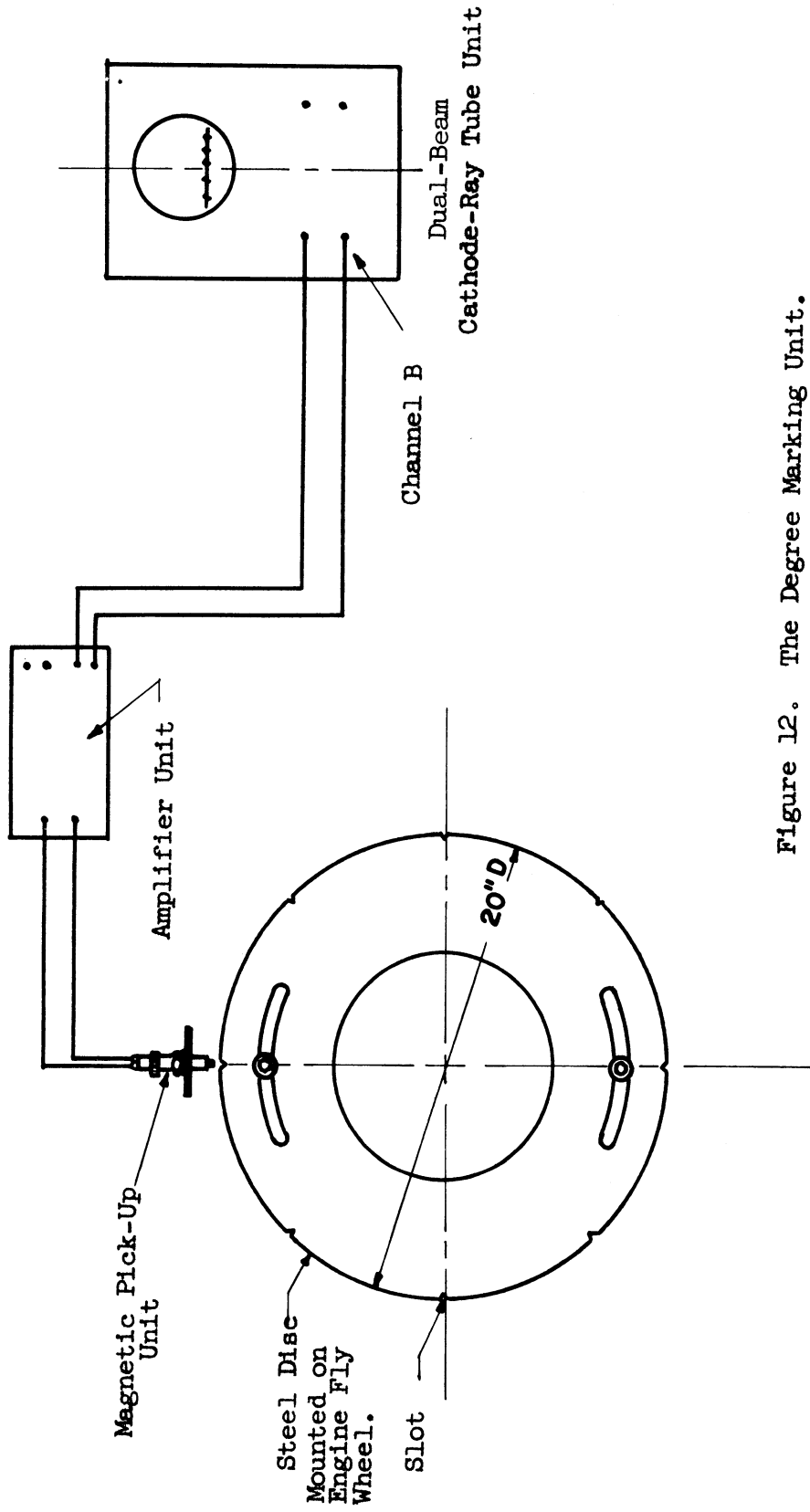


Figure 12. The Degree Marking Unit.

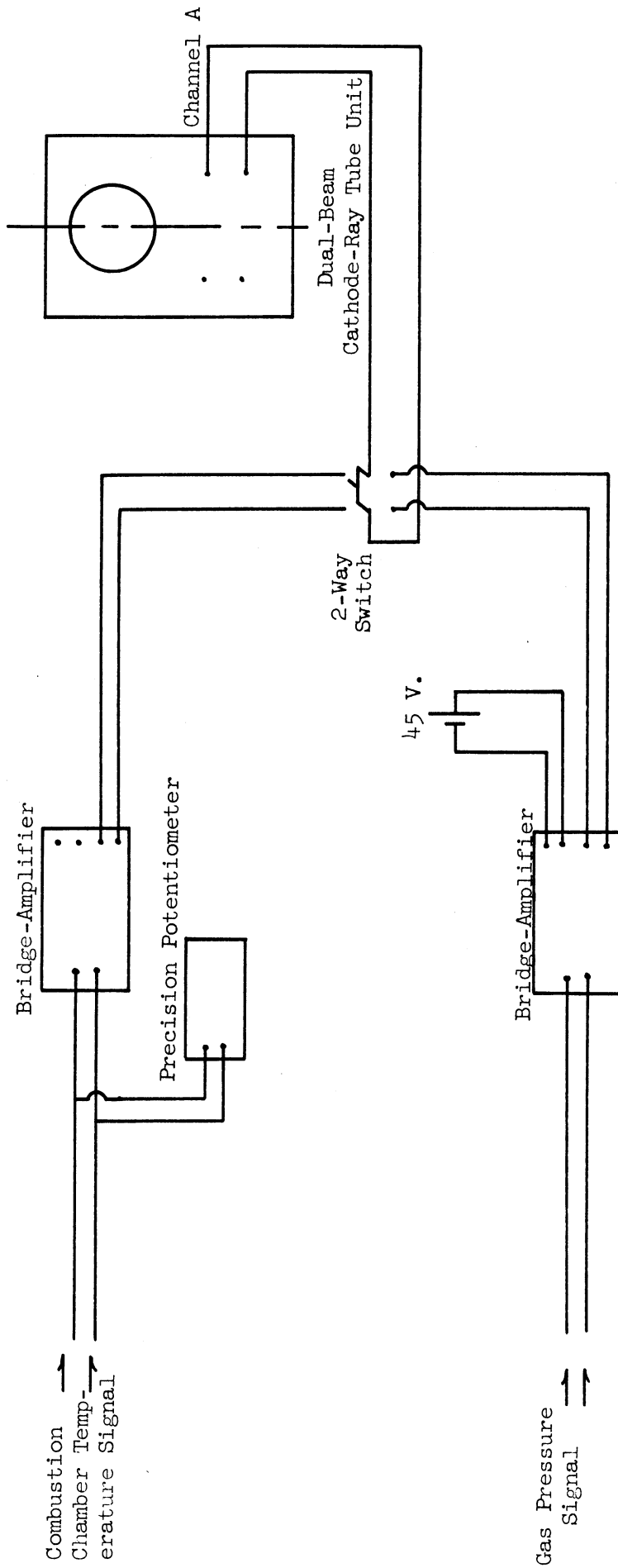


Figure 13. Layout of Electrical Circuits for Pressure and Temperature Recording.

Combustion-Chamber Thermocouple:

To measure the rapid temperature changes of the combustion-chamber-inside-surface a special Nickel-Steel thermocouple, manufactured by the Detroit Controls Corporation, was used. As shown in figure (14), it consisted of a: "Tyni-couple" basic unit, "Tyni-couple" mount, receptacle, plug, and coaxial cable. As described by the manufacturer, the basic unit, figure (15), was constructed by taking a 0.010" diameter nickel wire, applying a 0.00015" dielectric surface coating by oxidation, and swaging the wire into a slightly tapered hole in a small steel supporting body, thereby giving the assembled unit the ability to withstand very high pressures. The tip of the body and end of the wire were polished and plated with a 0.00025" thickness of nickel. The interface between the nickel plate and the steel body thus became the thermocouple junction. The basic unit was held in a steel mount, figure (14). The mount was equipped with external threads which were used to mount the unit on the cylinder head as shown in figure (16) and (17). Since the only electrical contact desired between the nickel and the steel was that existing at the hot junction, the internal nickel lead wire was insulated throughout its length from the steel parts of the thermocouple by a vinyl tubing. The nickel wire was soldered to the fitting in the receptacle. Shielded copper wires were used to carry the signal to the bridge-amplifier, then to the switch and the cathode ray oscilloscope. The layout of the temperature recording system being employed in the tests is shown in figure (13). The oscilloscope trace was photographed with a polaroid camera. The reference junction of the thermocouple circuit was at the ambient temperature.

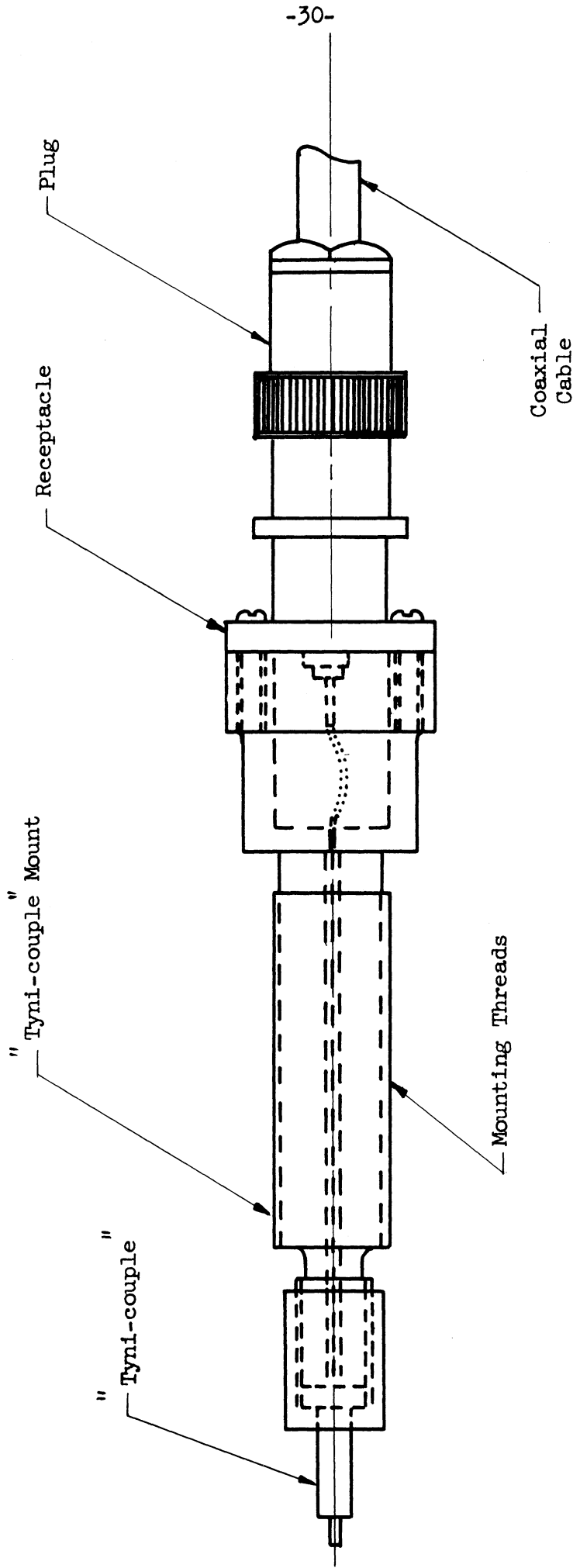


Figure 14. "Tyni-Couple" Assembly
 (Scale: Double Size)

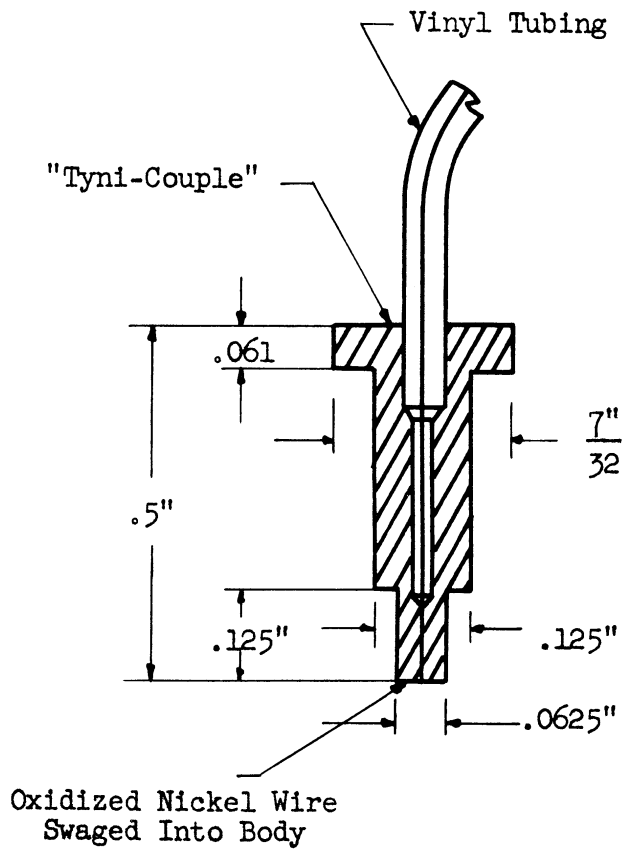


Figure 15. The Basic "Tyni-Couple" Unit

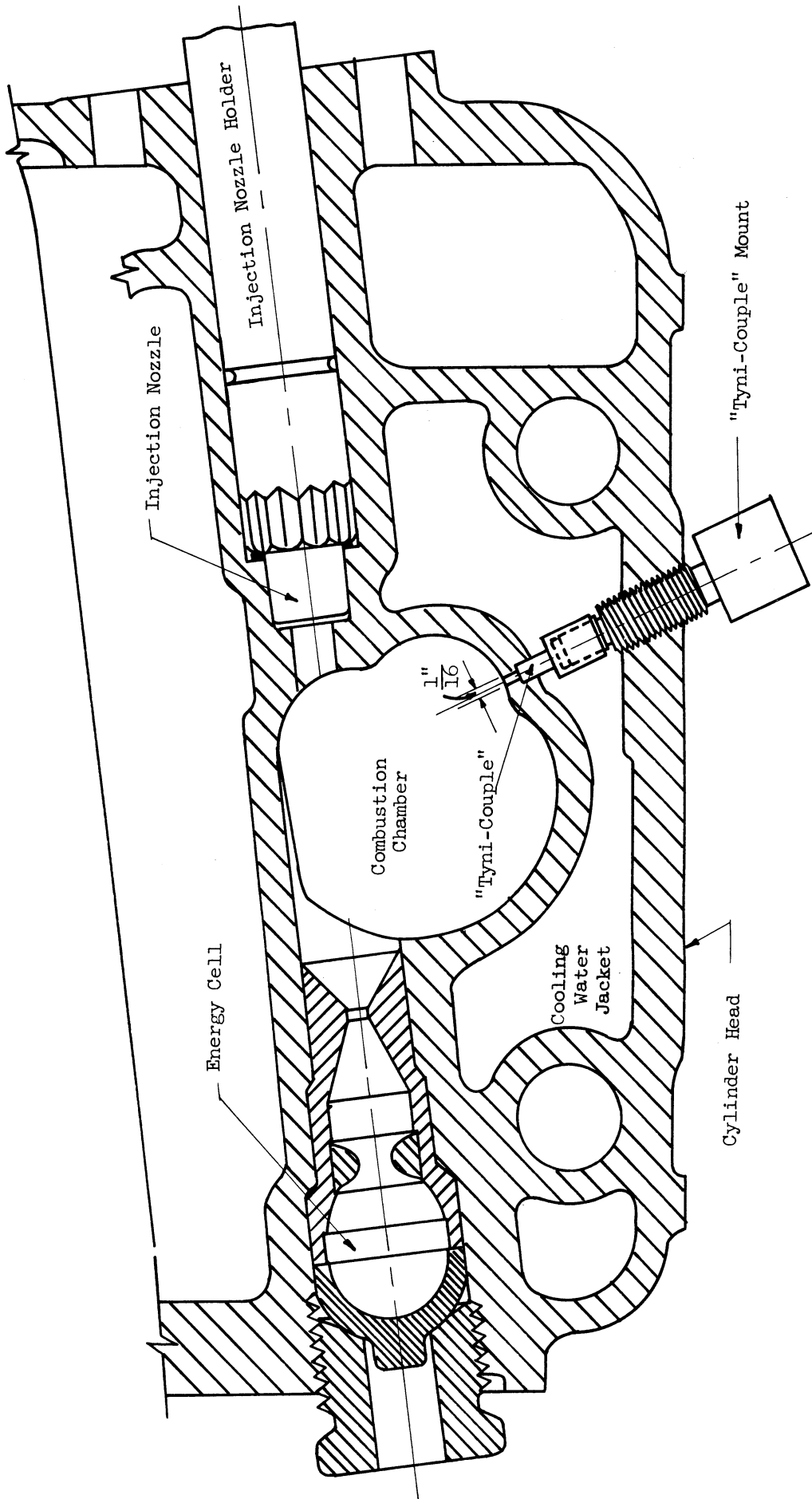


Figure 16. Sectional Plan of Cylinder Head Showing the Combustion-Chamber Thermocouple.

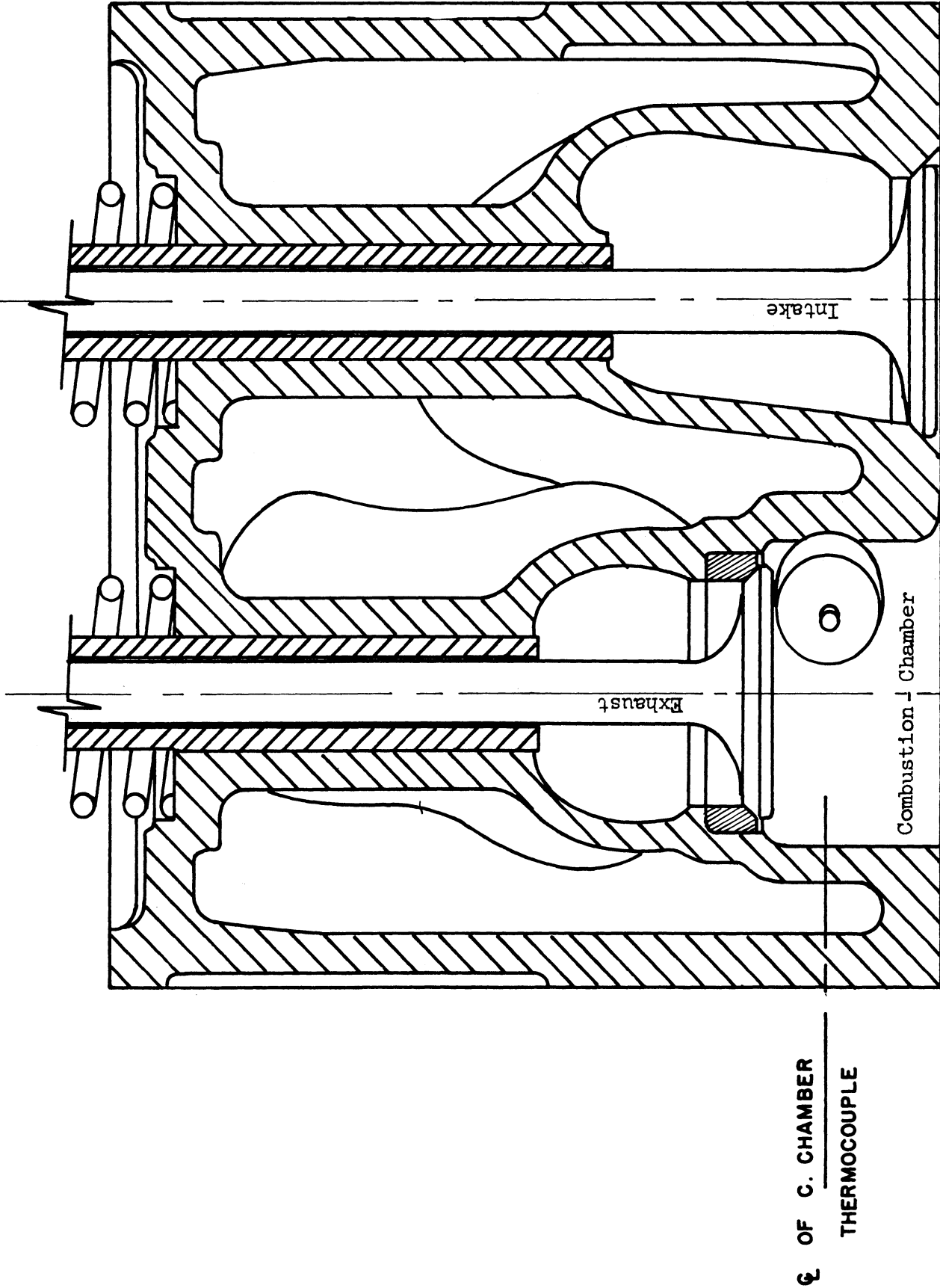


Figure 17. Sectional Elevation of Cylinder-Head Showing Position of Combustion-Chamber Thermocouple.

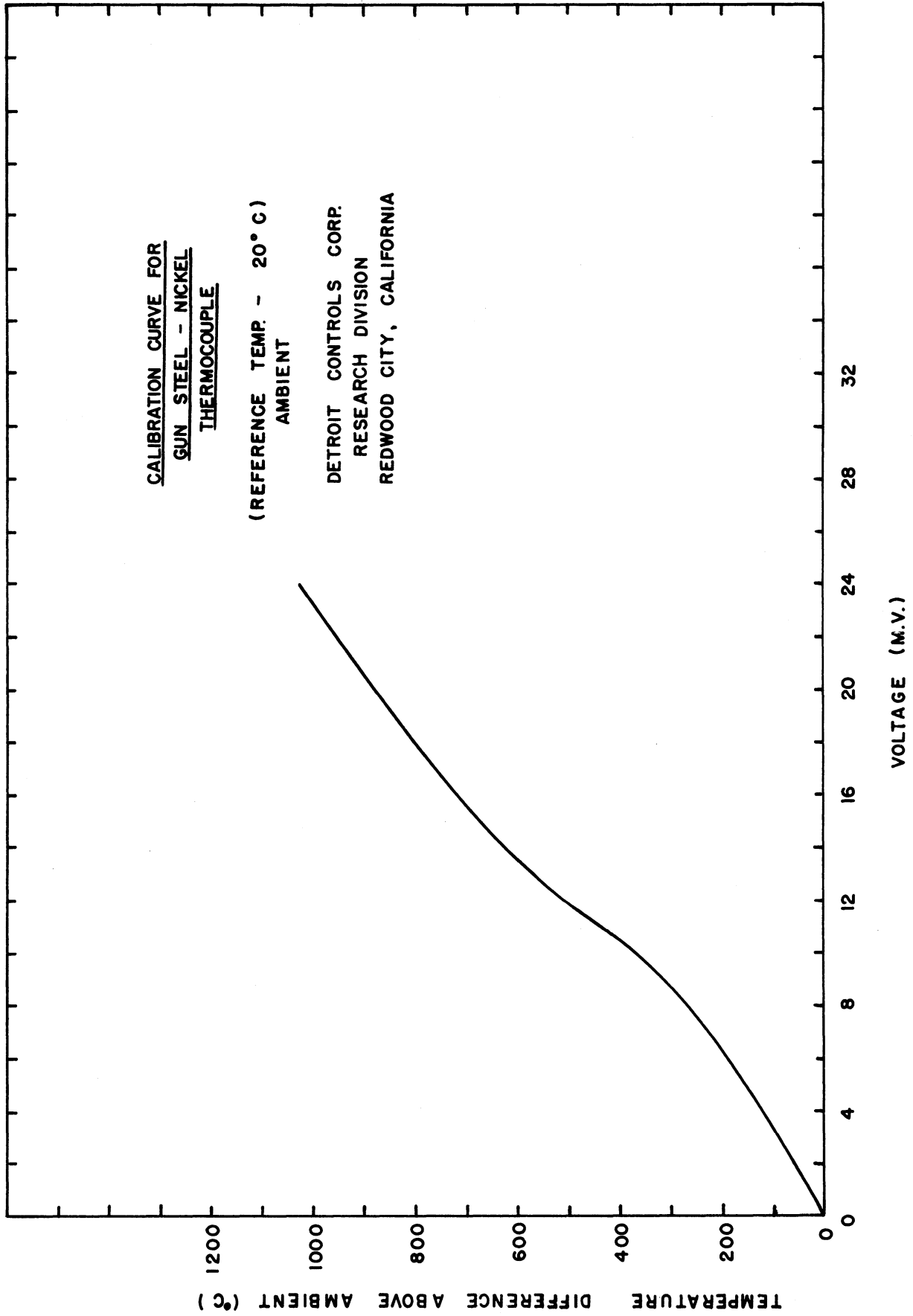
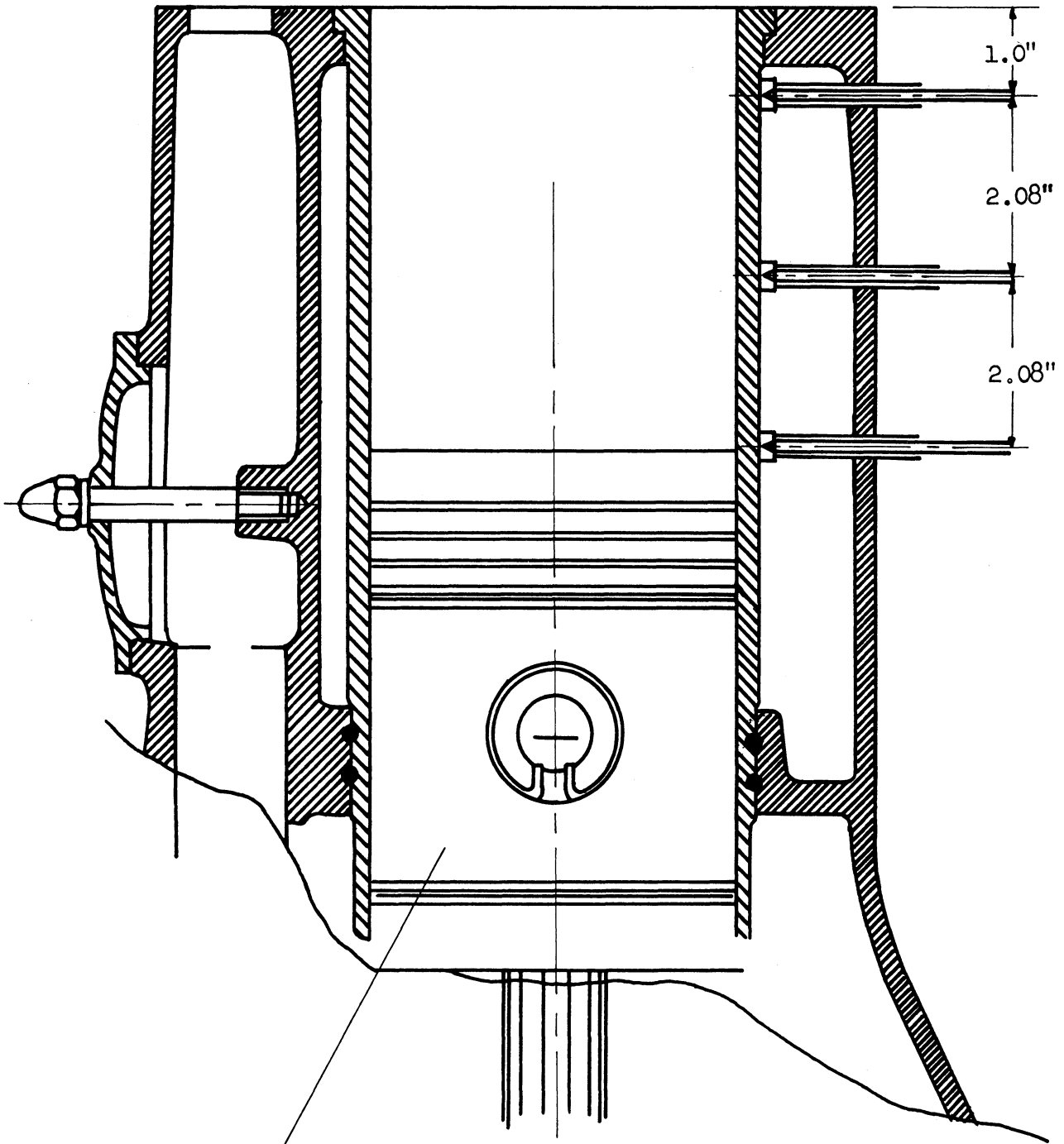


FIG.18 CALIBRATION CURVE FOR THE COMBUSTION CHAMBER THERMOCOUPLE
(Copy from figure delivered by manufacturer)



Piston at Bottom Dead Center

Figure 19. Thermocouples Positions on the Cylinder-Liner Walls

For the thermocouple, the theoretical response time, (time to reach 62.3% of imposed surface step change) = 4.5 microseconds. This time equals that required for the crank-shaft to rotate 0.034 crank-angle at an engine speed of 1200 R.P.M. Figure (18) shows a copy of the calibration curve for the thermocouple, as furnished by the manufacturer.

Engine Walls Thermocouples:

The thermocouples measured the surface temperatures of the liner, exhaust manifold, and the engine outer surface.

The liner wall coolant side temperature, was measured at three points in a vertical plane perpendicular to the crank shaft. One of the thermocouples measured the wall temperature near the T.D.C.; the other at the B.D.C.; and the third, midway between the other two. The positions of these thermocouples are shown in figure (19).

The exhaust manifold wall temperature was measured on the coolant side at a point midway between the exhaust valve and the manifold exit from the cylinder head. This temperature and the liner temperatures were used to calculate the coefficients of heat transfer from the gas to the walls, and from the walls to the cooling water.

The engine outer surface temperature was measured at five points: two on the cylinder head, one on the cylinder barrel, and two on the crank case. They were connected in parallel to give the average surface temperature.

IV. EXPERIMENTAL PROCEDURE

Procedure of Tests:

The engine was started, and after the necessary warming up period, the following data were taken for each run:

Air pressure in the surge tank of the intake system	P_m
Air pressure at the inlet tap of the orifice meter	P_a
Differential pressure across the air orifice	ΔP_a
Differential pressure across the cooling water orifice	ΔP_c
Air temperature at inlet to orifice meter	T_a
Air temperature at the intake manifold	T_m
Lubricating oil temperature in crank case	T_o
Wall temperature of the exhaust manifold	$T_{w.ex.}$
Wall temperature of liner at T.D.C.	T_{l_1}
Wall temperature of liner between T.D.C. and B.D.C.	T_{l_2}
Wall temperature of liner at B.D.C.	T_{l_3}
Engine outer surface temperature	T_s
Total rise in cooling water temperature	ΔT_c
Cooling water temperature at inlet to the engine	T_{c_1}
Cooling water temperature at inlet to the cylinder head	T_{c_2}
Cooling water temperature at exit from the engine	T_{c_3}
Exhaust gas temperature	$T_{exh.}$
Time for consumption of $\frac{1}{10}$ lb. of fuel	t_F
Revolutions of the crank shaft for the same period of time, t_F	N_{t_F}
Brake load	W_B

Pictures of the following traces:

Gas pressure and crank angles for the whole cycle.

Gas pressure and crank angles for the compression
and expansion strokes.

Calibration of the gas pressure trace.

Combustion chamber wall temperature and crank angles
for the whole cycle.

Combustion chamber wall temperature and crank angles
for the combustion period.

Calibration of the temperature trace.

A sample of these data is given in Appendix A, and a sample of the pictures is shown in figures (20), (21), (22) and (23). A few runs were **made** with the back pressure tank between the engine and the main exhaust conduit. These were to find the effect of the back pressure on the brake mean effective pressure.

Other data taken but not used in the calculations or results included lubricating oil pressure, lubricating oil temperatures before and after the cooler, current in the electric circuit of the air heater, air pressure after the reducing valve, and the **blow-by rate of flow**. Many of these were recorded for precautionary measures since by supercharging, the engine was overloaded beyond the design conditions.

The usual friction run was made at the end of each day's testing. For the brake horse power the formula was:

$$\text{B.H.P.} = \frac{W_B N}{4000}$$

where N = revolutions per minute

4000 = constant for the dynamometer

The indicated horsepower was obtained by adding, the brake horsepower at any given speed, to the friction horsepower at the same speed.

The cooling water temperatures at the inlet and exit from the engine were measured by two thermocouples connected to an ordinary "Leeds and Northrup" potentiometer. The difference between these two temperatures was also measured by two other thermocouples, connected to a potentiometer of the same type, but with greater precision reading temperatures down to 0.03°F . Four readings were taken for each run, and their average was used to calculate the heat losses to the cooling water. The water temperature was also measured at three of the four openings between the cylinder and cylinder head. During the first few runs, it was found that these three temperatures were almost equal. It was decided then, to connect the thermocouples in parallel, to get an average reading. The results given in Appendix A show the total rise in the cooling water temperature, the temperatures at the inlet to cylinder head and at the exit from the engine.

The Tests Covered the Following Ranges:

$\frac{F}{A}$ ratios from .0134 to .055

Air manifold pressures up to 45 inches mercury.

Air manifold temperatures up to 204°F .

Engine speeds from 560 to 1770 R.P.M.

Since the engine was designed to run under natural aspiration conditions, and to avoid troubles due to overloading by supercharging, the following limits were considered:

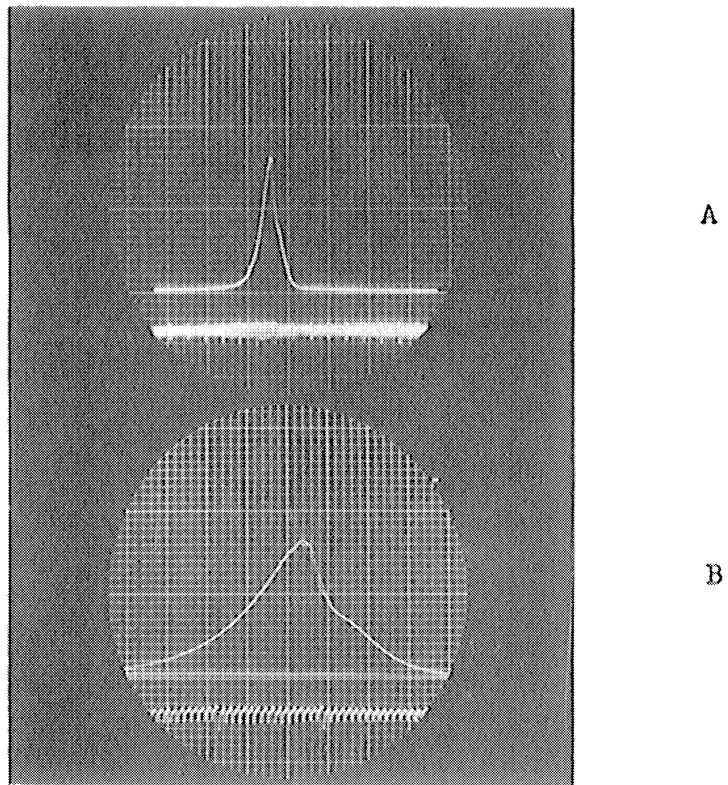
Exhaust temperatures not to exceed 1000°F .

Gas peak pressure in the cylinder not to exceed 1200 $\frac{\text{lbs.}}{\text{sq. in.}}$

The engine at the end of the tests was in a satisfactory condition, without any sign of failure in any of its parts.

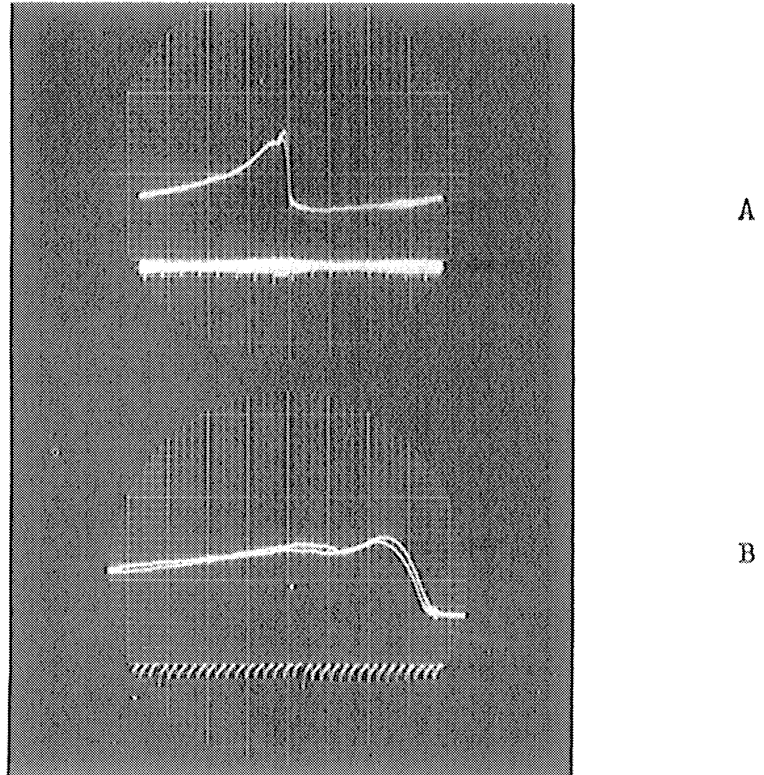
Calibration of the Combustion Chamber Thermocouple:

The calibration curve for the nickel-steel thermocouple, which was used to measure the combustion chamber wall temperature, was furnished by the manufacturer [Detroit Controls Corporation], and is shown in figure (18). To calibrate the temperature trace on the oscilloscope screen, the engine was stopped, and while the cylinder was still hot, the voltage produced by the thermocouple was measured by a precision potentiometer. At the same time a picture of the calibration trace was taken. The trace as shown in figure (23), is in the form of two parallel dashed lines; the vertical distance between them being equivalent to the voltage produced by the thermocouple. The reading of the potentiometer was in millivolts, and was converted to degrees fahrenheit by using the calibration curve figure (18). The scale of the temperature trace was then calculated from the calibration trace and the reading of the potentiometer.



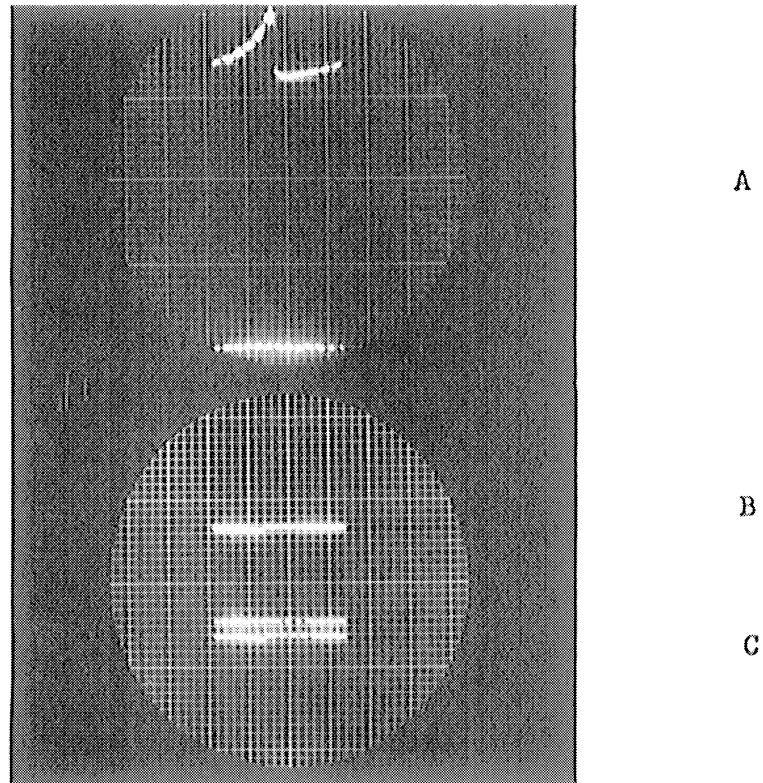
- A. Gas pressure and crank angles for the whole cycle
- B. Gas pressure and crank angles for the compression and expansion strokes

Figure 20. Gas Pressure During the Cycle.



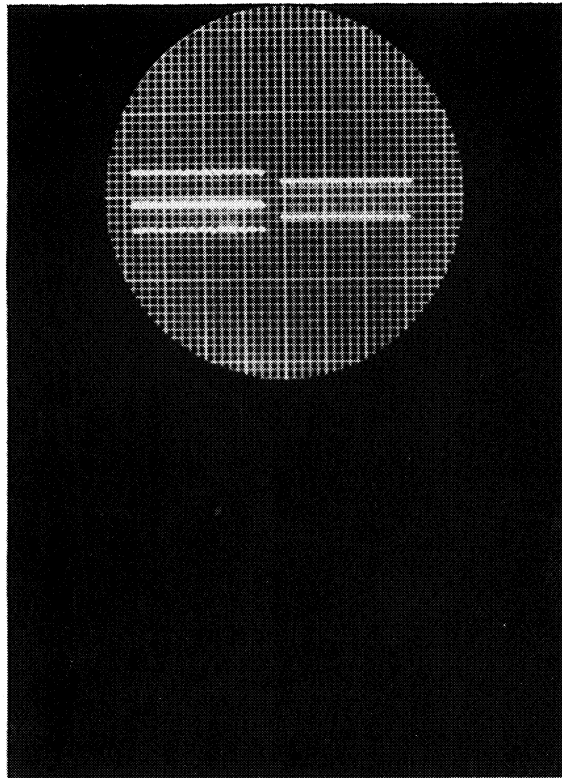
- A. Wall temperature and crank angles over the whole cycle (with 3 amplifiers)
- B. Wall temperature and crank angles for the combustion period (with 3 amplifiers)

Figure 21. Combustion Chamber Surface Transient-Temperature



- A. Wall temperature over the whole cycle and the atmospheric temperature. (With 3 amplifiers)
- B. Wall temperature over the whole cycle (With 2 amplifiers)
- C. Wall temperature over the whole cycle and the atmospheric temperature. (With 2 amplifiers)

Figure 22. Combustion Chamber Surface Transient-Temperature.



Pressure,(right): Deflection corresponds to $231.3 \frac{\text{lbs}}{\text{sq. in.}}$

Temperature,(left): Deflection corresponds to 33.1°F

- a. Deflection with 2 amplifiers (the two middle lines).
- b. Deflection with 3 amplifiers (the two outside lines).

Figure 23. Pressure and Temperature Calibration Traces.

V. EXPERIMENTAL RESULTS.

The results shown in this section covered the following range:

Series A. Runs At Variable Manifold Pressures:

Figures (24-32):

Average Speed = 800 R.P.M.

Average Manifold Temperature = 80°F

Manifold Pressures = 30" Hg - 45" Hg.

$\frac{F}{A}$ Ratios : .0134 - .055

Series B. Runs At Variable Manifold Temperatures:

Figures (33-38):

Average Speed = 1200 R.P.M.

Manifold Temperatures = 80 - 204°F

Average Manifold Pressure = 36" Hg.

$\frac{F}{A}$ Ratios : .0213 - .0468

These results are also given in **tables** (3-11). Other runs were made at different engine speeds and were used only to check the temperatures of the combustion chamber calculated from equation [2.14]. The results of these runs are shown in tables (12 and 13). Other set of runs was made before supercharging the engine to check the engine conditions while it was naturally aspirated. These are not of interest in the present investigation and their data are not given in this report.

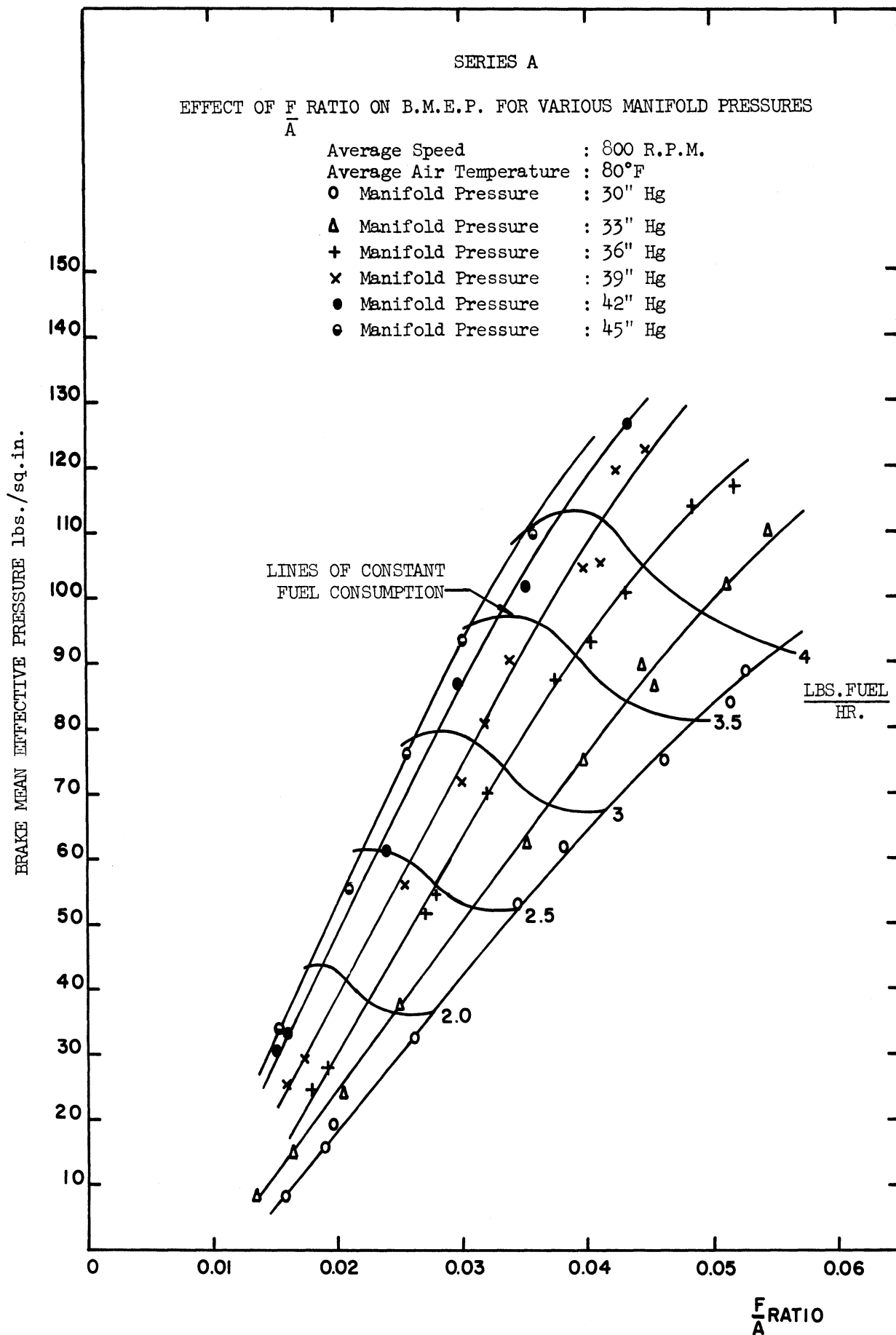


FIGURE 24

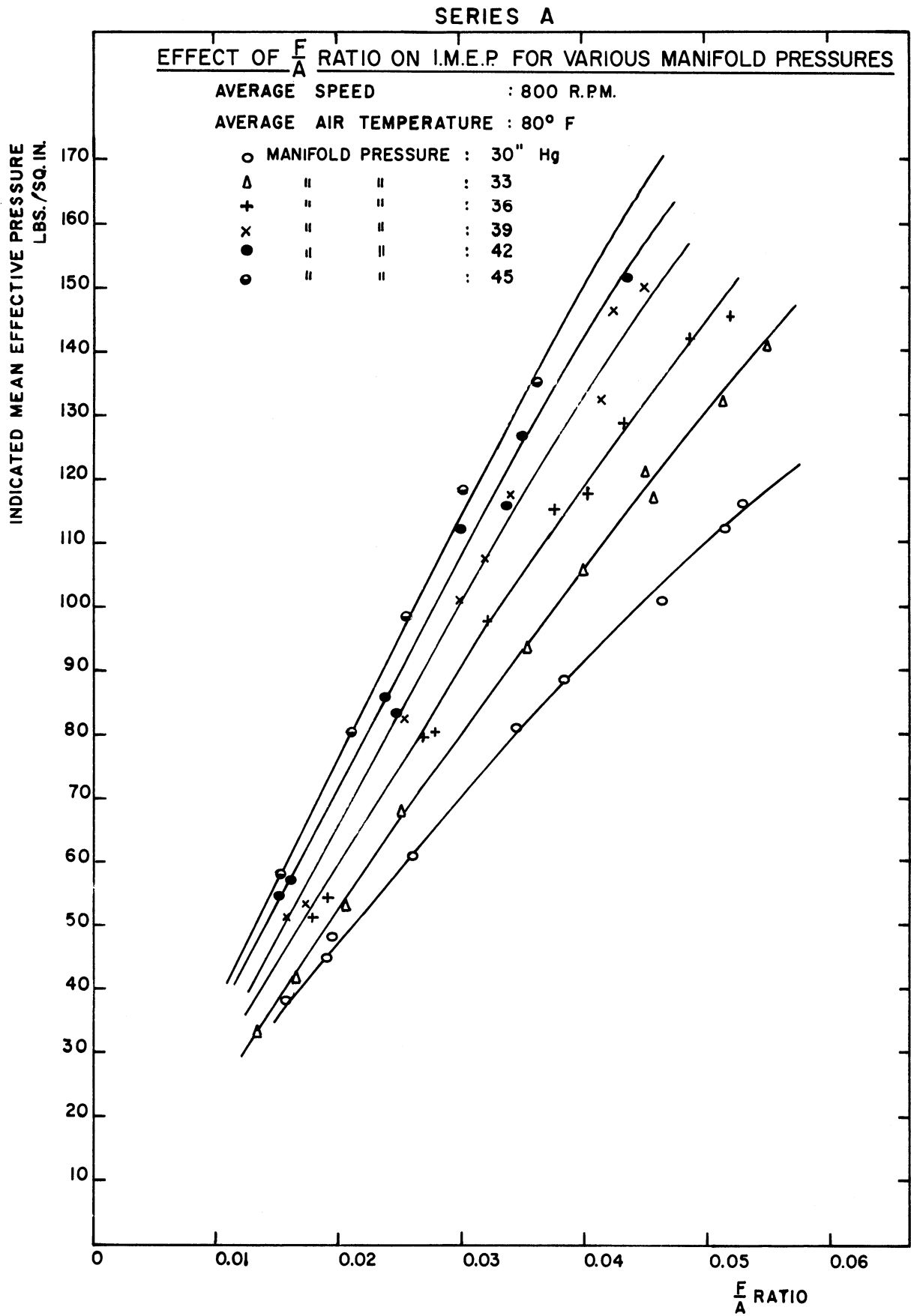


FIG. 25

Series A

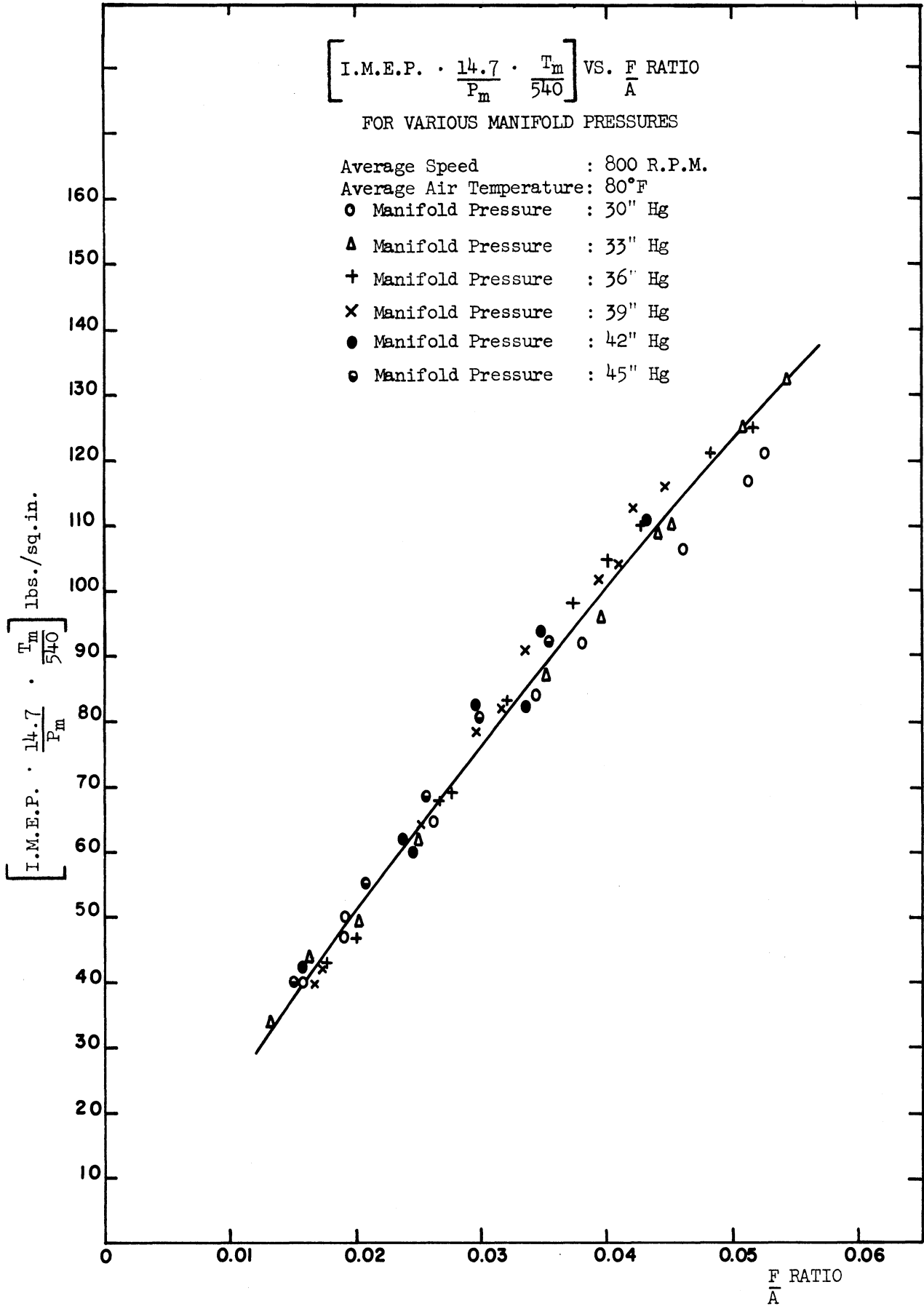


FIG. 26

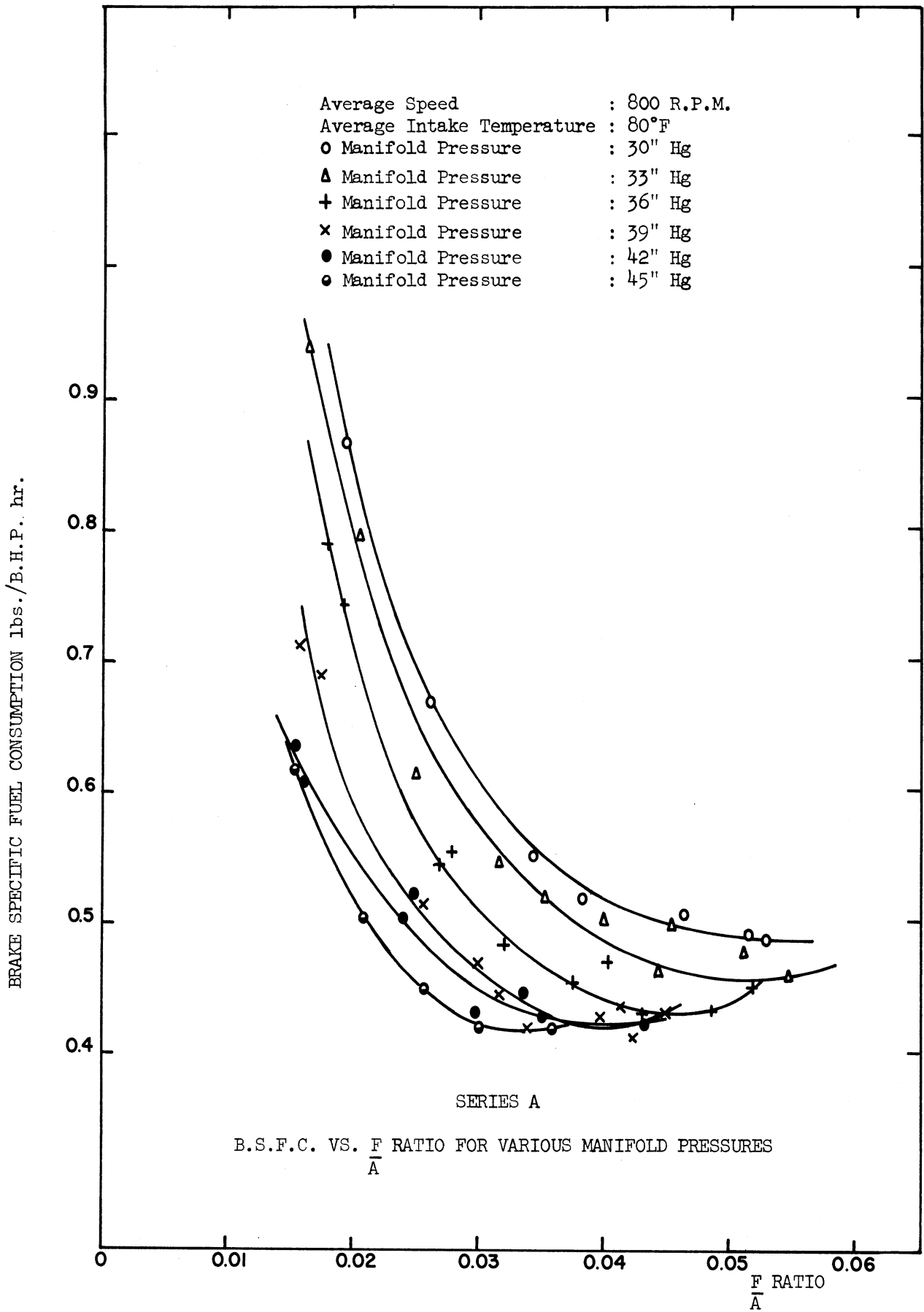


FIG. 27

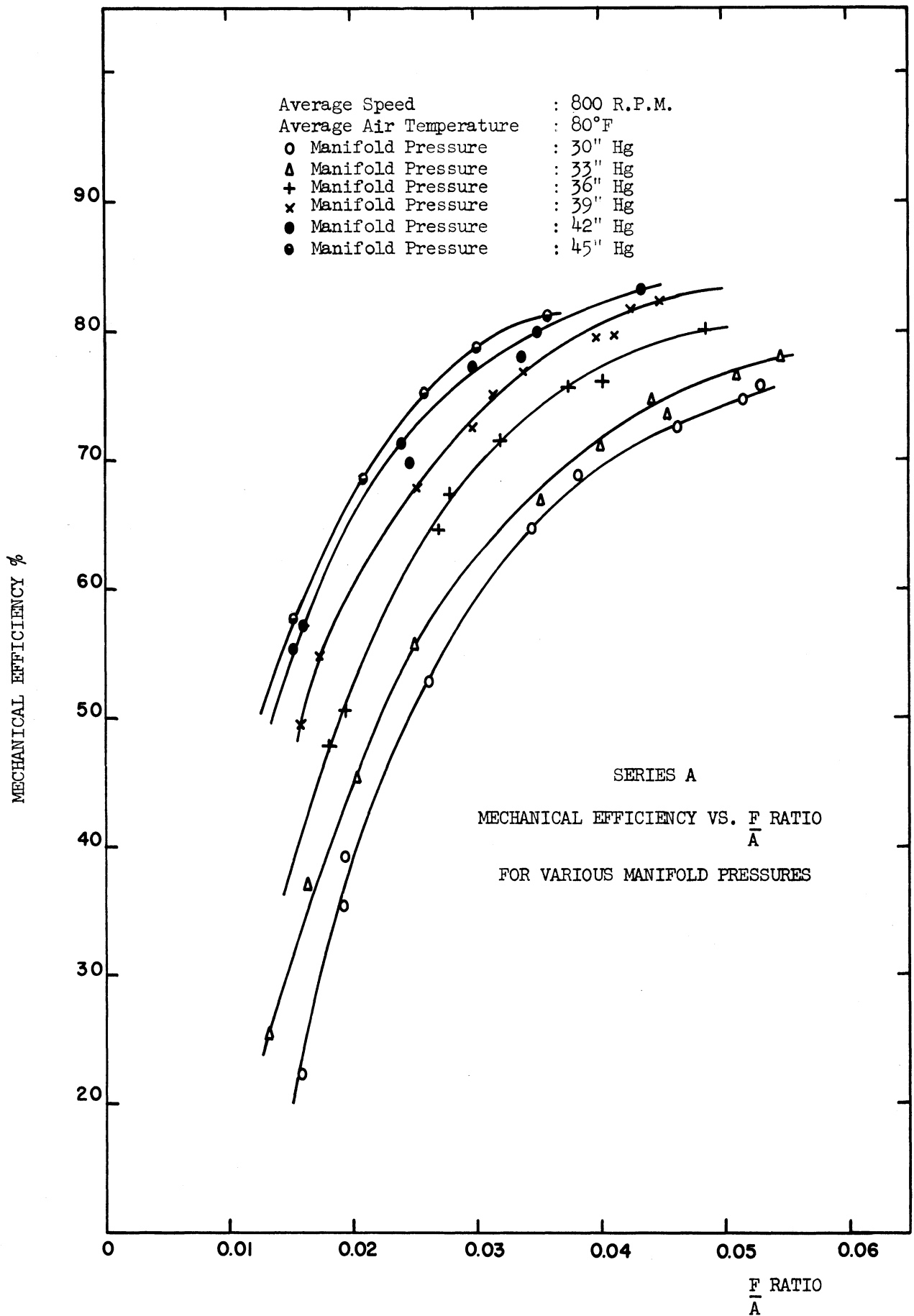


FIG. 28

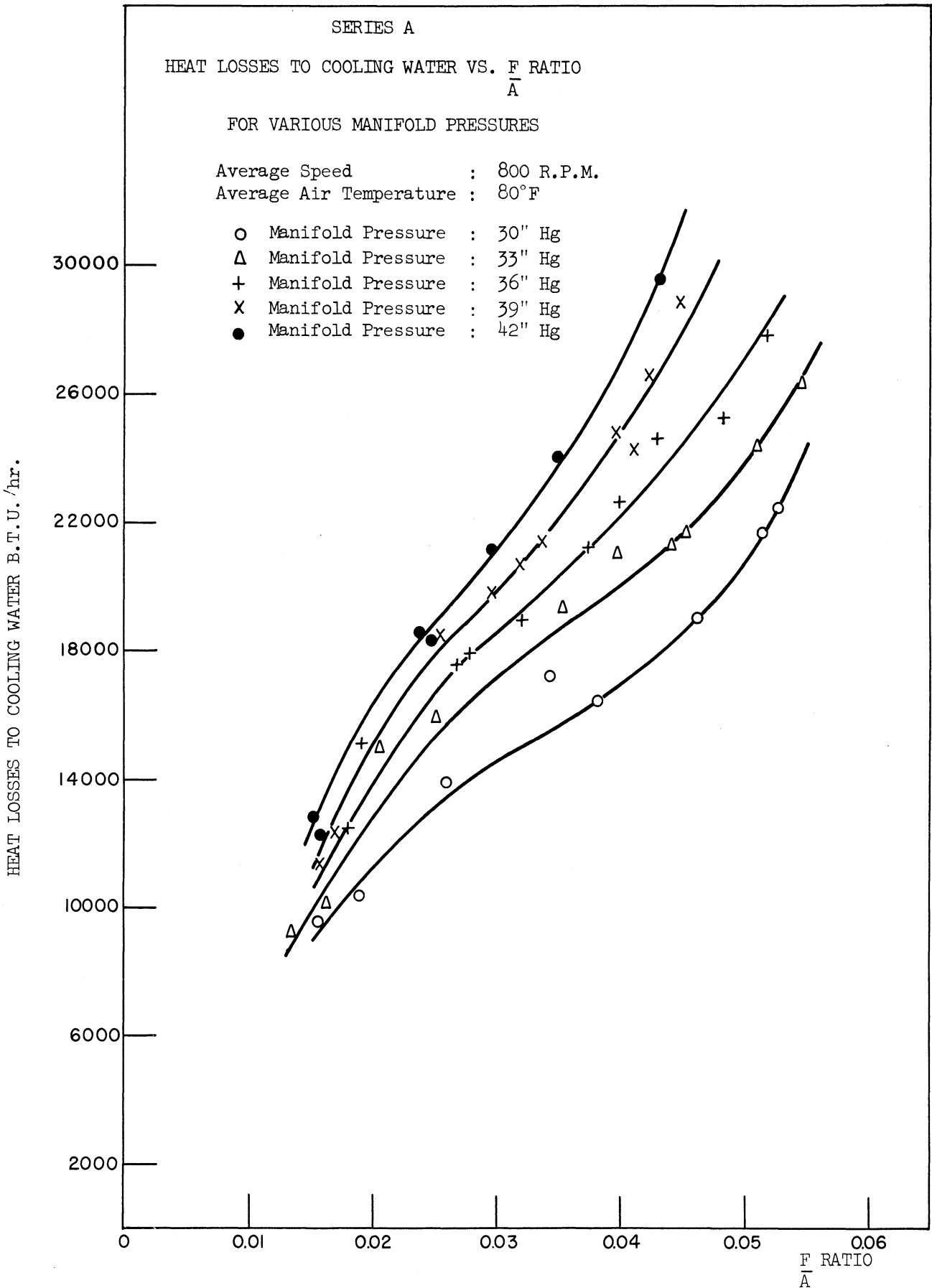


FIGURE 29

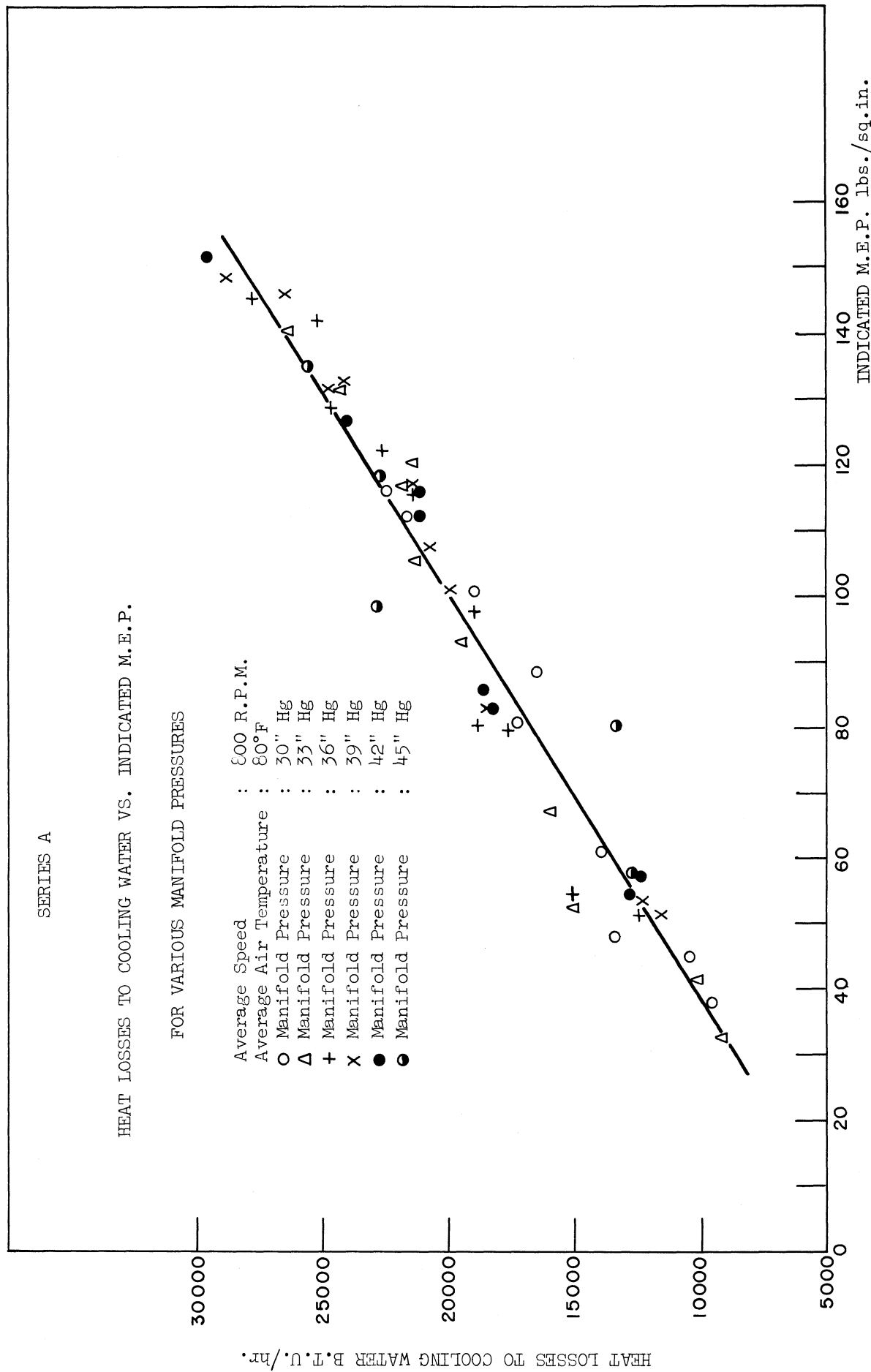


FIGURE 30

SERIES A

EXHAUST GAS TEMPERATURE VS. $\frac{F}{A}$ RATIO FOR VARIOUS MANIFOLD PRESSURES

- Average Speed : 800 R.P.M.
- Average Air Temperature : 80°F
- Manifold Pressure : 30" Hg
- △ Manifold Pressure : 33" Hg
- + Manifold Pressure : 36" Hg
- x Manifold Pressure : 39" Hg
- Manifold Pressure : 42" Hg
- ◐ Manifold Pressure : 45" Hg

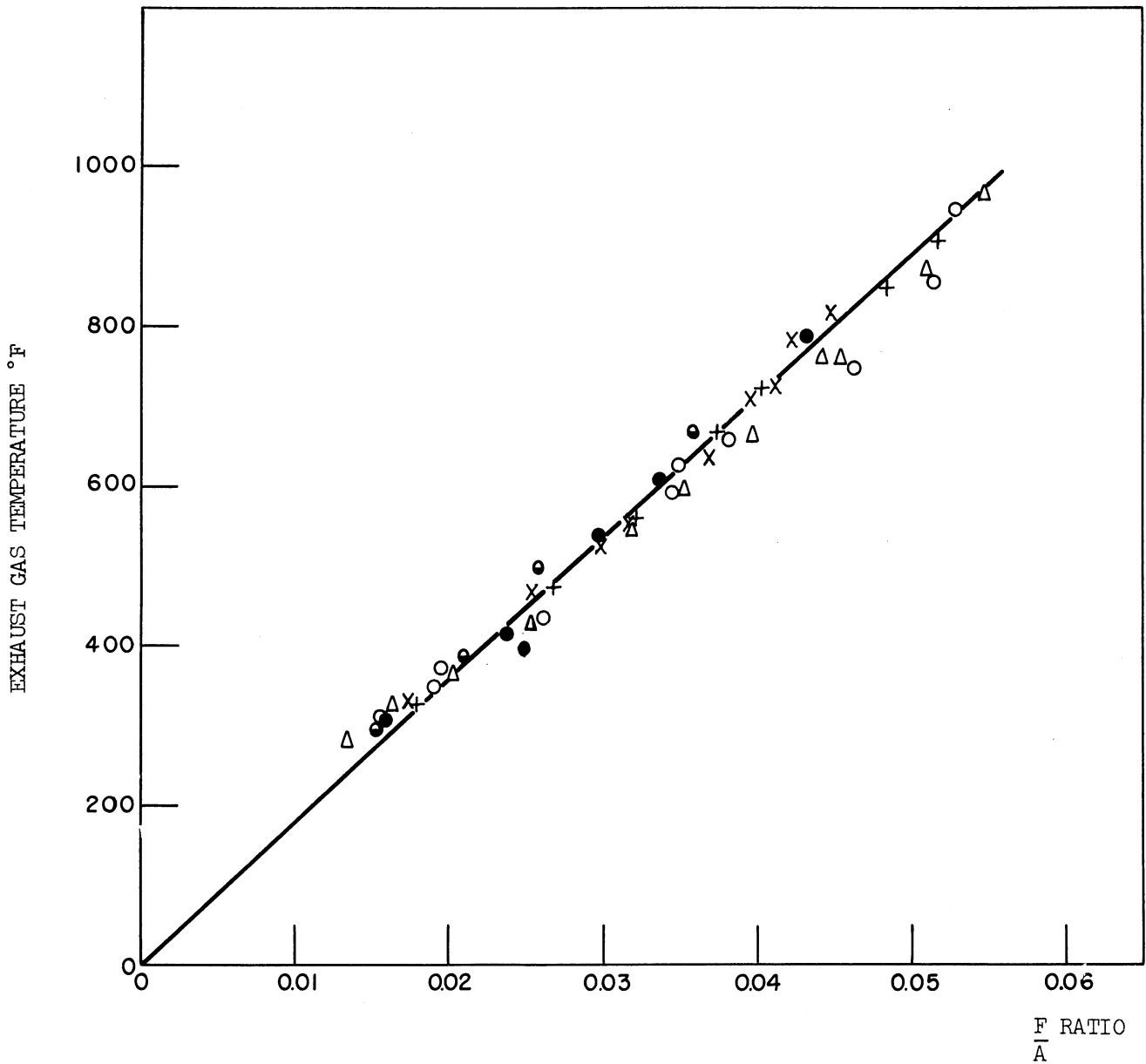


FIGURE 31

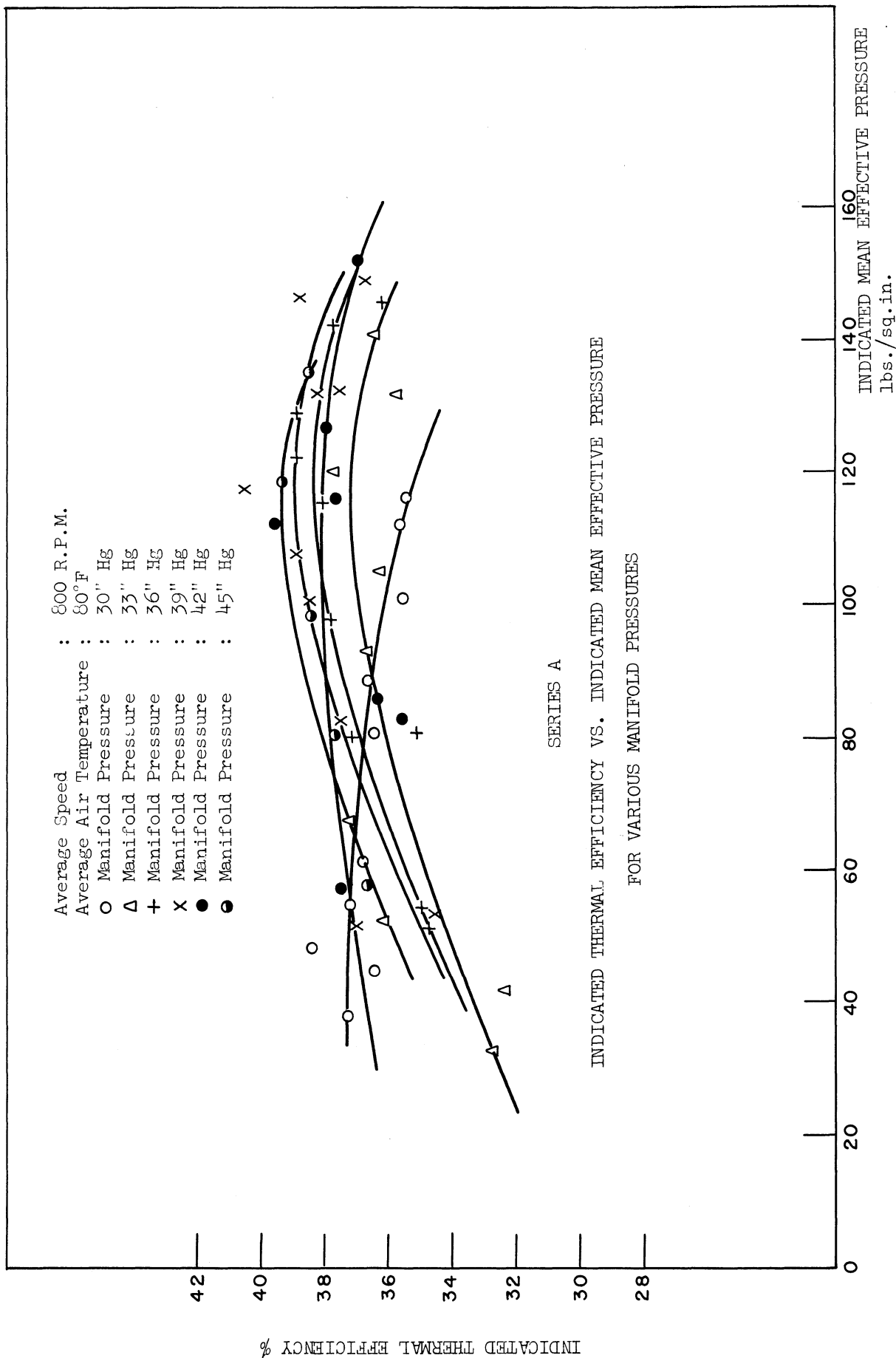


FIGURE 32

SERIES B

BRAKE MEAN EFFECTIVE PRESSURE VS. $\frac{F}{A}$ RATIO
FOR VARIOUS INTAKE AIR TEMPERATURES

Average Speed : 1200 R.P.M.
Average Air Pressure : 36" Hg
○ Intake Air Temperature: 80°F
X Intake Air Temperature: 140°F
+ Intake Air Temperature: 200°F

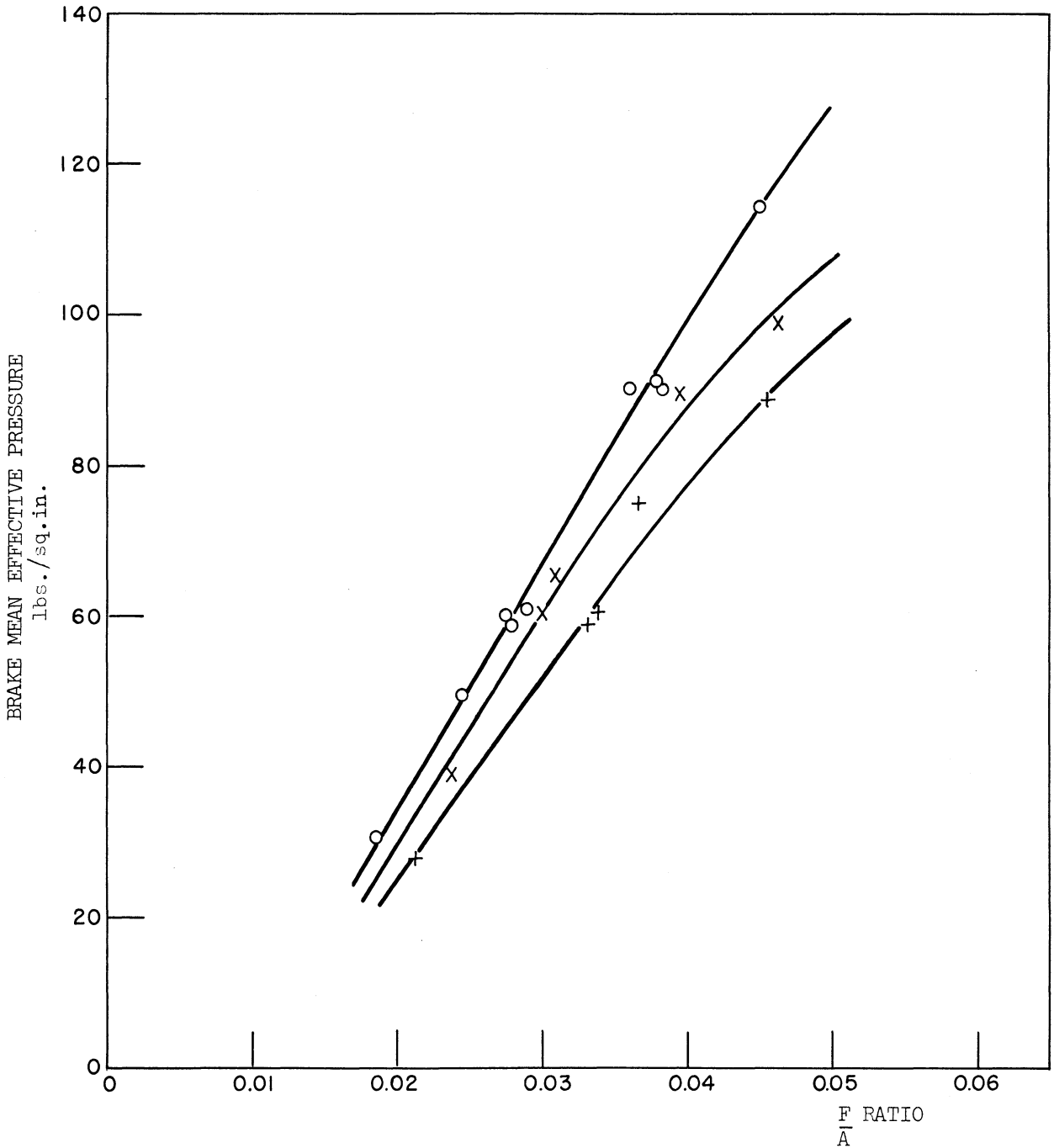


FIGURE 33

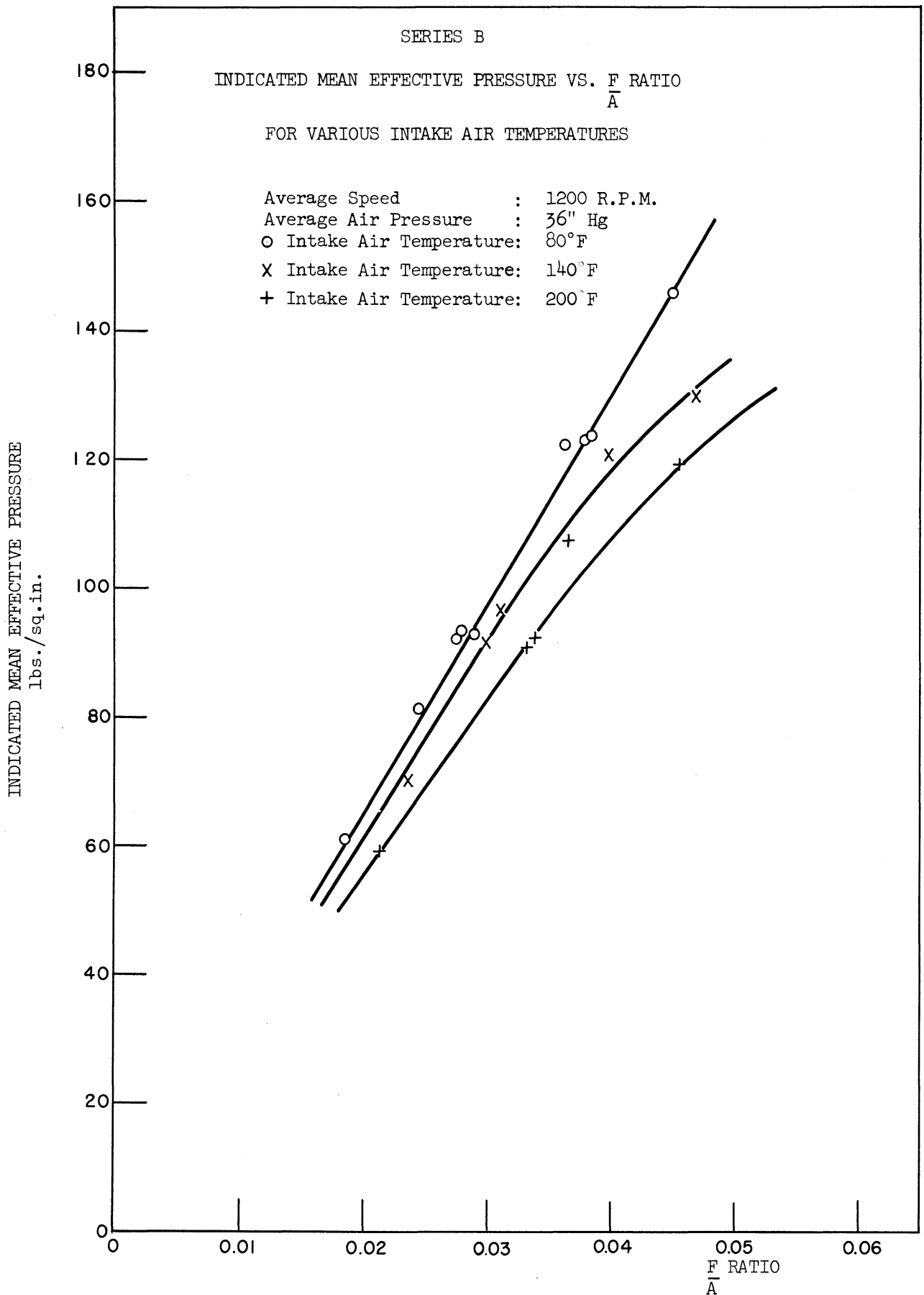


FIGURE 34

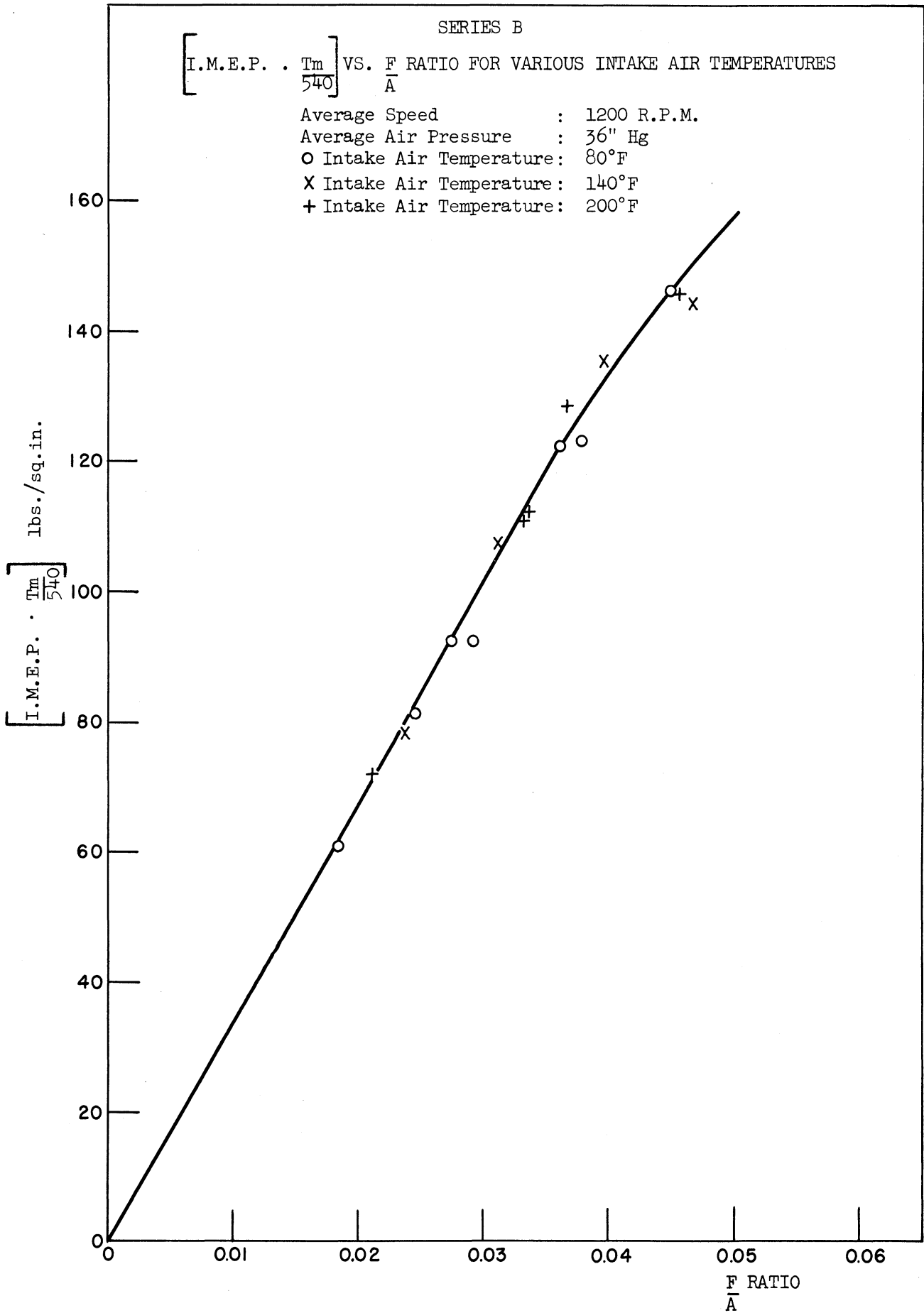


FIGURE 35

SERIES B

BRAKE SPECIFIC FUEL CONSUMPTION VS $\frac{F}{A}$ RATIO FOR

VARIOUS INTAKE AIR TEMPERATURES

Average Speed : 1200 R.P.M.

Average Air Pressure : 36" Hg

○ Intake Air Temperature : 80°F

× Intake Air Temperature : 140°F

+ Intake Air Temperature : 200°F

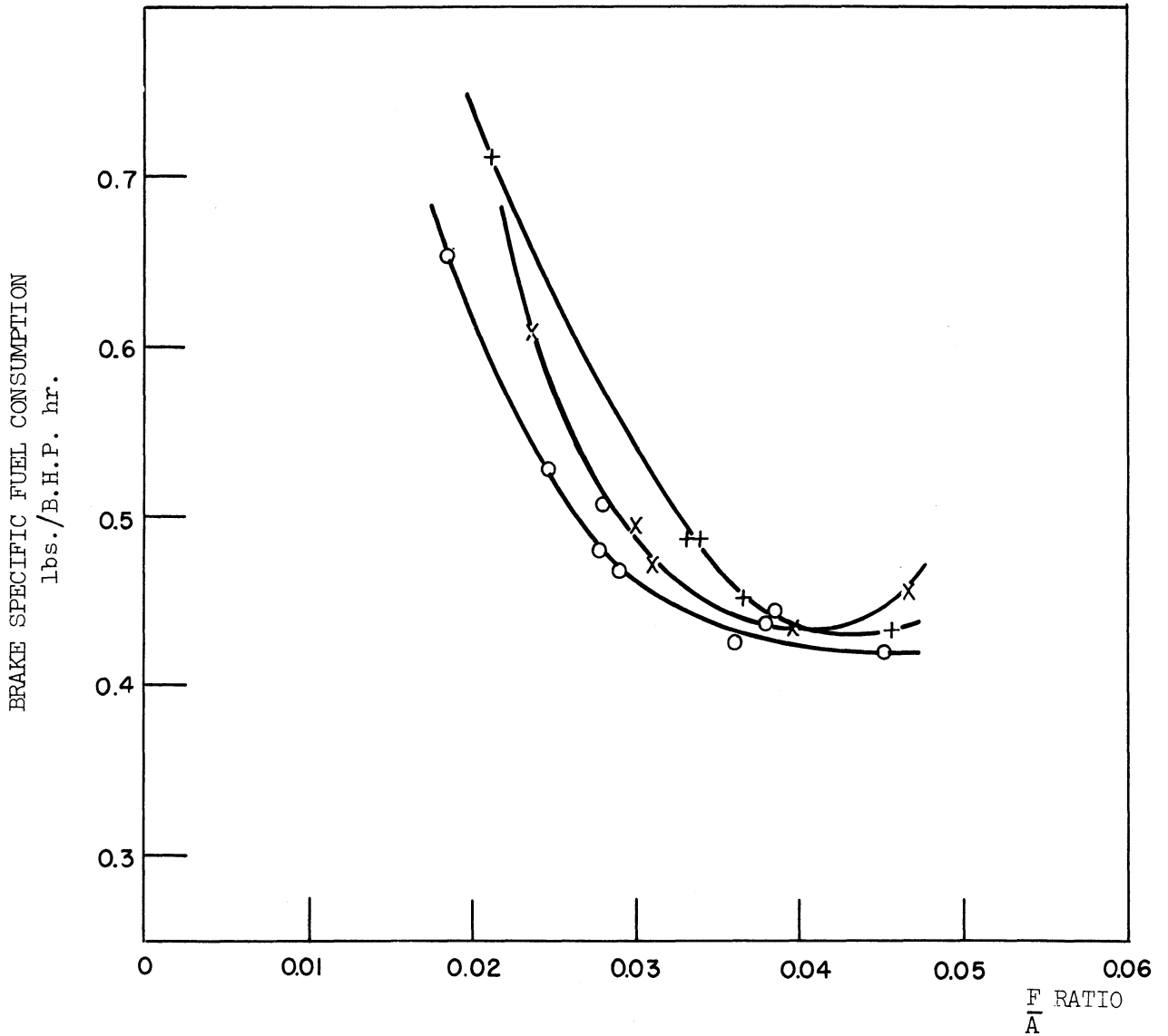


FIGURE 36

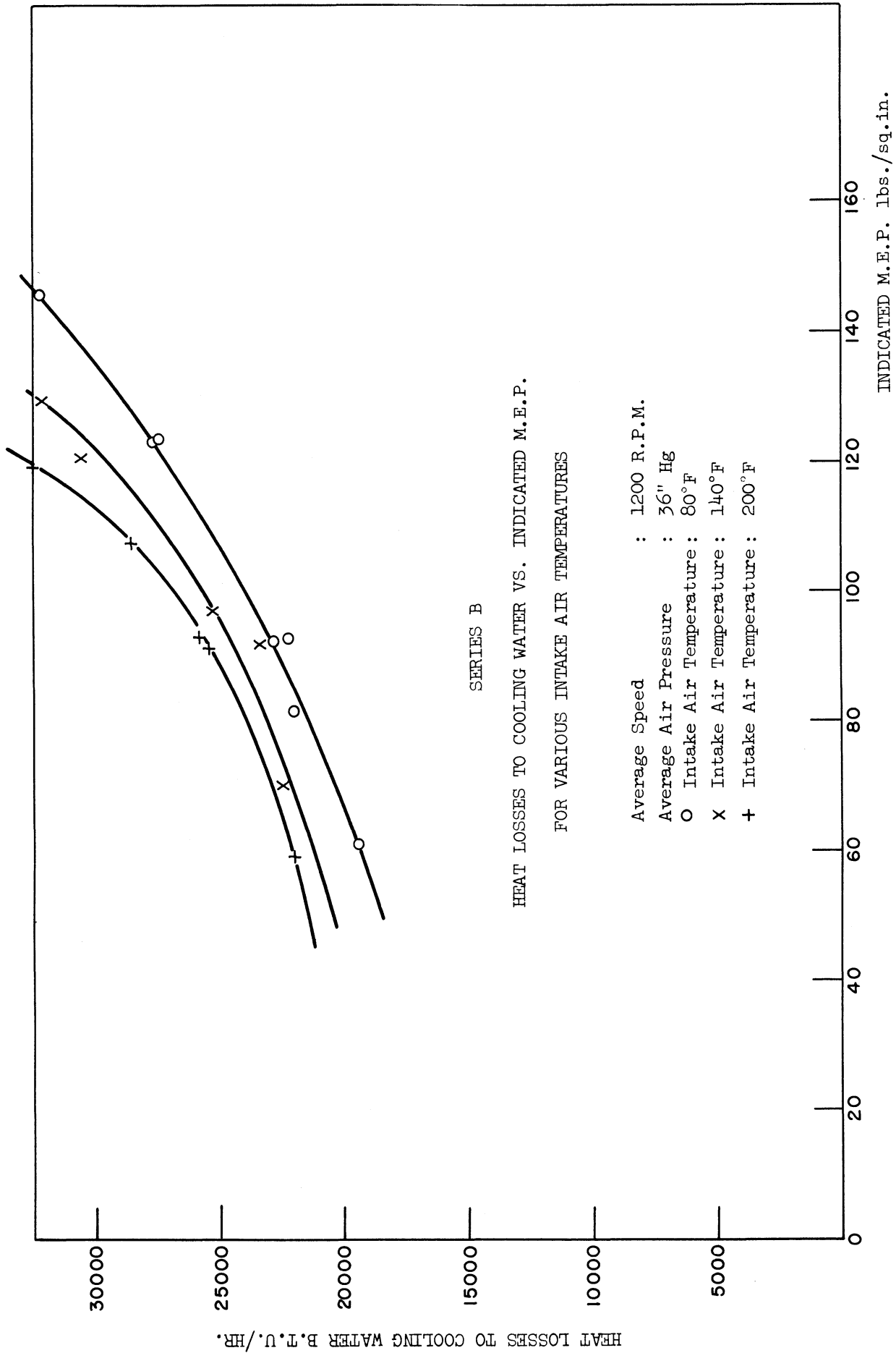


FIGURE 37

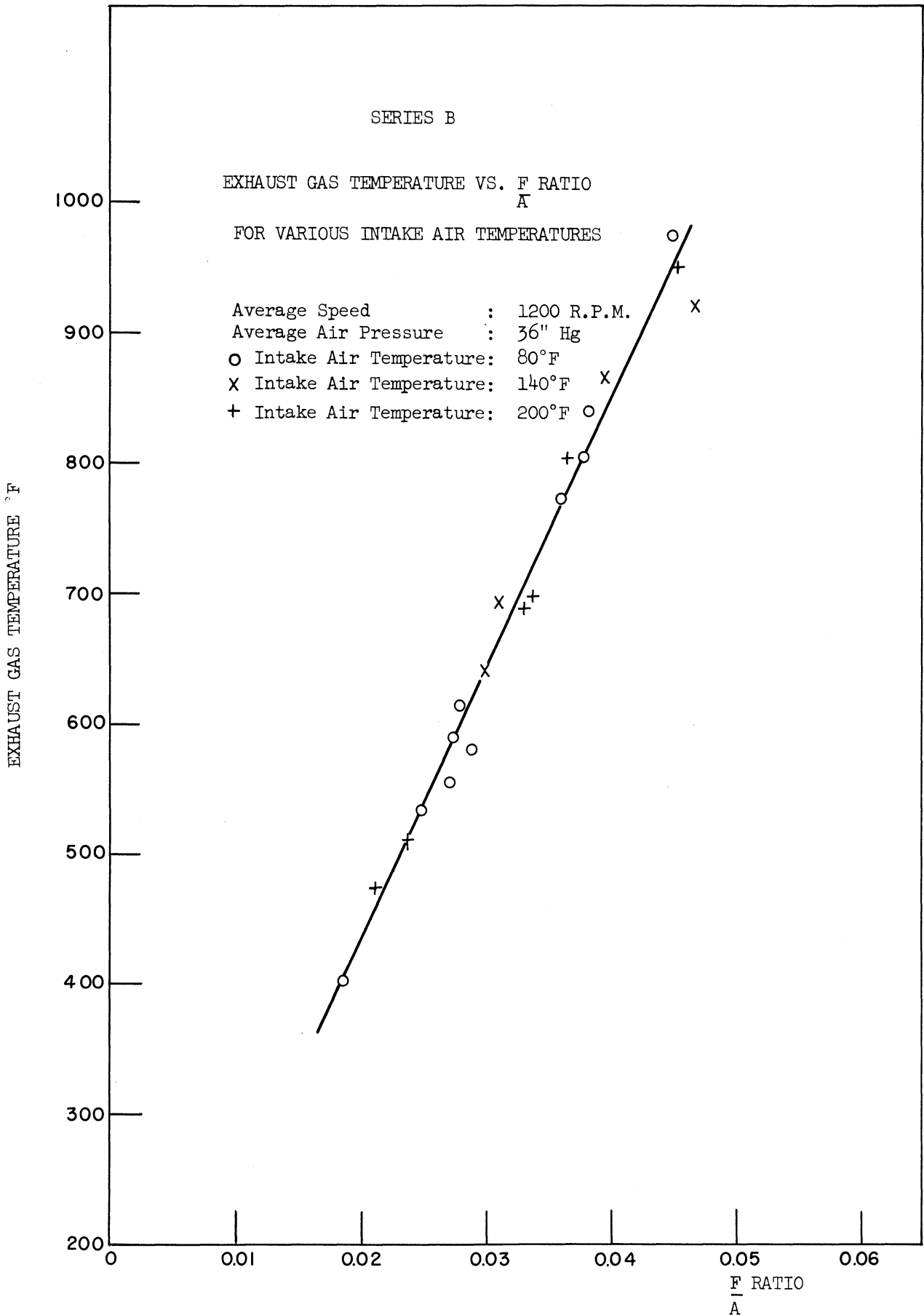


FIGURE 38

VI. DISCUSSION OF EXPERIMENTAL RESULTS

Series A. Runs At Variable Manifold Pressures:

Effect of $\frac{F}{A}$ ratio on B.M.E.P. for Various Manifold Pressures, Figure 24:

The B.M.E.P. of the engine increases with increasing $\frac{F}{A}$ ratios and supercharging pressures. The increase in the power output is mainly due to the increase in the amount of fuel used by the engine. This can be achieved either by increasing the fuel-air ratio at a constant intake manifold pressure, or by increasing the intake manifold pressure at constant fuel-air ratio. However, the power output obtained by using equal amounts of fuel at high manifold pressures is more than that obtained if the same amount were to be used without supercharging; therefore it would be better to increase the output by pressure charging rather than by increasing the $\frac{F}{A}$ ratio. This fact is illustrated by cross plotting the lines of constant fuel consumption per hour on the same figure. These lines show also that supercharging results in a rise in the B.M.E.P. up to a limiting pressure of about 40" Hg, beyond which there is no further increase; eventually there is a decrease. Some factors which might affect this limiting pressure are the fuel injection system design and timing, type of combustion chamber, and the inlet and exhaust valve timing.

Effect of $\frac{F}{A}$ ratio on I.M.E.P. at Various Manifold Pressures, Figure 25:

The engine I.M.E.P. curves follow the same shape as those for the B.M.E.P. But a sharp rise in the I.M.E.P. is noticed by comparing the atmospheric aspirated output with that obtained at

33" Hg manifold pressure. This is mainly due to the better scavenging efficiency resulting from any slight supercharging.

The sharp rise in power output is not noticed in the B.M.E.P. curves, due to the relatively poor mechanical efficiency of the engine at low supercharging pressures.

[I.M.E.P. x $\frac{14.7}{P_m}$ x $\frac{T_m}{540}$] vs $\frac{F}{A}$ ratio for Various Manifold Pressures, Figure 26:

It is noticed that practically all the points of figure (25) are well correlated by a single curve except for some of the runs at naturally aspirated conditions. This departure from the common curve is due to the poor scavenging efficiency of the engine at these conditions. From this figure it can be concluded that for any fuel-air ratio the power output varies in direct proportion to the weight of the air used by the engine.

B.S.F.C. vs $\frac{F}{A}$ for Various Manifold Pressures, Figure 27:

The better brake specific fuel consumption of the supercharged engine is due to its higher mechanical and indicated thermal efficiencies. Also, as will be shown later, the heat rejected to the cooling water is less, thus more of the fuel heat is left to be converted into net engine output.

Mechanical Efficiency vs $\frac{F}{A}$ ratio for Various Manifold Pressures, Figure 28:

The mechanical efficiency of the supercharged engine is higher than that of the naturally aspirated engine simply because the mechanical losses increase very little with increased engine output and percentage-wise become much smaller.

Heat Losses to Cooling Water vs $\frac{F}{A}$ ratio for Various Manifold Pressures, Figure 29:

The heat losses to the cooling water increase with both fuel-air ratio and intake manifold pressures. These losses consist of the direct heat loss from the gases, and the friction heat. The direct heat loss is a function of the gas temperature and the coefficient of heat transfer, which is discussed in detail in Chapter VII.

Heat Losses to Cooling Water vs I.M.E.P. for Various Manifold Pressures, Figure 30:

From this figure it can be concluded that the heat losses at any supercharging pressure and $\frac{F}{A}$ ratio is a function of the I.M.E.P., all other conditions being held constant. Also for the same B.M.E.P. the heat losses decrease with supercharging.

Exhaust Gas Temperatures vs $\frac{F}{A}$ ratio for Various Manifold Pressures, Figure 31:

The exhaust gas temperature is mainly a function of the fuel-air ratio, but for manifold pressures higher than 33 inches mercury the exhaust gas temperatures are slightly higher than those for normal atmospheric operation. This is due to the relatively higher temperatures reached in the cycle with boosted inlet pressures.

Indicated Thermal Efficiency vs I.M.E.P. for Various Manifold Pressures, Figure 32:

Although the points for each manifold pressure do not fall on a smooth curve, yet from the average curves drawn for the different pressures it can be noticed that at high I.M.E.P.'s the thermal efficiency of the supercharged engine is better than that of the naturally aspirated engine. This is due to the fact that the supercharged engine operates at a lower fuel-air ratio and with a better scavenging efficiency. The slight drop in the indicated thermal efficiency of

naturally aspirated engine, as the I.M.E.P. increases, is caused by the high fuel-air ratios used and the high gas temperatures reached at the beginning of the compression stroke.

Series B. Runs At Constant Manifold Pressures And Variable Manifold Temperatures:

Effect of $\frac{F}{A}$ ratio on Power Output for Various Manifold Temperatures, Figures 33 and 34:

The heating of the air before it enters the engine causes a drop in the power output. This is mainly due to the drop in the mass-rate of air flow caused by an increase in the specific volume of the air at the time the inlet valve closes.

As the cycle starts from a higher initial temperature the gas temperatures throughout the cycle are increased, causing some decrease in the indicated thermal efficiency, accompanied by an increase in the heat lost to the cooling water.

$\left[\frac{\text{I.M.E.P.} \times \frac{T_M}{540}}{\frac{F}{A}} \right]$ vs $\frac{F}{A}$ ratio at Various Manifold Temperatures, Figure 35:

This figure confirms the conclusion reached from figure (26), i.e., with constant $\frac{F}{A}$ ratio, the power output varies in direct proportion to the weight of air used by the engine.

B.S.F.C. vs $\frac{F}{A}$ for Various Manifold Temperatures, Figure 36:

The poor fuel economy at higher manifold temperatures is caused by the drop in the thermal efficiency as explained in the discussion for figures (33) and (34).

Heat Losses to Cooling Water vs $\frac{F}{A}$ I.M.E.P. ratio for Various Manifold Temperatures, Figure 37:

The heat losses to the cooling water increase with an increase in the manifold temperature. This is due to the high temperatures

and coefficients of heat transfer reached during the cycle.

Exhaust Gas Temperatures vs $\frac{F}{A}$ ratio for Various Manifold
Temperatures, Figure 38:

The exhaust gas temperature is a function of the fuel-air ratio for all intake manifold temperatures.

VII. HEAT-TRANSFER ANALYSIS OF THE EXPERIMENTAL RESULTS.

The purpose of this analysis is to apply equation [2.14] and [2.17] to calculate the combustion-chamber-wall inside-surface temperature and the thermal loading on the cylinder walls, and to check the values calculated, with those measured. This analysis was made in the following steps:

1. Study of the effect of the manifold pressure and temperature, and the mean piston speed, on the gas mean effective temperature, and coefficient of heat transfer.
 2. Evaluation of some constants for the engine.
 3. Calculation and check on the wall temperature.
 4. Calculation and check on the thermal loading.
1. Effect of P_m , T_m and S on $T_{M.E.}$ and α_M :

$T_{M.E.}$ and α_M are the main factors affecting the process of heat transfer from the gas to the walls. The following procedure was followed to find an equation for them in terms of P_m , T_m , S and the I.M.E.P.

- a. Calculation of the gas pressure all around the cycle from the pictures taken for each run. A sample is shown in figure (20).
- b. Calculation of the gas temperature all around the cycle from the weights of air and fuel consumed for each run.
- c. Substituting in equation [2.1], the values of the pressure and temperature previously calculated, and

the value of the mean piston speed measured during the tests; to get the coefficients of heat transfer.

- d. Plotting the values of α_g against the crank angles, (as in figure 52) and by graphical integration getting the mean value of α_g , known as α_M .
- e. Calculating $\alpha_g T_g$ all around the cycle by multiplying the instantaneous value of α_g with the corresponding value of T_g .
- f. Plotting $\alpha_g T_g$ against the crank angles, (as in figure 53) and by graphical integration getting the mean value of $\alpha_g T_g$, known as $(\alpha_g T_g)_M$.
- g. Using equation [2.8] to calculate the gas mean effective temperature over the cycle.

A sample of these calculations is given in Appendix A. This cycle-analysis was made for many runs covering the following range:

P_m :	28.75	-	44.25	inches Hg.
T_m :	73.5	-	204	°F
S :	11.3	-	17.97	$\frac{\text{ft.}}{\text{sec.}}$
N :	775	-	1231	R.P.M.

The results of these analyses are given in tables (16) and (17).

The best correlation for these results was found by plotting:

$$\frac{\alpha_M}{\sqrt[3]{S}} \times \frac{1}{\sqrt[3]{P_m T_m}} \quad \text{vs} \quad \text{I.M.E.P. Figure (39)}$$

and

$$\frac{\alpha_M}{\sqrt[3]{S}} \cdot \frac{T_{M.E.}}{T_m} \quad \text{vs} \quad \text{I.M.E.P. Figure (40)}$$

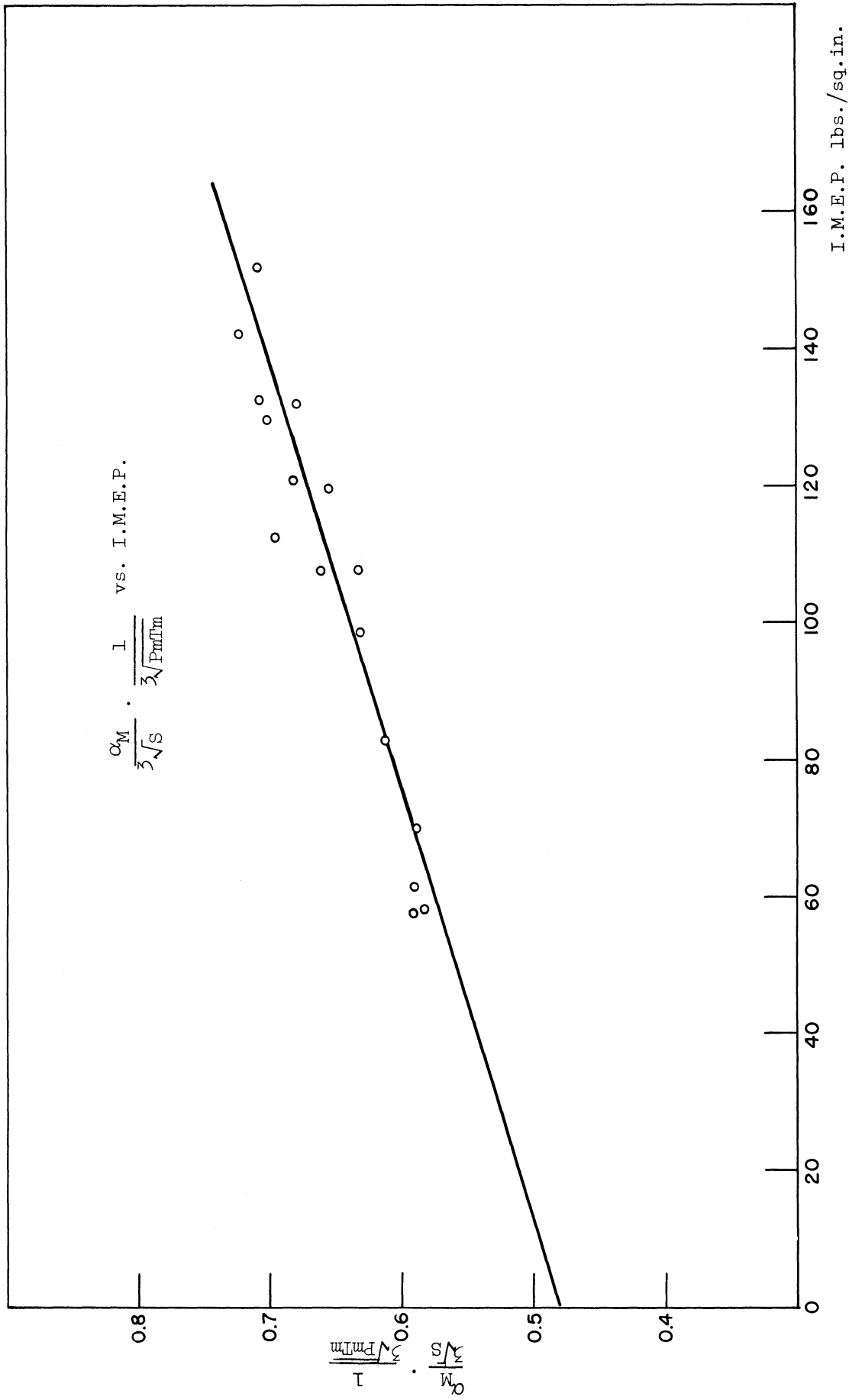


FIGURE 39

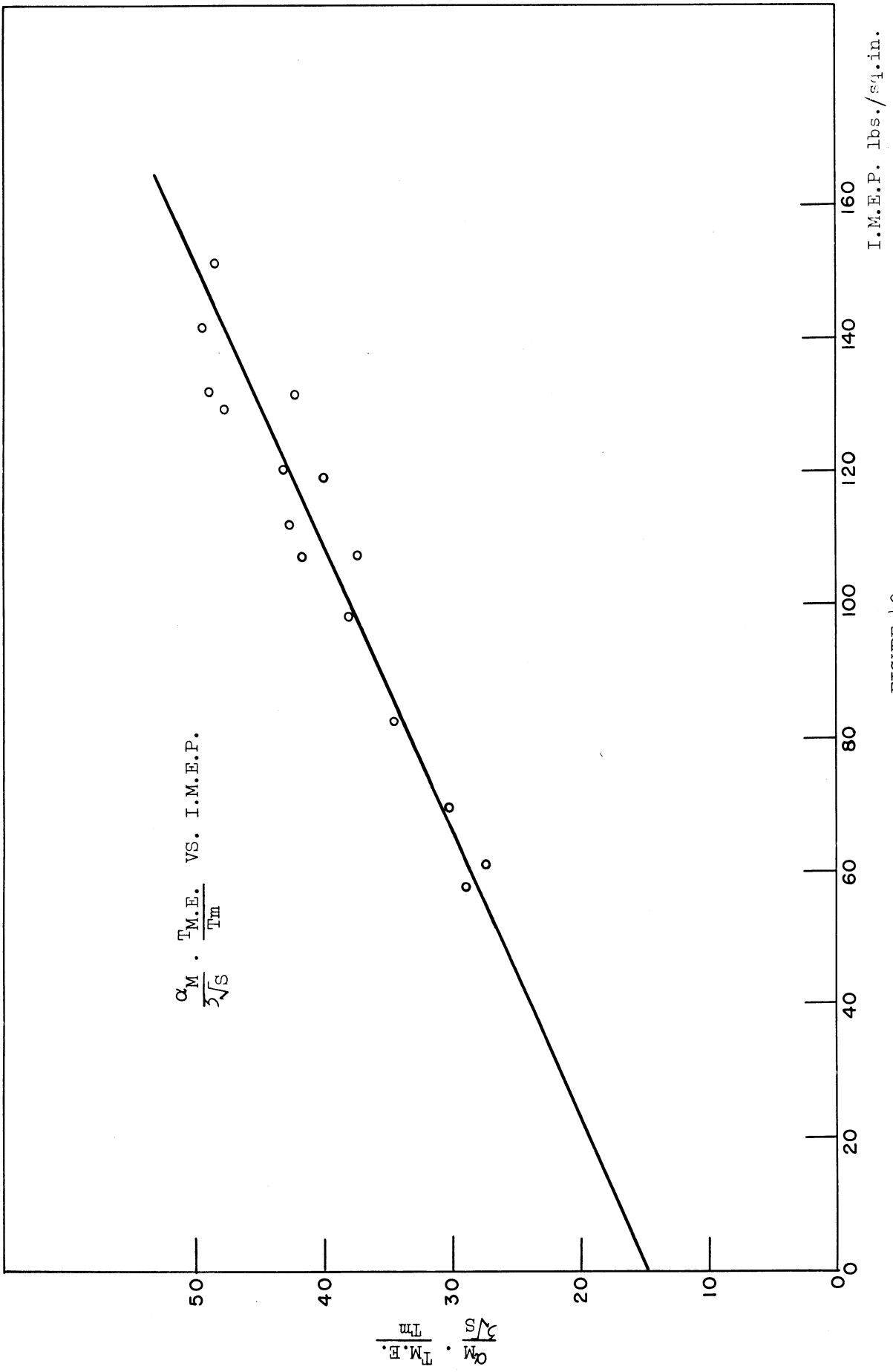
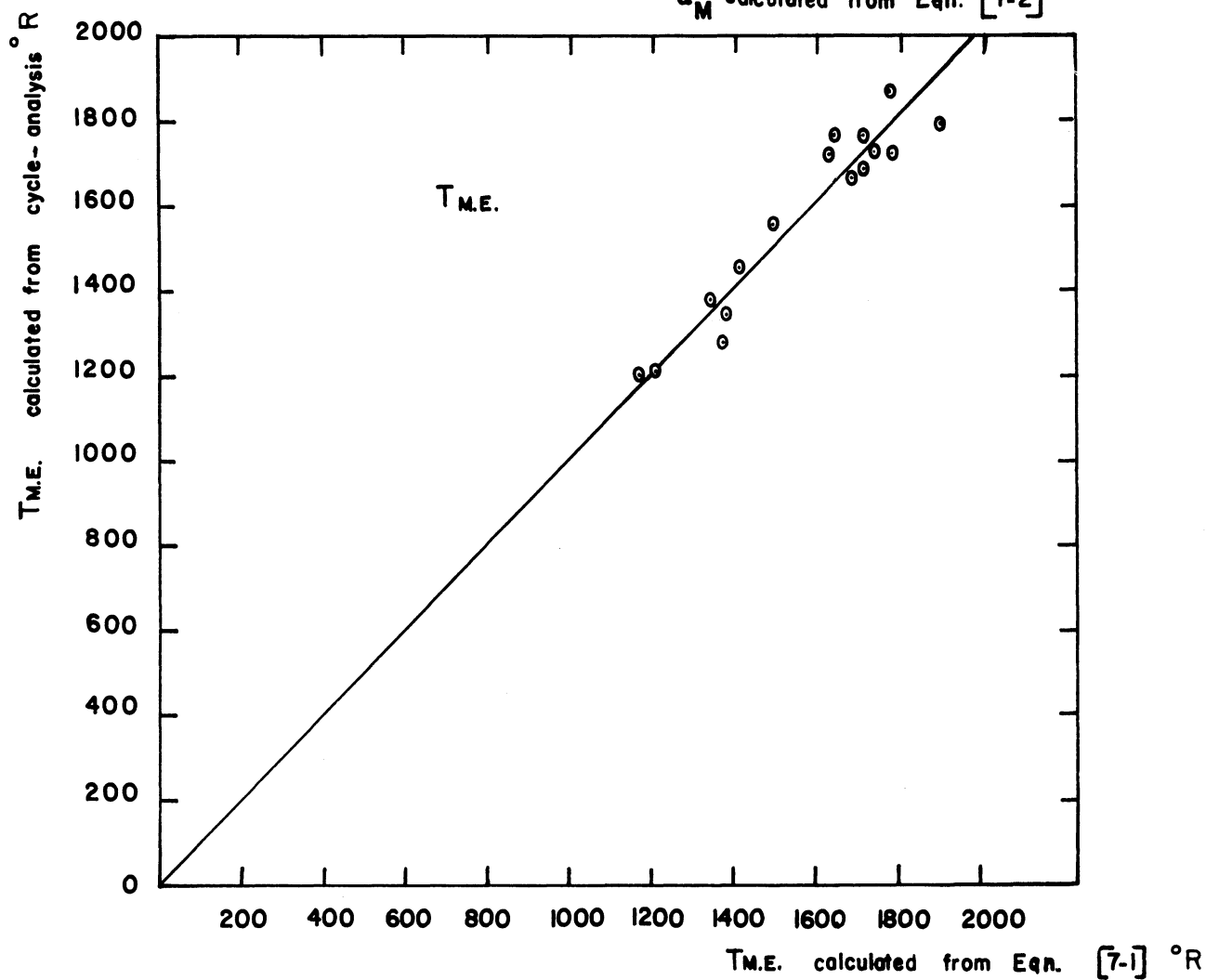
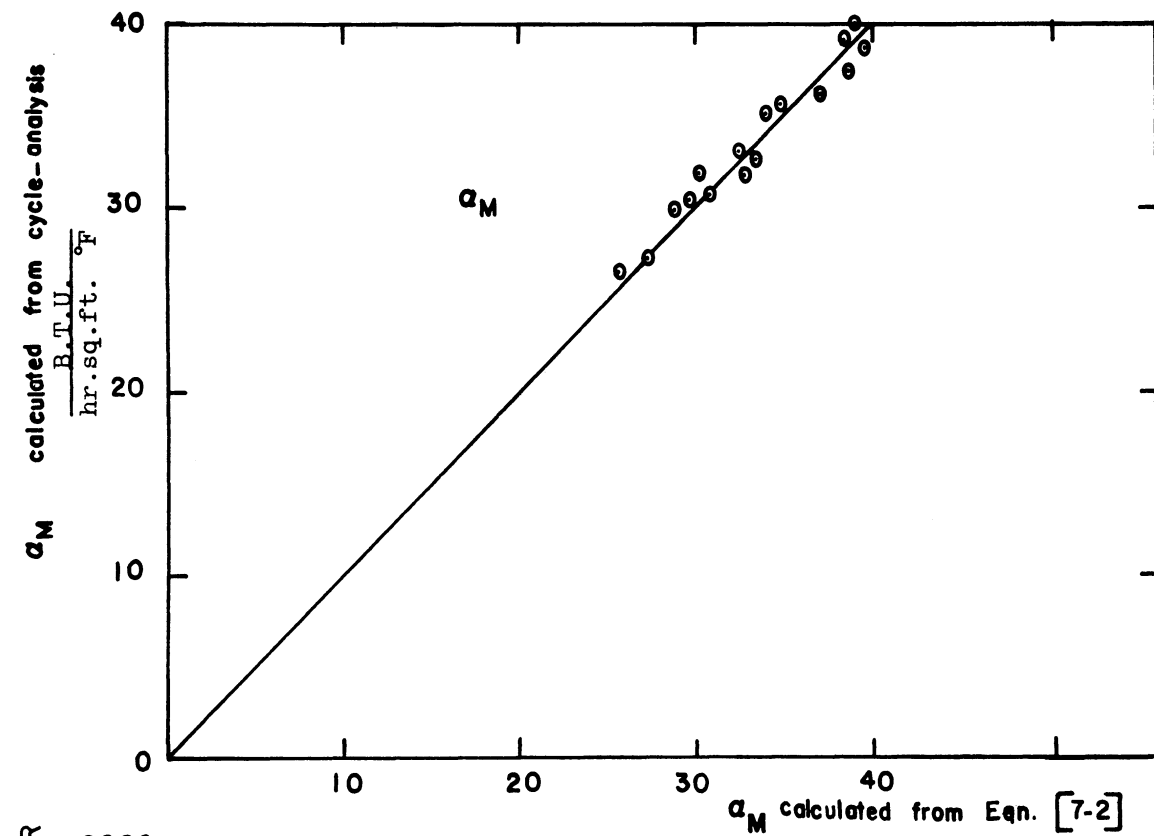


FIGURE 40



The relation between these variables were found to be of the form:

$$\frac{\alpha_M}{\sqrt[3]{S}} \times \frac{1}{\sqrt[3]{P_m T_m}} = 0.48 + 0.00157 \text{ (I.M.E.P.)}$$

and

$$\frac{\alpha_M}{\sqrt[3]{S}} \times \frac{T_{M.E.}}{T_m} = 14.71 + 0.233 \text{ (I.M.E.P.)}$$

From these two equations:

$$T_{M.E.} = \frac{T_m}{\sqrt[3]{P_m T_m}} \frac{14.71 + 0.233 \text{ (I.M.E.P.)}}{0.48 + 0.00157 \text{ (I.M.E.P.)}} \quad [7.1]$$

and

$$\alpha_M = \sqrt[3]{S} \times \sqrt[3]{P_m T_m} [0.48 + 0.00157 \text{ (I.M.E.P.)}] \quad [7.2]$$

The values of $T_{M.E.}$ and α_M calculated from equations [7.1] and [7.2] were plotted against those found from the cycle-analysis, in figure (41). The maximum errors in $T_{M.E.}$ and α_M are 7.2% and 4.5% respectively.

2. Evaluation of Some Constants for the Engine:

a. Constant C in equation [2.11].

$$C = \frac{\alpha_c}{\left(\frac{W_c}{\mu}\right)^{0.6} \left(\frac{c\mu}{k}\right)^{0.4}} \quad [7.3]$$

W_c was taken from the cooling water flow rates measured for each run.

$c, \mu,$ and k were evaluated at the average temperature of the cooling water.

α_c was calculated from: Q , the heat carried by the cooling water; $A_{W.C.}$, the area of cylinder

walls in contact with coolant; and the mean temperature difference between the walls and the water. The area of cylinder walls, $A_{W.C.}$ consists of:

- (i) the barrel area
- (ii) the combustion chamber area
- (iii) the exhaust manifold area enclosed in the cylinder head.

The mean average temperature for these areas was calculated by adding the multiple of each part by its temperature, then averaging the sum over the whole area.

Since the flow of water past the surface was a mixture of parallel, counter, and cross flows; α_c was calculated in terms of the arithmetic mean temperature difference between the surface and water.

A sample of these calculations is shown in Appendix B. The results of similar calculations for other runs are tabulated in tables (14) and (15), and were plotted in figure (57).

From figure (57)

$$C \text{ for the engine} = 3.15 \quad [7.4]$$

Thus

$$\alpha_c = 3.15 \left(\frac{W_c}{\mu}\right)^{0.6} \left(\frac{c\mu}{k}\right)^{0.4}$$

b. Area factors for the combustion chamber:

The shape of the combustion chamber is shown in figures (16) and (17). To evaluate the area factors,

the combustion chamber wall was considered as cylindrical, with an inside diameter of 2 inches, and an outside diameter of 2.56 inches.

Mean area factor a_m :

$$a_m = \frac{A_g}{A_m} = \frac{2}{2.28} = .877 \quad [7.5]$$

Cooling area factor a_c :

$$a_c = \frac{A_g}{A_c} = \frac{2}{2.56} = .782 \quad [7.6]$$

Wall equivalent thickness x :

$$\begin{aligned} x &= r_m \ln \frac{D_2}{D_1} \\ &= \frac{2 + 2.56}{2} \times \ln \frac{2.56}{2} = 0.282 \text{ inch.} \end{aligned} \quad [7.7]$$

c. Thermal conductivity of the metal:

$$k_w^* = 27 \frac{\text{B.T.U.}}{\text{hr. sq. ft. } \left(\frac{^\circ\text{F}}{\text{ft}}\right)} \quad [7.8]$$

3. Calculation and Check on the C. Chamber Wall Temperatures:

By equating the values of: $T_{M.E.}$, equation [7.1]; α_M , equation [7.2] and the constants, equations [7.4] to [7.8]; in equation [2.14]; the values of $T_{w.g.}$ could be calculated from: $P_m, T_m, S, I.M.E.P., W_c, T_{c3}$ and the engine constants.

Using this procedure, $T_{w.g.}$ was calculated for several runs covering the following range of operating conditions:

* (Reference No. 33)

P_m :	28.75	-	44.7	inches Hg.
T_m :	72	-	204	°F
N :	789	-	1769	R.P.M.
I.M.E.P.:	51.3	-	152	$\frac{\text{lbs.}}{\text{sq. in.}}$

The results are shown in tables (18) and (19). These calculated temperatures were compared with those measured by the thermocouple and were found to be in fair agreement. The maximum error is 12.7%. The values measured are shown also in tables (18) and (19). The deviation of the measured temperature from that calculated is due to the following experimental errors:

a. The time when the picture of the wall-temperature was taken was not exactly the same time the cooling water was measured, during which a change in the water temperature might have taken place. The change in the water temperature was within $\pm 5^\circ\text{F}$ during the run and a result of the thermostatic control being not very sensitive.

b. The indicated mean effective pressure used to calculate the wall temperature was evaluated by adding the friction load measured at the end of the day's tests to the brake load for the run. The friction load, being a function of the lubricating oil temperature, was not constant for all the runs of the day, and caused an error in the indicated mean effective pressure.

c. The cooling water temperature T_{c3} , used in the calculations, being lower than the water temperature near the combustion chamber wall, caused the majority of the calculated wall temperatures to be lower than those measured by the thermocouple.

4. Calculation and Check on the Thermal Loading:

By equating the values of: $T_{M.E.}$, equation [7.1]; α_M , equation [7.2] and the constants, equations [7.4] to [7.8]; in equations [2.16], [2.17] and [2.18]; the thermal loading could be calculated from P_m , T_m , S , I.M.E.P., W_c , $(\frac{T_{c1} + T_{c3}}{2})$ and the engine constants. Equation [2.18] was simplified by assuming the mean effective area equal to the mean arithmetic area, therefore

$$\begin{aligned} A_M &= A_{c.ch.} + A_{P.T.} + \frac{A_{bore}}{2} \\ &+ \left[\frac{A_{int.man.} + A_{exh.man.}}{4} \right] \\ &= 32.5 + 15.9 + 37.1 + \left[\frac{34.3 + 26.6}{4} \right] = 100.7 \text{ sq.ins.} \end{aligned}$$

The results of the calculations are shown in Tables (20) and (21) as compared with the measured cooling water heat losses. The calculated thermal loadings are in general less than the measured heat losses which included part of the friction heat. The deviation between the calculated and measured values increases at high engine speeds due to the increase in the friction heat. Another factor which affects the measured losses is the heat losses from the outer surface of the engine.

VIII. INVESTIGATION ON THE EFFECT OF AFTERCOOLING

To investigate the effect of aftercooling on the operation of the turbocharged engine, the following calculations were made, based on the conclusions reached from the experimental work. The power output, the maximum temperature of the piston crown and the intensity of thermal loading were calculated for different degrees of aftercooling.

The arrangement on which calculations were based is shown diagrammatically in figure (42). The conditions of operation assumed were as follows:

Compressor Efficiency	=	80%
Atmospheric Conditions		
Pressure	=	30 inches Hg.
Temperature	=	80 °F
Drop in air pressure between the compressor outlet and the engine manifold	=	0.5 $\frac{\text{lb}}{\text{sq. in.}}$
Aftercooler Effectiveness	=	0, 50% and 100%

Method of Calculation:

a. Calculation of I.M.E.P. for different aftercooler effectiveness:

After being compressed in the turbocharger, the air will be at a temperature higher than that of the atmospheric. If an aftercooler is used between the compressor and the engine, the air temperature will drop to a value depending on the aftercooler effectiveness; and the power output will be greatly affected. It was found from the results of the experiments that the I.M.E.P. is inversely proportional to the absolute manifold temperature. Thus the power of the turbocharged engine, at

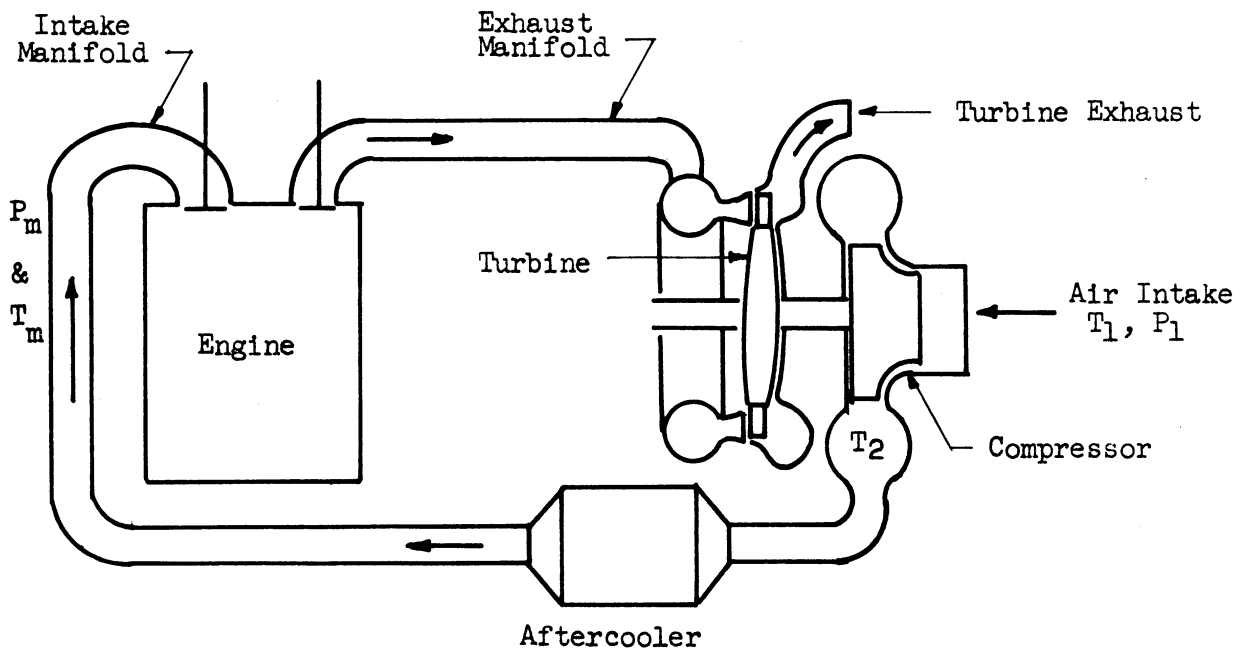


Figure 42. Diagram of Assumed Turbocharged C.I. Engine

any manifold pressure and with any aftercooler effectiveness, can be calculated by multiplying the I.M.E.P. from the test-results [figure (25)] by a temperature factor $\frac{540}{T_m}$. The test-results were considered (after being corrected to a manifold temperature of 540°R and manifold pressures of 30 to 45" Hg) to represent the engine performance with 100% aftercooling effectiveness. These are shown in figure (43).

b. Calculation of the maximum temperature of the piston-crown:

For these calculations, the following constants were evaluated:

x : the thickness of the piston-crown = $\frac{3}{4}$ inch

k_w : coefficient of thermal conductivity = 27 $\frac{\text{B.T.U.}}{\text{hr. sq. ft. } (\frac{^\circ\text{F}}{\text{ft}})}$

T_a : the temperature of the hot gases in the crank case = 160°F

α_a : coefficient of heat transfer from the bottom of the crown to the hot gases, calculated from equation [2.1]

with

$$P = 14.7$$

$$T = 460 + 160 = 620 \text{ R}$$

$$S : \text{ at 800 R.P.M.} = 11.672 \frac{\text{ft.}}{\text{sec.}}$$

$$\therefore \alpha_a = 12.22 \frac{\text{B.T.U.}}{\text{hr. sq. ft. } ^\circ\text{F}}$$

c. Calculation of Intensity of thermal loading on the combustion chamber walls:

This was calculated from equation [2.15]:

$$q = U (T_{M.E.} - T_c)$$

U was calculated from equation [2.16] by using equations [7.2], [2.11] and [7.4] to [7.8] and $T_{M.E.}$ was calculated from equation [7.1].

A sample calculations for the effect of aftercooling on the engine performance, piston-crown maximum temperature and intensity of thermal loading is given in Appendix G. The results of similar calculations are given in tables (22), (23) and (24). They are plotted in the following figures:

Figures (43), (60) and (61) for 100% aftercooler effectiveness.

Figures (44), (62) and (63) for 50% aftercooler effectiveness.

Figures (45), (64) and (65) for 0% (No aftercooling).

Figures (43), (44) and (45) illustrate the engine performance for conditions of, constant manifold pressures, piston-top maximum temperatures, and intensities of thermal loads. The curves for the indicated mean effective pressures were calculated from figure (43) and the temperature factors. The other curves are cross plots from figures (60) to (65).

At the end of this chapter calculations were made, to find the effect of aftercooling on the intensity of thermal loading, piston maximum temperature, and power output, at a manifold pressure of 45 inches Hg. The results are shown in figures (46), (47), (48), (49), and (50).

Discussion of Results of Calculations:

Performance with 100% aftercooler effectiveness, figure 43:

This figure shows that increasing the power output at any supercharging pressure causes an increase in both the thermal loads and the piston temperatures. This is mainly due to the increase in the amount of fuel used per cycle. Also, the thermal loading and piston temperatures at high supercharging pressures and low $\frac{F}{A}$ ratios, are lower than those at lower supercharging pressures and higher $\frac{F}{A}$

Performance With 100% Aftercooler Effectiveness

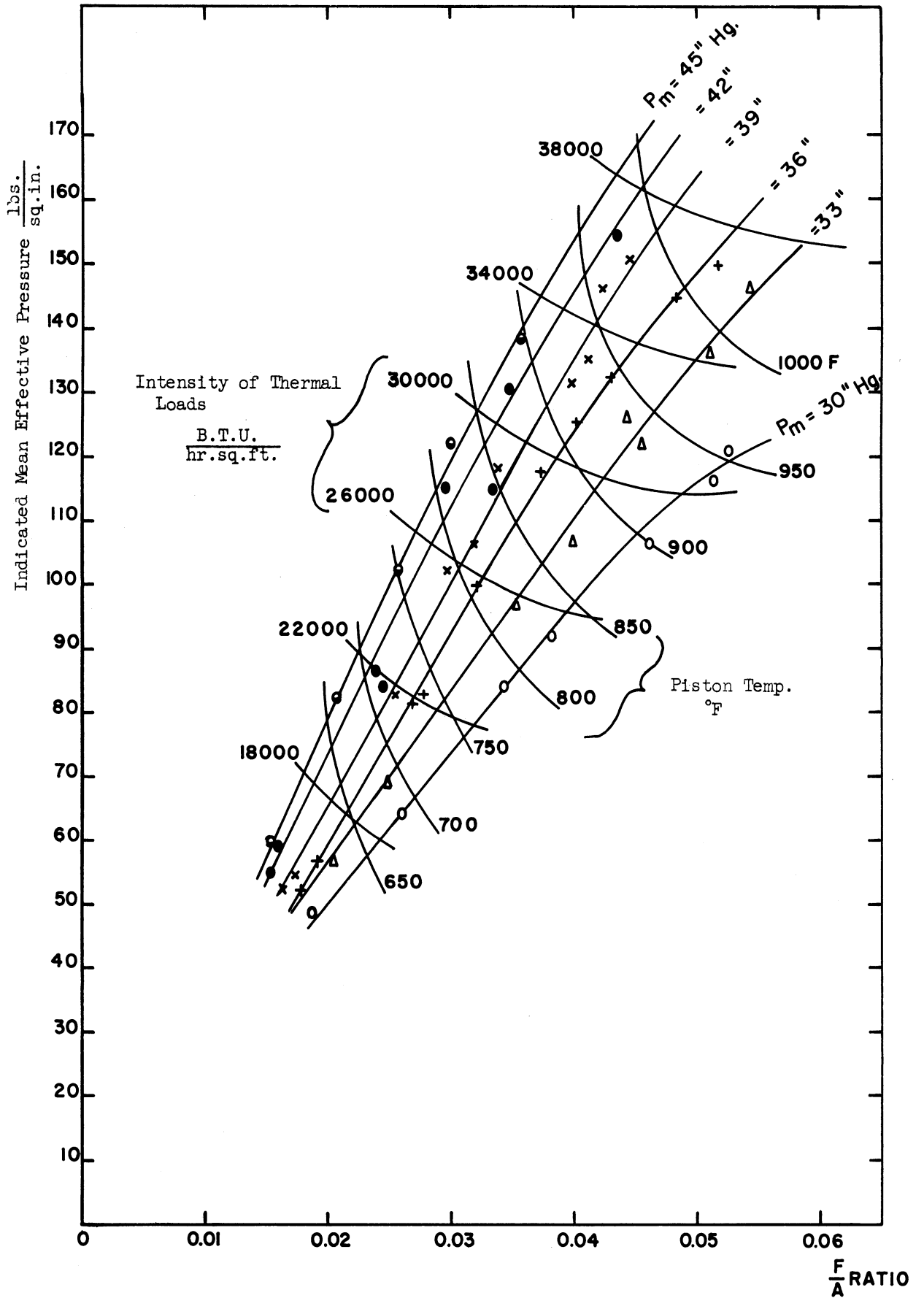


FIGURE 43

Performance With 50% Aftercooler Effectiveness

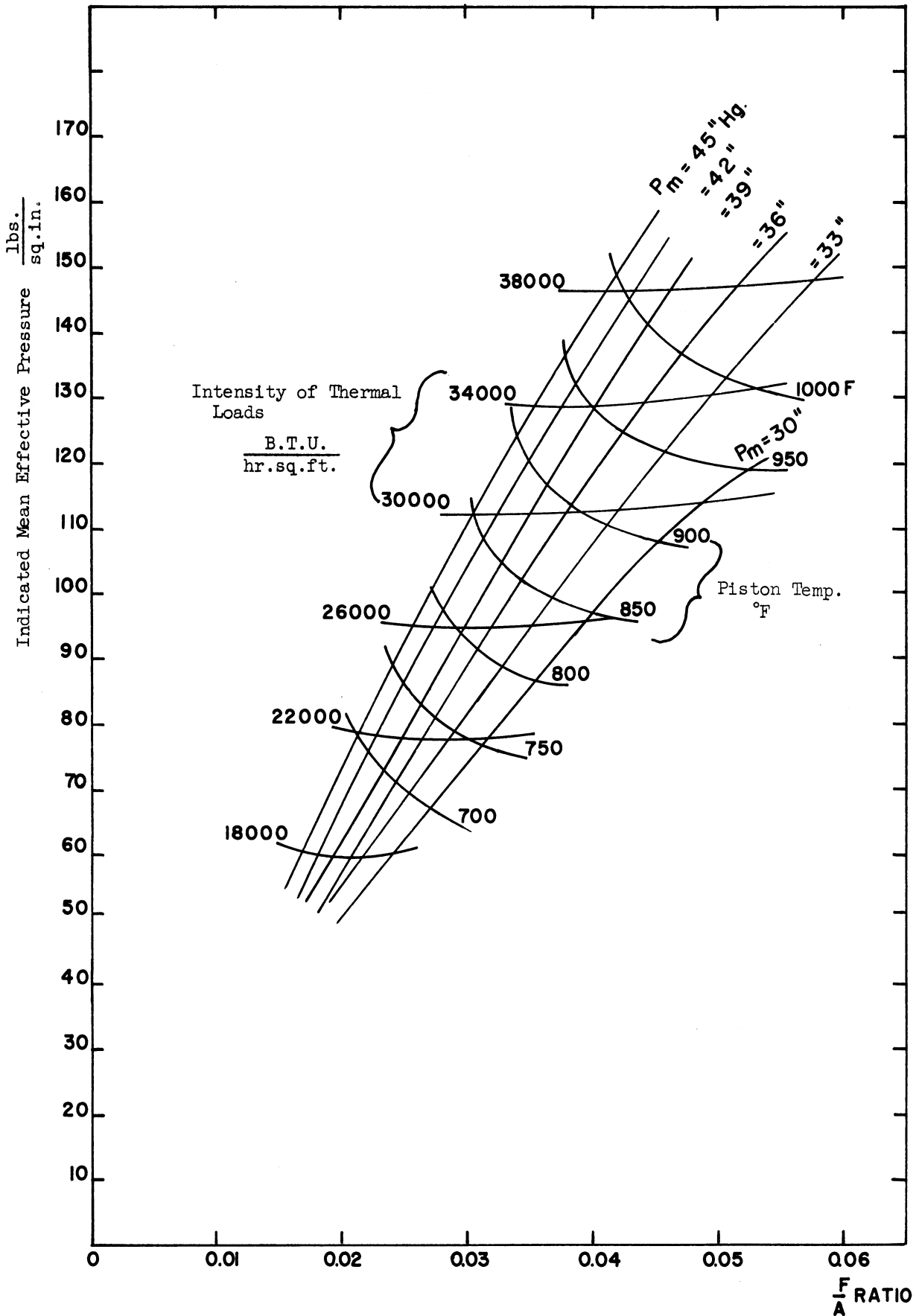
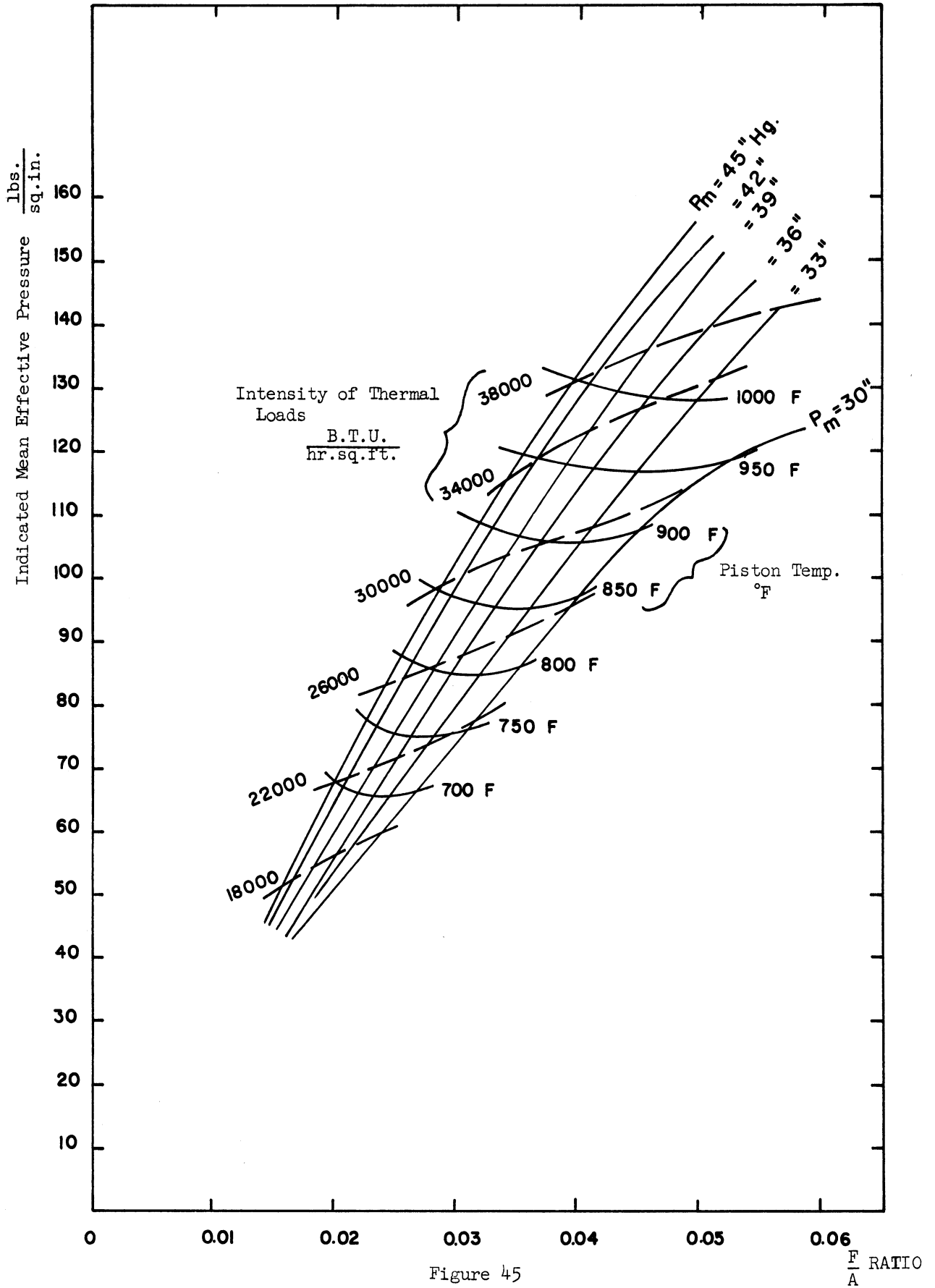


FIG. 44

Performance Without Aftercooling



ratios. Thus for equal power outputs it is better to operate the engine at the highest supercharging pressure, with the lowest $\frac{F}{A}$ ratio. This will also result in the best fuel economy.

Performance with 50% aftercooler effectiveness, figure 44:

This figure also shows that for any supercharging pressure, both the thermal loads and piston temperatures increase with the power output. In this case, the thermal loads are functions, only, of the I.M.E.P., for any $\frac{F}{A}$ ratio or supercharging pressure. For the same I.M.E.P. the piston maximum temperature drops with supercharging. For any brake mean effective pressure, it is still better to run the engine at the highest supercharging pressure, since the thermal loading and the piston temperature will be lower.

Performance with 0% aftercooler effectiveness, figure 45:

Here also both the thermal loads and piston temperatures increase with the engine output.

Although the same I.M.E.P. could be reached at lower $\frac{F}{A}$ ratios with supercharging, yet the thermal loads increased and the piston maximum temperatures remained constant. However, for equal brake mean effective pressures, the piston temperatures will decrease with supercharging and the thermal loading will remain constant.

For the turbocharged engines without aftercooling we have to choose either, the low efficiency and low mechanical loading of the low supercharged engine, or the higher efficiency but higher mechanical loading of the higher supercharged engine, without any

reduction in its thermal loading.

Engine performance with different aftercooling effectiveness, figures 46 and 47:

Both figures are for a constant manifold pressure of 45 inches mercury, with the variables arranged in two different ways. It can be noticed that:

a. The wall temperatures and intensities of thermal loading are functions, not only of the fuel-air ratios, but also of the after-cooler effectiveness. For the same fuel-air ratio the thermal loading and wall temperatures decrease with better aftercooling.

b. The fuel-air ratio required for equal power outputs decreases with better aftercooling, resulting in a reduction in the thermal loading and piston temperatures, and a better thermal efficiency.

Effect of aftercooling on thermal loading:

Figure (48a) shows the intensity of thermal loading with different supercharging pressures and aftercooling effectiveness, for an indicated mean effective pressure of 150 lbs. per sq. in., with a compressor efficiency of 80%.

Curve for $\epsilon = 100\%$:

This is the case of supercharging and cooling to a constant manifold temperature of 540°R, (this is the condition of series "A" of the experiments). The thermal loading decreases continuously with supercharging. That is to say, the increasing manifold pressure has a reducing effect on the thermal loading, a pressure rise of 15" Hg causes a reduction of 7.7%. This reduction is not noticed in figure (30), because the manifold temperature and the friction heat were not constant for all the runs.

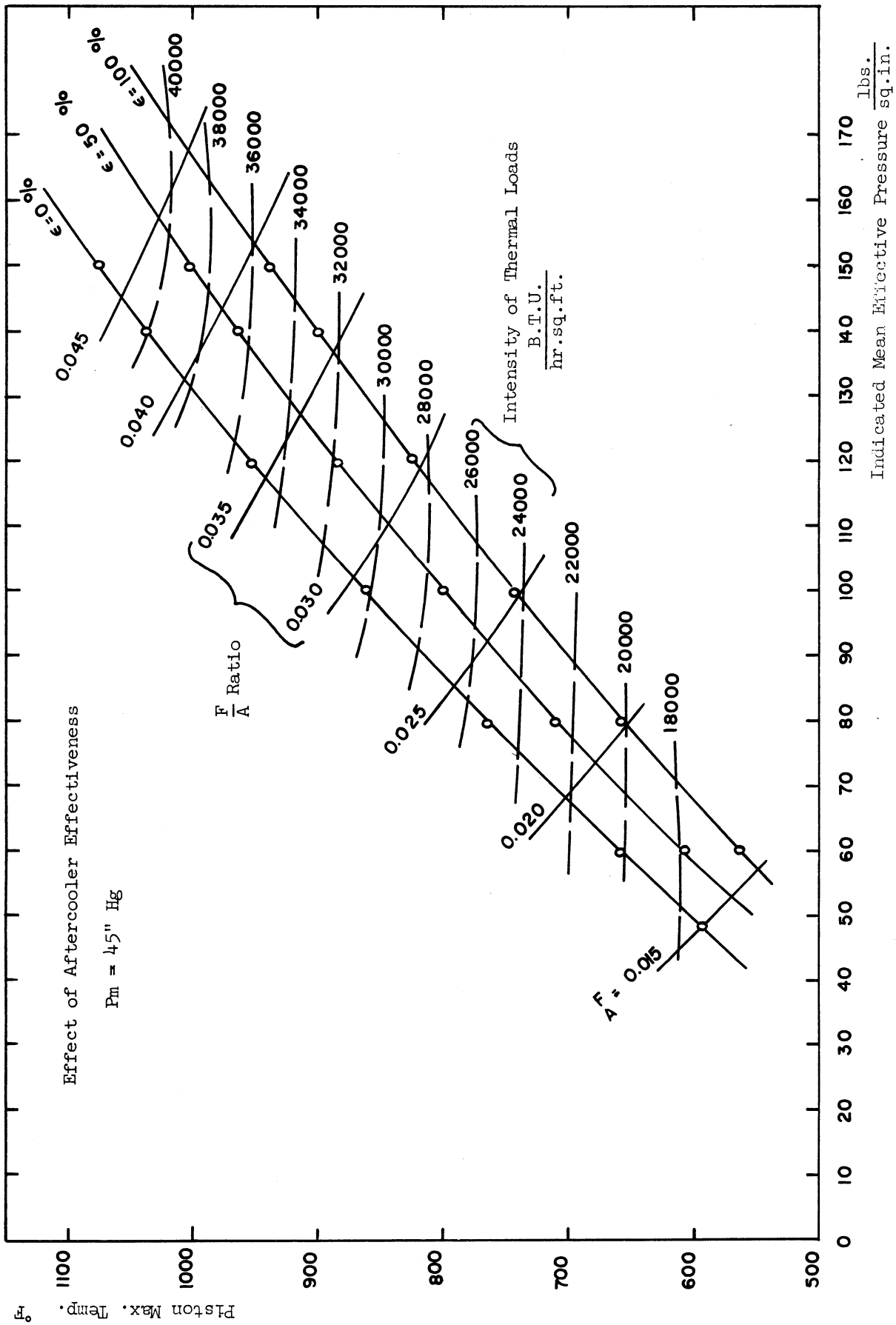
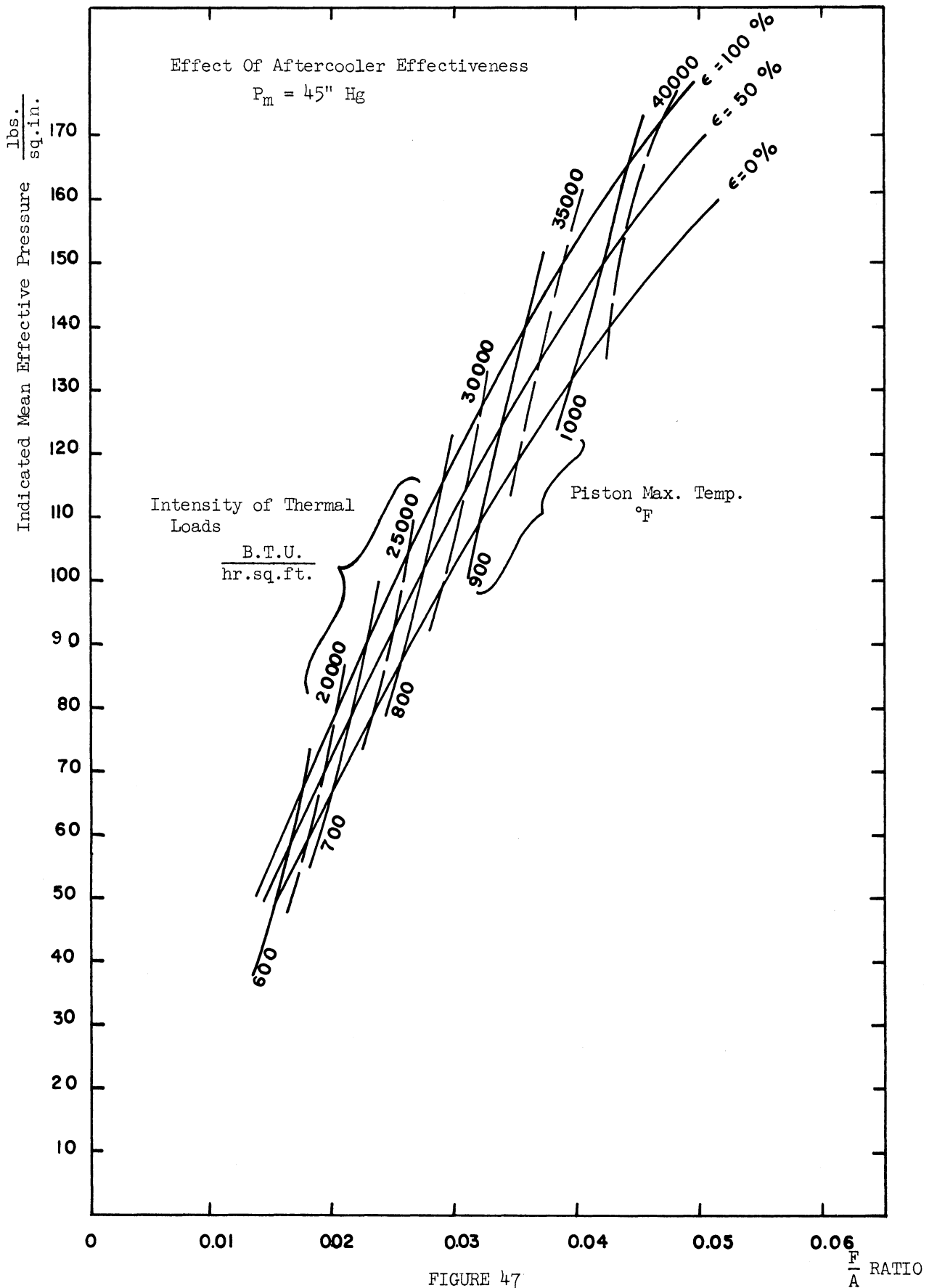


FIGURE 46



Curve for $\epsilon = 0\%$:

This curve represents the case of turbocharging without aftercooling. The increase in the thermal loading with turbocharging is mainly due to the increase in the manifold temperature, which has a much greater effect on increasing the thermal loading than the reducing effect of the increasing manifold pressure. An increase of 87°F due to turbocharging to 45" Hg, caused an increase of 22.5% in the thermal loading.

If the thermal loading was not permitted to increase by turbocharging, it would be better to use low manifold pressures with better aftercooling than to use high manifold pressures and poor aftercooling. In other words, an effective cooler which might cause a bigger pressure drop, will be preferred to an ineffective cooler which will cause a small pressure drop.

It is worthwhile to add here that, for an I.M.E.P. of 140, the thermal loading on the engine-cooling-system, is reduced by an amount twice as much as the heat removed from the air in the aftercooler. This is illustrated in figure (50).

Effect of aftercooling on the maximum temperature of the piston-crown

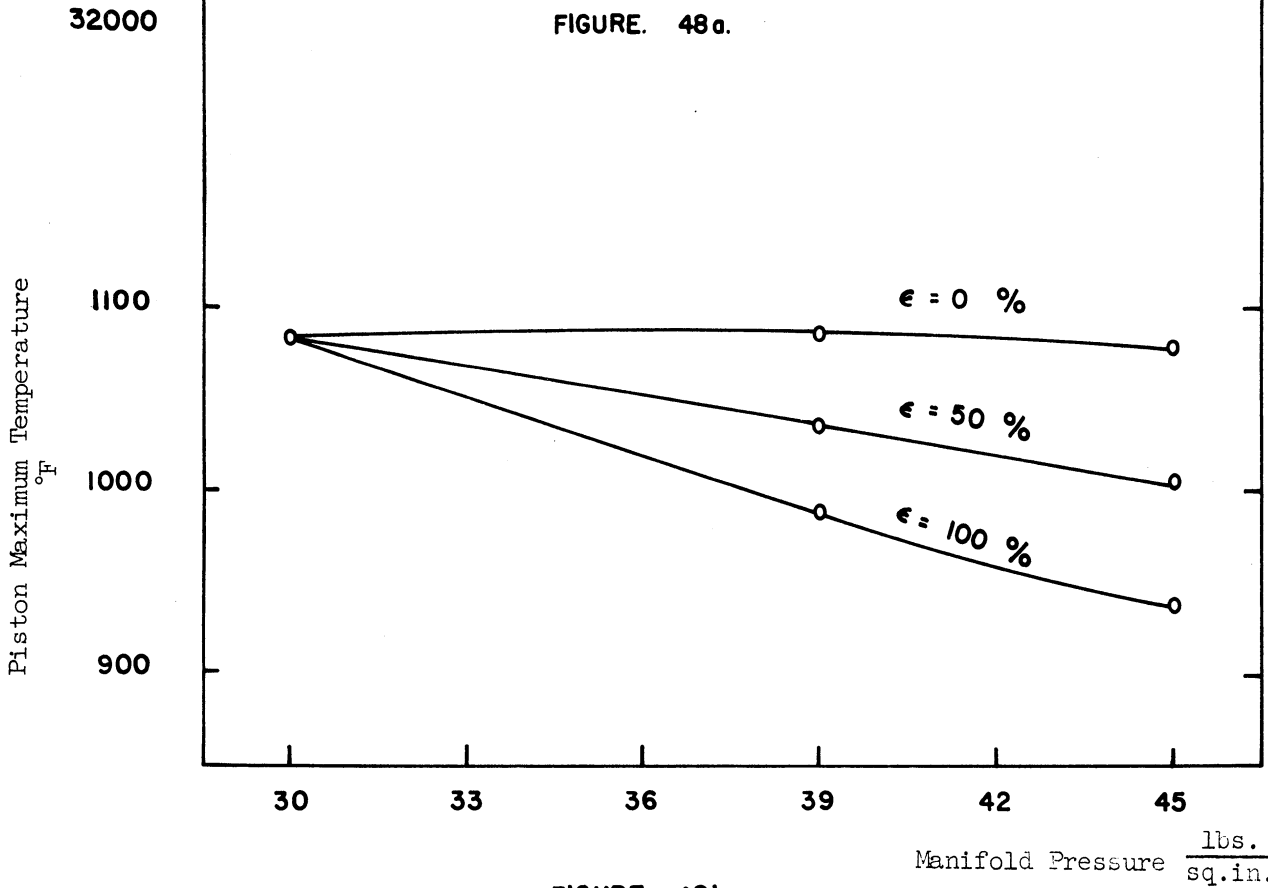
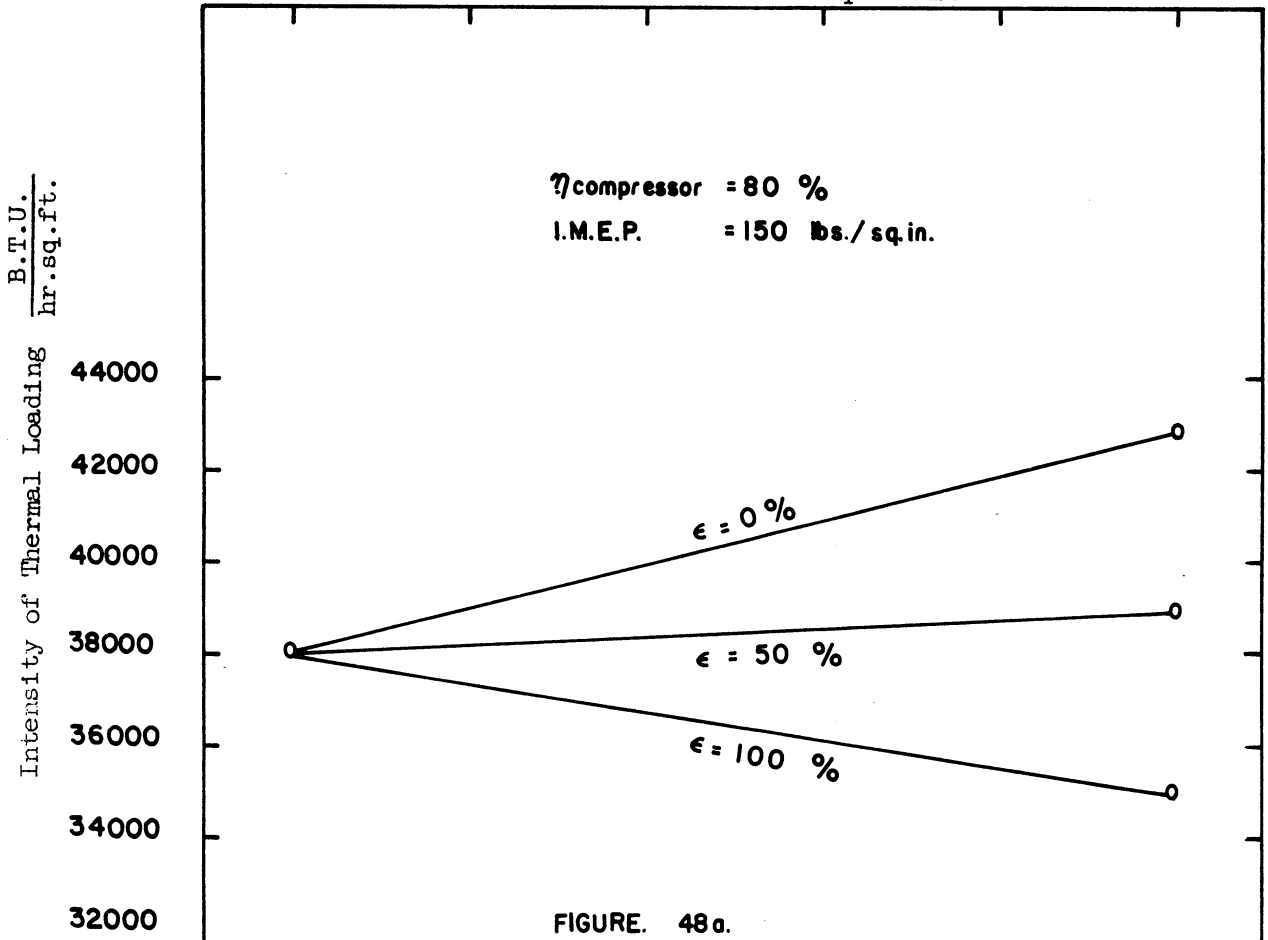
Figure (48,b) shows the piston-crown maximum temperature for different supercharging pressures and aftercooling effectiveness and an indicated mean effective pressure of 150 lbs. per sq. in., with a compressor efficiency of 80%. It indicates that the piston temperature drops with better aftercooling for any supercharging pressure.

Effect of aftercooling on power output:

Figure (49) shows the increase in the power output by supercharging and different degrees of aftercooling.

A horizontal dotted line representing an I.M.E.P. of 129 lbs. per sq. in. was drawn to intersect with the lines of $\epsilon = 0, 50$ and 100% . This line indicated that with better cooling, lower manifold pressures are required to give the same I.M.E.P. This means that, with an air pressure of 45" Hg at the exit from the compressor, it would be better, in the interest of lowering the thermal loading, to use an aftercooler with $\epsilon = 50\%$, which might cause a pressure drop up to 3.8" Hg, rather than to exclude the cooler and keep the pressure at 45" Hg.

Effect of Aftercooling on Intensity of Thermal Loading and Piston Maximum Temperature



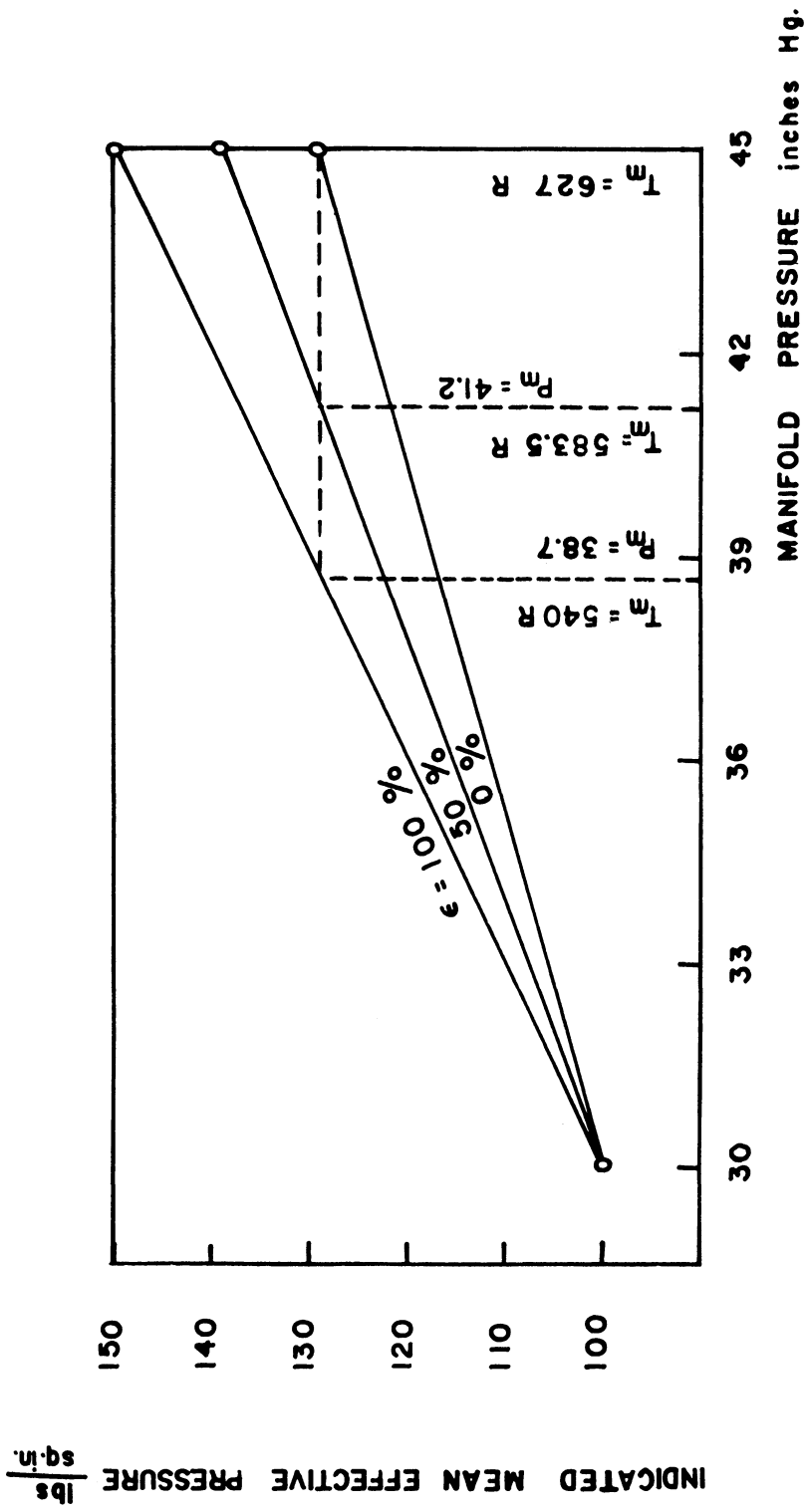


FIG. 49

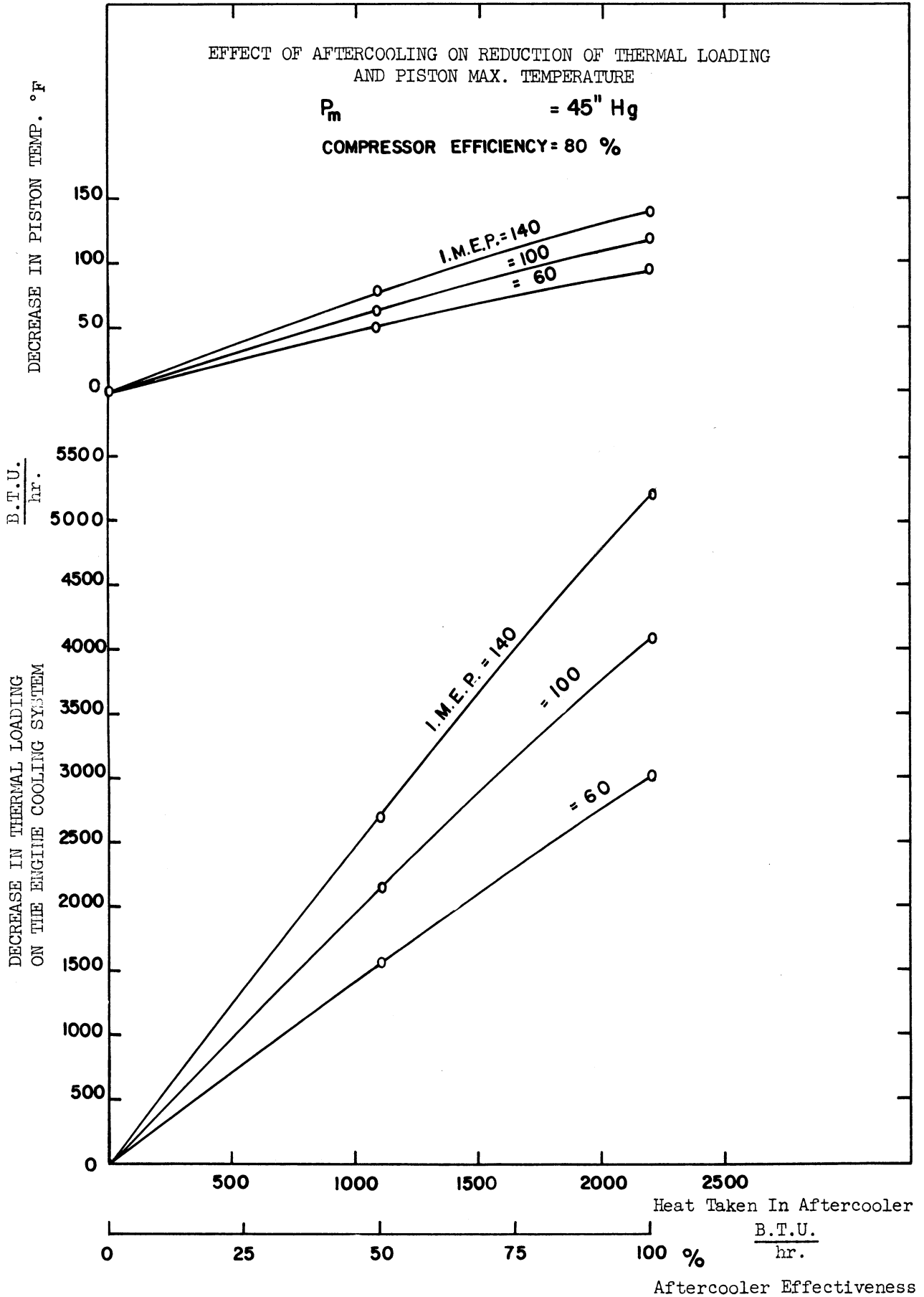


FIG. 50

IX. CONCLUSIONS AND RECOMMENDATIONS

Conclusions:

From the foregoing analysis it is concluded that:

1. The thermal loading and wall temperatures of a turbocharged compression ignition engine are primarily related to the indicated power output and are affected to a lesser degree by intake manifold conditions and the engine speed. Results of this investigation show that:
 - a. Thermal loading and wall temperatures increase in direct proportion to the indicated mean effective pressure.
 - b. For the same indicated power output:
 - (i) Boosting the intake manifold pressure without heating the air will reduce the thermal loading and wall temperatures
 - (ii) Raising the intake manifold temperature will increase the thermal loading and wall temperatures
 - (iii) Thermal loading changes in direct proportion to the cube root of the mean piston speed.
 - c. For the same intake manifold pressure the wall temperature changes in direct proportion to the thermal loading.
2. For the operation of turbocharged engines at constant power output and no aftercooling, one of the following two conditions prevails:

- a. High supercharging resulting in better fuel economy
- b. Low supercharging resulting in poor fuel economy but reduced thermal and mechanical loadings, without any reduction in the wall temperatures.

3. The turbocharged engine performance is improved by increasing the air density and reducing its temperature in the intake manifold resulting in higher specific power outputs and lower thermal loadings and wall temperatures. Aftercooling is one method used for increasing air density by decreasing the air temperature. Even though the pressure drop increases as the aftercooler effectiveness increases, general engine performance will be improved by using an aftercooler with high effectiveness. Improving the compressor efficiency will also increase the specific power output, and reduce the thermal loading and wall temperatures.

4. Aftercooling is necessary if high power outputs are to be obtained at high turbocharging pressures.

Recommendations:

It is recommended that further investigations be made along the following lines:

1. Apply the equations derived in this work to turbocharged engines operating with aftercoolers and, for tests at high supercharging pressures, compare the measured values for the engine performance, thermal loading, and wall temperatures, with those predicted from these equations.

2. Study the relationship between aftercooler pressure-drop and effectiveness required for maximum air-density and minimum air-temperature in the intake manifold. These two conditions will give maximum specific power output and minimum thermal loading and wall temperatures.
3. Make a study of possible methods for effectively cooling the air after its compression in the turbocharger.
4. Investigate the effect of valve timing and exhaust manifold pressure ~~and~~ both the cylinder wall temperature and energy of the exhaust gases necessary to drive the turbocharger.
5. Study the distribution of the heat losses during the cycle, over the cylinder of the turbocharged engine.

APPENDIX A

SAMPLE CALCULATIONS
Run Number 95

Test Conditions:

P_b	Barometric pressure	= 29.52 inches Hg.
P_m	Air gauge pressure at the intake manifold in surge tank	= 3.1 inches Hg.
P_a	Air gauge pressure at inlet tap of orifice meter	= 3.7 inches Hg.
ΔP_a	Differential pressure across the air orifice	= 7.05 inches water.
ΔP_c	Differential pressure across the cooling water orifice	= 8.3 inches water.
T_a	Air temperature at air orifice	= 79 °F
T_m	Air temperature at intake manifold	= 90 °F = 550°R
T_o	Oil temperature in crank case	= 164 °F
$T_{w.ex}$	Exhaust manifold wall temperature	= 202 °F
T_{l1}	Liner wall outer side temperature at T.D.C.	= 225 °F
T_{l2}	Liner wall outer side temperature between T.D.C. and B.D.C.	= 201 °F
T_{l3}	Liner wall outer side temperature at B.D.C.	= 191 °F
T_s	Average temperature of the engine outside wall	= 141 °F
$\Delta T_c = (T_{c3} - T_{c1})$	Rise in water temperature	= 9.95 °F
T_{c2}	Cooling water temperature at inlet to barrel	= 167 °F
T_{c3}	Cooling water temperature at exit from cylinder head	= 173 °F

T_{exh}	Exhaust gas temperature	= 875 °F
t_F	Average time for consumption of 0.1 lb of fuel	= 1.433 minutes
N_{t_F}	Tachometer reading for the time t_F	= 1176.8 revolutions
W_B	Brake load	= 42.9 lbs.
W_F	Friction load	= 13.06 lbs.
N	Revolutions per minute	= $\frac{1176.8}{1.433} = 821$
S	Mean Piston speed	= $\frac{2LN}{60} = \frac{2 \times 5.25 \times 821}{12 \times 60} = 11.98 \frac{\text{ft}}{\text{sec}}$
H.V.	Heating Value of fuel	= 19500 $\frac{\text{B.T.U.}}{\text{lbs.}}$

Air Flow Rate:

D_1	Actual inside diameter of 2" pipe	= 2.0052 inches
A_1	Area of the 2" pipe	= $\frac{\pi}{4} \times (2.0052)^2 = 3.16 \text{ sq. ins.}$
D_2	Diameter of the sharp edged orifice	= 0.7018 sq. ins.
A_2	Area of the sharp edged orifice	= $\frac{\pi}{4} \times (0.7018)^2 = 0.387 \text{ sq. ins.}$
P_a	Absolute air pressure at inlet tap of orifice meter	= 29.52 + 3.7 = 33.22 inches Hg.
ΔP_a		= $\frac{7.05}{12} \frac{62.2}{144} = 0.254 \frac{\text{lbs.}}{\text{sq. in.}}$
$\frac{\Delta P_a}{P_a}$		= $\frac{0.254}{33.22 \times 0.49} = 0.0156$
	Assume the Reynold's number	= 14,300
$K (2)^*$	Flow coefficient [for $\frac{D_2}{D_1} = \frac{0.7018}{2.0052} = 0.35$]	= 0.6155
$E (2)$	Area multiplier for thermal expansion of the orifice plate (stainless steel)	= 1
$Y (2)$	Emperical expansion factor [for $\frac{\Delta P_a}{P_a} = .0156$]	= 0.995
ρ_a	Density of air at inlet to orifice	= $\frac{P_a}{RT_a} = \frac{33.22 \times 0.49 \times 144}{53.34 (460 + 79)} = 0.0816 \frac{\text{lb.}}{\text{cu. ft.}}$

* References are given in Bibliography.

$$\begin{aligned} \omega_a^{(2)} \text{ Air flow rate} &= 0.668 \cdot A_2 \cdot K.E.Y. \cdot \sqrt{\rho_a \Delta P_a} \quad \frac{\text{lbs}}{\text{sec}} \\ &= 0.668 \times 0.387 \times 0.6155 \times 0.995 \sqrt{0.0816 \times 0.254} \\ &= 0.0228 \quad \frac{\text{lbs}}{\text{sec}} \end{aligned}$$

$$\text{Air flow rate} = 0.02275 \times 3600 = \underline{82.1} \quad \frac{\text{lbs}}{\text{hr}}$$

Check on Reynold's Number:

$$Re = \frac{GD_1}{\mu \text{ air}}$$

G = Air flow rate per sq. ft. hr.

μ_{air} = Absolute viscosity of air $\frac{\text{lb}}{\text{ft. hr.}}$

$$Re: \quad \frac{82.1 \times 144}{3.16} \times \frac{2.0052}{12 \times 0.0438} = 14,300$$

Cooling Water Flow Rate:

The orifice meter used for measuring water flow rates had the same dimensions as that for air. Using the same symbols used for the air flow rate, the equation for the rates of cooling water flow is

$$\begin{aligned} \omega_c &= 0.668 A_2 \cdot K.E.Y. \cdot \sqrt{\rho_c \Delta P_c} \quad \frac{\text{lbs.}}{\text{sec.}} \\ \text{Assume the Reynold's Number} &= 19700 \\ K &= 0.6123 \\ E \text{ at } T = 163^\circ\text{F for stainless steel} &= 1.0011 \\ \rho_c \text{ at } T = 163^\circ\text{F} &= 61 \quad \frac{\text{lbs.}}{\text{cu. ft.}} \\ \Delta P_c &= \frac{8.3}{12} \times \frac{62.2}{144} = 0.2986 \quad \frac{\text{lb.}}{\text{sq. in.}} \\ A_2 &= 0.387 \text{ sq. ins.} \\ W_c &= 0.668 \times 0.387 \times 0.6123 \times 1.0011 \sqrt{61 \times 0.2986} = 0.676 \quad \frac{\text{lb.}}{\text{sec.}} \\ &= 0.666 \times 3600 = \underline{2435} \quad \frac{\text{lbs}}{\text{hr}} \end{aligned}$$

Check on Reynold's Number:

$$\mu \text{ water at } 163^{\circ}\text{F} = 0.944 \frac{\text{lb.}}{\text{ft. sec.}}$$

$$\text{Re} = \frac{2435 \times 144 \times 2.0052}{3.16 \times 12 \times 0.944} = 19,650$$

Fuel Rate of Consumption:

$$\text{Consumption per hour} = \frac{0.1}{t_F} \times 60 = \frac{0.1}{1.433} \times 60 = 4.19 \text{ lbs.}$$

$$\frac{F}{A}: \text{ Fuel air ratio} = \frac{4.19}{82.1} = 0.051$$

Power Output:

The equation for the engine horse power as measured by the dynamometer is:

$$\text{Horse Power} = \frac{W \times N}{4000}$$

where W = load on the dynamometer arm.

N = revolutions per minute.

4000 = a constant for the dynamometer.

$$\text{B.H.P. Brake horse power} = \frac{W_B \times N}{4000}$$

$$= \frac{42.9 \times 821}{4000} = 8.8 \text{ H.P.}$$

$$W_I \text{ Indicated load} = W_B + W_F = 42.9 + 13.06 = 55.96 \text{ lbs.}$$

B.M.E.P. Brake mean effective pressure

$$= \text{B.H.P.} \times \frac{33000}{V_s} \times \frac{2}{N} \times 12$$

where V_s is the swept volume = 83.48 in.³

$$\text{B.M.E.P. (uncorrected)} = 8.8 \times \frac{33000}{83.48} \times \frac{2}{821} \times 12 = 101.9 \frac{\text{lbs.}}{\text{sq. in.}}$$

$$\text{Correction factor of the B.M.E.P. for the effect of back pressure.} = 0.6 \frac{\text{lbs.}}{\text{sq. in.}}$$

$$\text{B.M.E.P.} = 101.9 - 0.6 = 101.3 \frac{\text{lbs.}}{\text{sq. in.}}$$

$$\text{B.H.P.} = 101.3 \times \frac{83.48}{33000} \times \frac{821}{2} \times \frac{1}{12} = 8.76$$

$$\eta_m \quad \text{Mechanical efficiency} = \frac{W_B}{W_I} = \frac{42.9}{55.96} = 76.7 \%$$

$$\text{I.M.E.P.} \quad = \frac{101.3}{.767} = 132 \quad \frac{\text{lbs.}}{\text{sq. in.}}$$

$$\text{I.H.P.} \quad = 132 \times \frac{83.48}{33000} \times \frac{821}{2} \times \frac{1}{12} = 11.42 \quad \text{H.P.}$$

B.S.F.C. Brake specific fuel consumption

$$= \frac{4.19}{8.76} = 0.477 \quad \frac{\text{lb.}}{\text{B.H.P. hr.}}$$

$$\text{I.S.F.C.} \quad = \frac{4.19}{11.42} = 0.3663 \quad \frac{\text{lb.}}{\text{I.H.P. hr.}}$$

$$\begin{aligned} \eta_{B.Th.} &= \text{Brake thermal efficiency} \\ &= \frac{8.76 \times 550 \times 60 \times 60 \times 100}{778 \times 4.19 \times 19,500} = 27.35 \% \end{aligned}$$

$$\begin{aligned} \eta_{I.Th.} &= \text{Indicated thermal efficiency} \\ &= \frac{\eta_{B.Th.}}{\eta_m} = \frac{27.35}{0.767} = 35.62 \% \end{aligned}$$

$$\begin{aligned} \text{Heat to cooling water} &= \omega_c \times \text{sp.ht.} \times \Delta T_c \\ &= 2435 \times 1 \times 9.95 = 24220 \quad \frac{\text{B.T.U.}}{\text{hr.}} \end{aligned}$$

(P-V) and (Wall Temperature-Crank Angles) diagrams:

Scale of pressure

$$\text{Calibration pressure} = 231.3 \quad \frac{\text{lb}}{\text{sq. in.}}$$

This corresponds to a calibrating resistance of $\frac{1}{2}$ ohm
in the "Bridge-Amplifier".

Deflection on the oscillograph screen, figure (23)
= 4.5 screen divisions.

$$\text{Scale of trace} = \frac{231.3}{4.5} = 51.5 \quad \frac{\text{lbs.}}{\text{sq. in.}} \text{ per division.}$$

Scale of temperature

Voltage across the thermocouple ends
(as measured by the precision potentiometer) = 0.585 m.v.

Voltage corresponding to 100°F temperature
 difference between thermocouple junction
 and reference junction temperatures
 (In the range of 40°C to 150°C, figure (18)) = 1.765 m.v.

Temperature difference corresponding to .585 m.v. = $\frac{.585}{1.765} \times 100 = 33.1^\circ\text{F}$

Corresponding deflection on the oscillograph
 screen = 7 screen
 division

Scale of trace = $\frac{33.1}{7} = 4.73 \frac{^\circ\text{F}}{\text{division}}$

Weight of the Residual Gases in the Clearance Volume:

Assume the pressure at the end of the exhaust stroke = $14.7 \frac{\text{lbs}}{\text{sq. in}}$

Clearance volume = 6.393 cu.ins.

R_{ex} : Gas constant for exhaust gases (20) = $53.175 \frac{\text{ft. lb.}}{\text{lb. } ^\circ\text{F.}}$

Wt. of residual gases = $\frac{PV}{RT} = \frac{14.7 \times 144 \times 6.393}{53.175 \times 144 \times 12} = .000109 \text{ lb.}$
 per cycle

Wt. of scavenging air per sec. = $.00764 \sqrt{\frac{3.1}{6.3}} \times \frac{537}{550} = 0.00526 \frac{\text{lb.}}{\text{sec.}}$
 (Appendix F)

Time for scavenging per cycle = $\frac{60 \times 36}{821 \times 360} = 0.00731 \text{ sec.}$

Wt. of scavenging air per cycle = $0.00526 \times 0.00731 = 0.0000385 \text{ lb.}$

Wt. of fresh air trapped in the cylinder per cycle

= $\frac{82.1 \times 2}{60 \times 821} - 0.0000385$

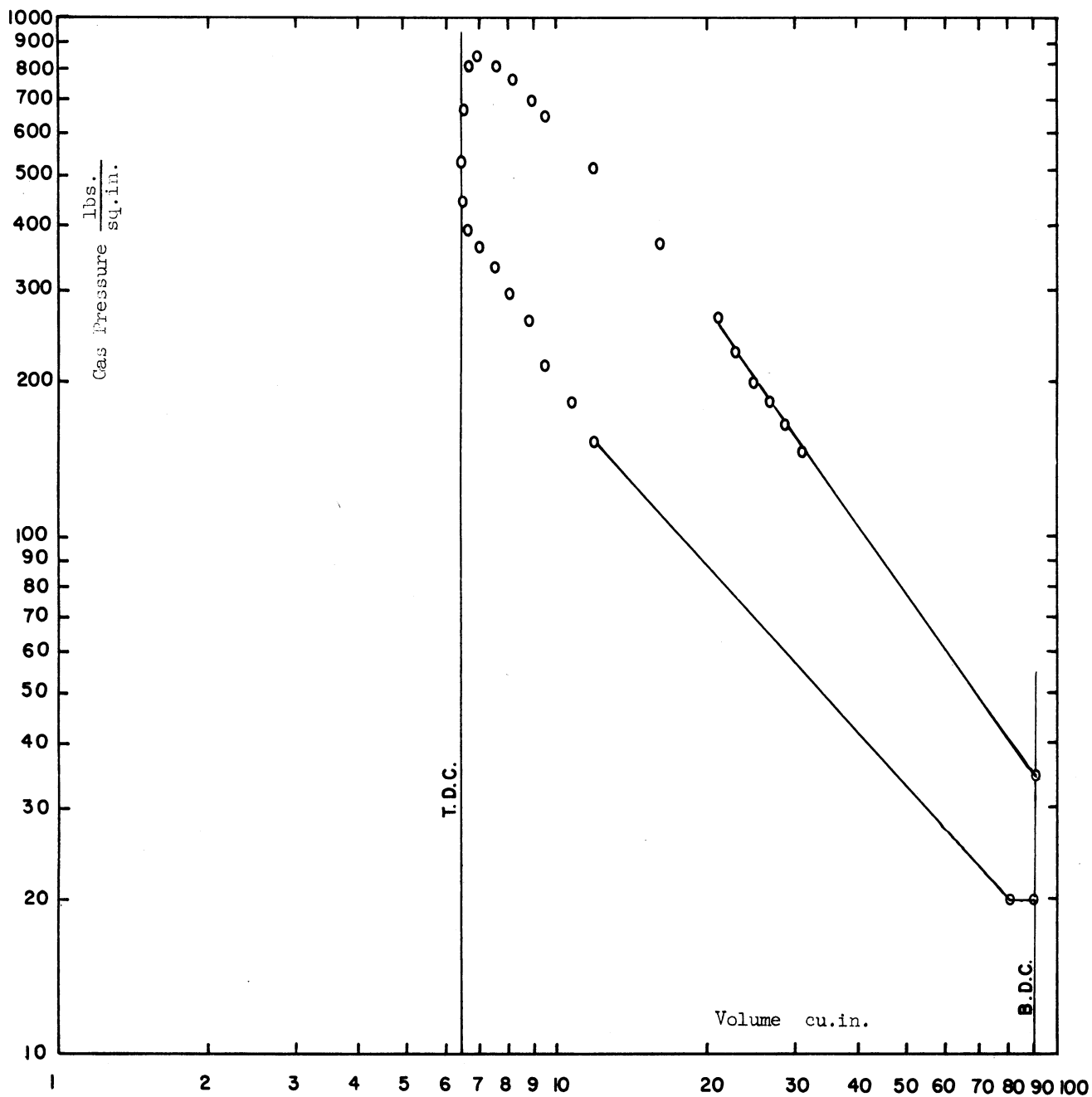
= $0.003,33 - 0.000,039 = 0.00329 \text{ lb.}$

Wt. of gases during the compression stroke

= $0.00329 + 0.00011 = 0.0034 \text{ lb.}$

Wt. of fuel used per cycle = $\frac{4.19}{\frac{821}{2} \times 60} = 0.00017 \text{ lb.}$

Wt. of gases during the expansion stroke = $0.0034 + 0.00017 = 0.00357 \text{ lb.}$



P-V DIAGRAM
(Run Number 95)

FIG. 51

For any point on the compression stroke,

$$T = \frac{P \times V}{12 \times 53.34 \times 0.0034} = \underline{0.458 \text{ P.V.}}$$

For any point on the expansion stroke,

$$T = \frac{P \times V}{12 \times 53.175 \times 0.00357} = \underline{0.438 \text{ P.V.}}$$

To draw the pressure-crank angles diagram near B.D.C., allow for all the runs, 0.75 lb.per.sq.in.drop in air pressure below the manifold pressure at the time the I.V. closes.

$$\therefore \text{Pressure at close of I.V.} = 32.62 \times 0.49 - 0.75 = 15.27 \frac{\text{lb.}}{\text{sq. in.}}$$

Allow, for all the runs, 20°F drop in gas temperature between the end of the expansion stroke and the measured exhaust temperature,

$$\begin{aligned} \therefore T \text{ at the end of expansion stroke} &= 875 + 20 = 895^\circ\text{F} \\ &= 1355^\circ\text{R} \end{aligned}$$

$$\& P \text{ at the end of expansion stroke} = \frac{1355}{0.438 \times 89.87} = 34.4 \frac{\text{lbs.}}{\text{sq. in.}}$$

Heat Transfer Analysis For The Cycle:

Equation [2.1]:

$$\alpha_g = 0.0564 \sqrt[3]{s} \sqrt{PT}$$

for this run

$$s = \frac{2LN}{60} = \frac{2 \times 5.25}{12} \times \frac{821}{60} = 11.98 \frac{\text{ft.}}{\text{sec.}}$$

thus α_g at any crank angle where the gas is at a pressure P and temperature T

$$\begin{aligned} &= 0.0564 \sqrt{11.98} \sqrt{PT} \\ &= 0.1291 \sqrt{PT} \end{aligned}$$

The values of α_g and $(\alpha_g \cdot T_g)$ for the compression and expansion strokes are shown in tables (1) and (2). For the intake and exhaust strokes, the method used is as follows:

Intake stroke:

For the intake stroke the effective gas temperature was calculated by equating the heat gained by air to the heat transferred from the walls.

$$\omega_a \times c_p \times \Delta t = A_m \times \alpha_g \times (T_{w.g.} - T_E) \quad [10.1]$$

where Δt is the temperature rise in the mixture of air and residual gases, due to the heat from the walls. The temperature of the mixture of residual exhaust gases and air was calculated from the following equation:

$$\begin{aligned} (\omega_{\text{air}} + \omega_{\text{exh.}}) h_{\text{mix.}} &= \omega_a \times h_a + \omega_{\text{exh.}} \times h_{\text{exh.}} \\ h_a \text{ at } 90^\circ\text{F} &= 131.46 \frac{\text{B.T.U.}}{\text{lb.}} \\ h_{\text{exh.}} \text{ at } 875^\circ\text{F} &= 321.5 \frac{\text{B.T.U.}}{\text{lb.}} \end{aligned}$$

$$h_{\text{mix.}} = \frac{.00333 \times 131.46 + .00011 \times 321.5}{.00333 + .00011} = 137.4 \quad \frac{\text{B.T.U.}}{\text{lb.}}$$

$$T_{\text{mix.}} = 115^{\circ}\text{F}$$

Temperature of the gases at the time when I.V. closed

$$= \frac{PV}{\omega R} = \frac{15.27 \times 144 \times 82.97}{144 \times 12 \times 0.0034 \times 53.34} = 582^{\circ}\text{R} = 122^{\circ}\text{F}$$

Rise in gas temperature due to heat from walls

$$= 122 - 115 = 7^{\circ}\text{F}$$

75% of this heat was assumed to be gained during the intake stroke, and the rest during the compression stroke before the inlet valve closed.

$$\text{Heat gained during the intake stroke} = 82.1 \times 0.24 \times 7 \times .75 = 103.5 \quad \frac{\text{B.T.U.}}{\text{hr.}}$$

Mean wall temperature during the suction stroke = 212°F
(Appendix E)

To get the coefficient of heat transfer between the gases and wall, assume 1 lb. per sq. in. drop in air pressure below the manifold pressure during the intake stroke.

$$\therefore P = 32.62 \times .49 - 1 = 15.02 \quad \frac{\text{lbs.}}{\text{sq. in.}}$$

$$\text{Average gas temperature} = \frac{122 + 115}{2} = 118.5^{\circ}\text{F} = 578.5^{\circ}\text{R}$$

$$\alpha_M = 0.1291 \sqrt{15.02 \times 578.5} = 12.02 \quad \frac{\text{B.T.U.}}{\text{hr. sq. ft. }^{\circ}\text{F}}$$

$$A_M = \text{Comb}^n \text{ ch. area} + \frac{1}{2} \text{ liner area} + \text{intake manifold area}$$

$$= 48.4 + \frac{74.2}{2} + 34.3 = 119.8 \quad \text{sq. ins.}$$

From equation [10.1]

$$T_{\text{w.g.}} - T_E = \frac{103.5 \times 144}{12.02 \times 119.8} = 10.35^{\circ}\text{F}$$

$$T_E = 212 - 10.35 = 201.65^\circ\text{F} = 661.65^\circ\text{R}$$

$$\alpha_M T_E = 12.02 \times 661.65 = 0.796 \times 10^4$$

Exhaust stroke:

The gas pressure during this stroke is assumed to be

$$1 \frac{\text{lb.}}{\text{sq. in.}} \text{ higher than the atmospheric pressure} = 14.5 + 1 = 15.5 \frac{\text{lbs.}}{\text{sq.in.}}$$

$$\text{Exhaust gas temperature} = 875 + 460 = 1335^\circ\text{R}$$

$$\alpha_M = 0.1291 \sqrt{15.5 \times 1335} = 18.56 \frac{\text{B.T.U.}}{\text{hr. sq. ft. }^\circ\text{F}}$$

$$\alpha_M T = 18.56 \times 1335 = 2.48 \times 10^4$$

At the end of the expansion stroke the pressure was considered half way between the exhaust pressure and that from extrapolation of the expansion curve. The temperature was found by extrapolation.

Values Of α_M And $T_{M.E.}$ As Calculated From Figures 52 and 53:

Stroke	Intake	Compression	Expansion	Exhaust	Total Cycle
α_M	12.02	26.55	70.3	18.56	31.86
$\alpha_M T_{M.E.}$	0.796×10^4	2.415×10^4	15.5×10^4	2.48×10^4	5.298×10^4
$T_{M.E.}^\circ\text{R}$	661.7	910	2205	1335	1660
$T_{M.E.}^\circ\text{F}$	201.7	450	1745	875	1200

TABLE I

Heat Transfer Analysis For The Cycle: (Run #95)

Stroke	Crank Angles From T.D.C.	Deflection of trace screen divisions	Gauge	P	V	T	\sqrt{PT}	α_g	$\alpha_g \cdot T_g$ $\times 10^{-4}$
			Pressure	Absolute Pressure	Volume	Temper- ature			
			lbs. sq. in.	lbs. sq. in.	cu. ins.	°R			
COMPRESSION	0	10.2	520	534.5	6.393	1552	910	117.6	18.25
	3	8.3	428	442.5	6.474	1305	760	98.1	12.8
	6	7.3	376	390.5	6.675	1186	680	87.8	10.4
	9	6.8	350	364.5	7.031	1166	652	84.2	9.82
	12	6.2	319	333.5	7.613	1157	620	80.1	9.27
	15	5.45	281	295.5	8.158	1098	570	73.6	8.08
	18	4.8	247	261.5	8.946	1063	528	68.2	7.26
	21	3.9	201	215.5	9.6	942	452	58.4	5.5
	24	3.25	167.3	181.8	10.887	899	404	52.2	4.69
	27	2.7	139	153.5	11.998	837	358	46.3	3.88
	36	-	-	108	16.175	794	293	37.85	3.03
	45	-	-	78	21.22	754	242.5	31.35	2.36
	63	-	-	45	33.3	682	175	22.6	1.54
	72	-	-	36.6	39.95	666	156	20.16	1.34
	90	-	-	25.8	53.32	626	127	16.4	1.03
	108	-	-	20.2	65.72	604	110.4	14.28	0.86
	126	-	-	16.8	76.05	581	98.8	12.76	0.74
	142	-	-	15.25	82.97	575	93.7	12.11	0.7
180	-	-	15.02	89.87	573	92.8	12	0.69	

TABLE II

Heat Transfer Analysis For The Cycle: (Run #95)

Stroke	Crank Angles From T.D.C.	Deflection of trace screen division	Gauge	P	V	T	\sqrt{PT}	α_g	$\alpha_g \cdot T_g$ 10^{-4}
			Pressure <u>lbs.</u> sq. in.	Absolute Pressure <u>lbs.</u> sq. in.	Volume cu.ins.	Temper- ature °R			
	0	10.2	520	534.5	6.393	1552	910	117.6	18.25
	3	12.7	654	668.5	6.474	1890	1123	145.2	27.42
	6	15.55	800	814.5	6.675	2377	1390	179.6	42.6
	9	16.2	835	849.5	7.031	2610	1490	192.5	50.3
	12	15.5	798	812.5	7.613	2706	1482	191.4	51.9
	18	13.3	685	699.5	8.946	2740	1383	178.8	49
	21	12.25	631	645.5	9.60	2710	1320	170.5	46.2
	27	9.8	505	519.5	11.998	2720	1188	153.3	41.7
	36	6.9	355	369.5	16.175	2612	982	127	33.17
	45	4.9	252	266.5	21.22	2475	812	105	26
	48	4.15	214	228.5	23.103	-	-	-	-
	51	3.6	185.5	200	24.993	-	-	-	-
	54	3.3	170	184.5	27.013	2180	634	81.6	17.8
	57	2.95	152	166.5	29.073	-	-	-	-
	60	2.6	134	148.5	31.163	-	-	-	-
	63	-	-	137	33.3	1992	522	67.5	13.45
	72	-	-	107	39.95	1868	447	57.8	10.8
	90	-	-	72.5	53.32	1690	350	45.2	7.65
	108	-	-	55	65.72	1580	294.2	38	6
	126	-	-	45	76.05	1497	259.5	33.5	5.01
	135	-	-	42	80.24	1475	248.5	32.15	4.74
	180	-	-	25	89.87	1353	184	23.75	3.22

Expansion

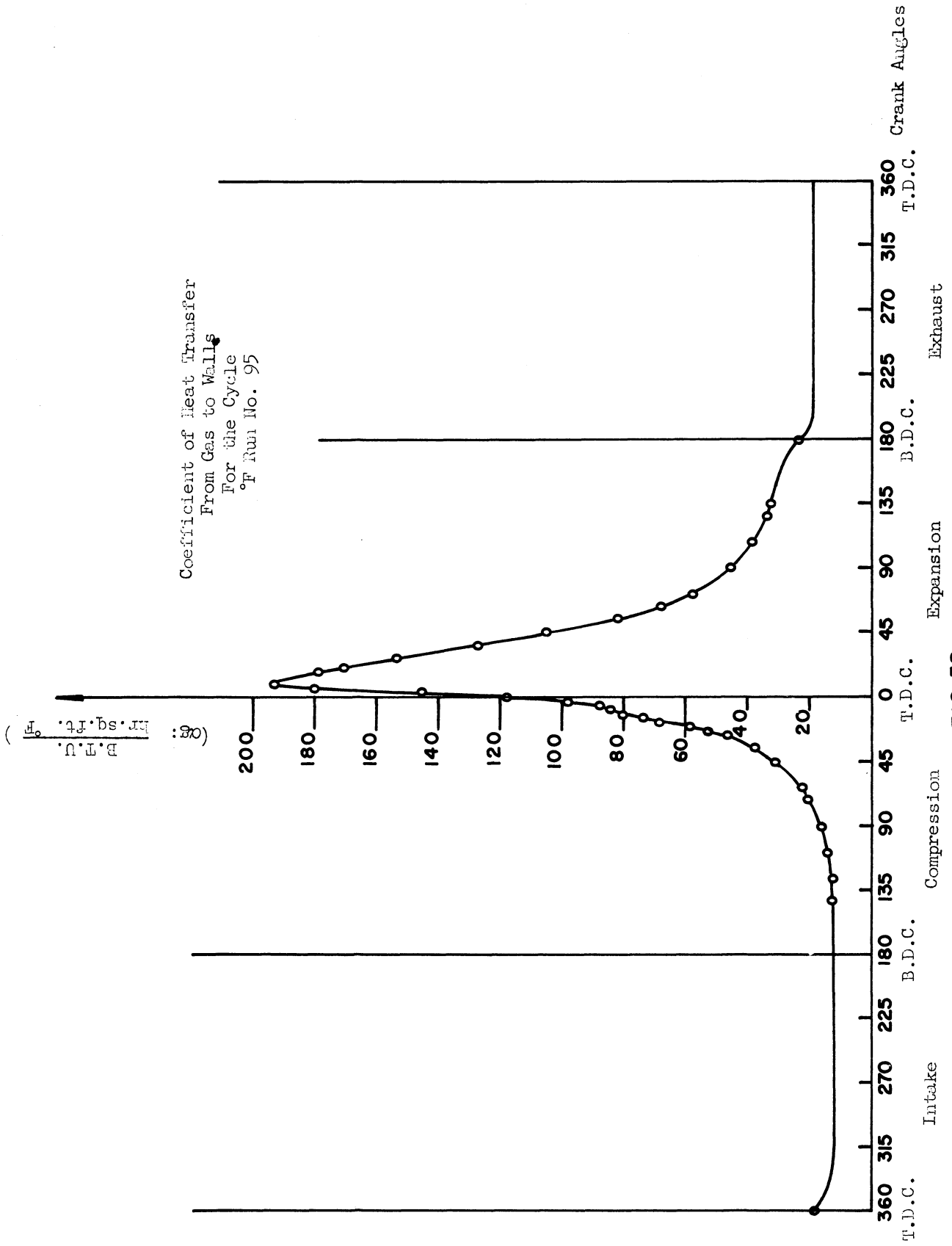
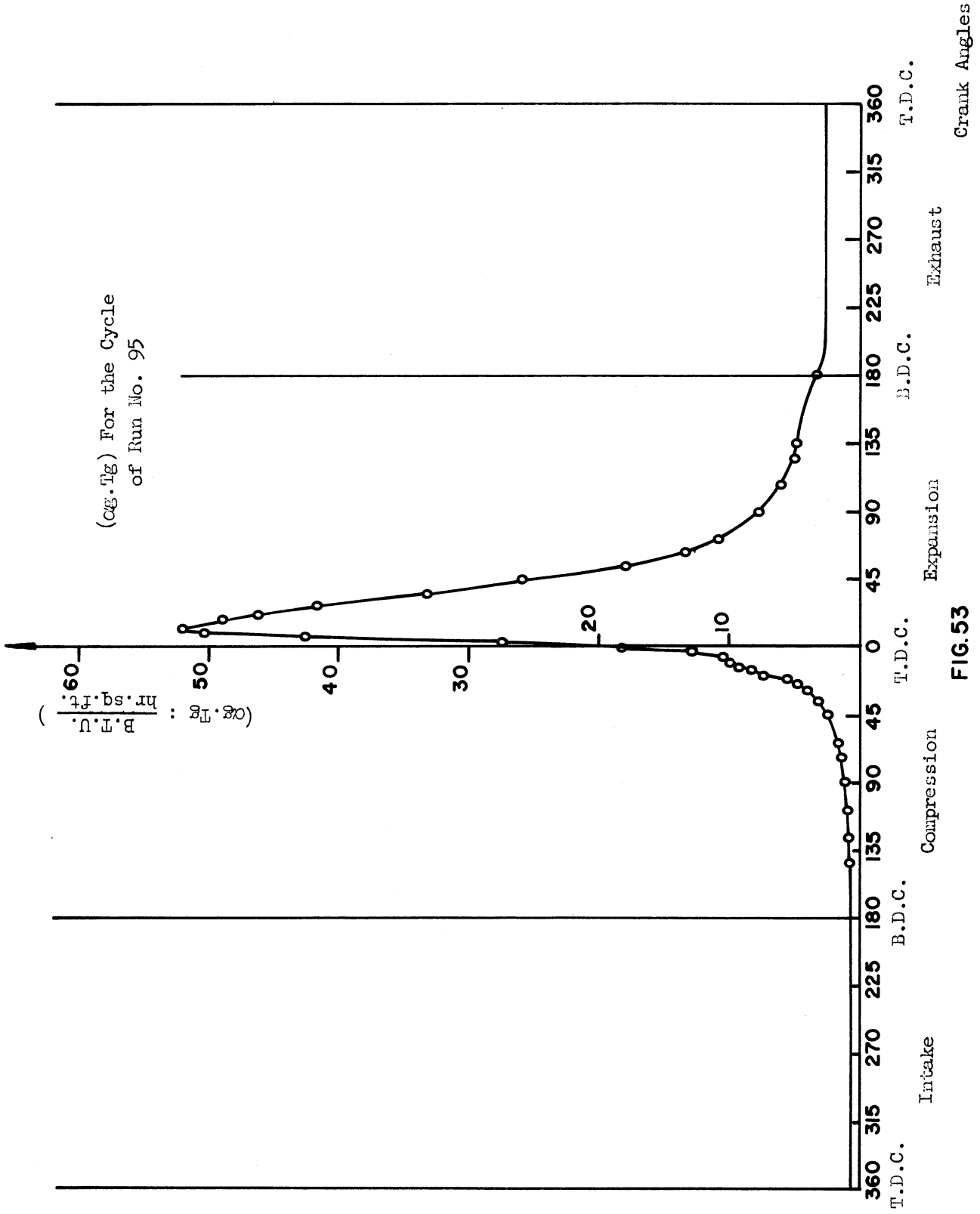


FIG. 52



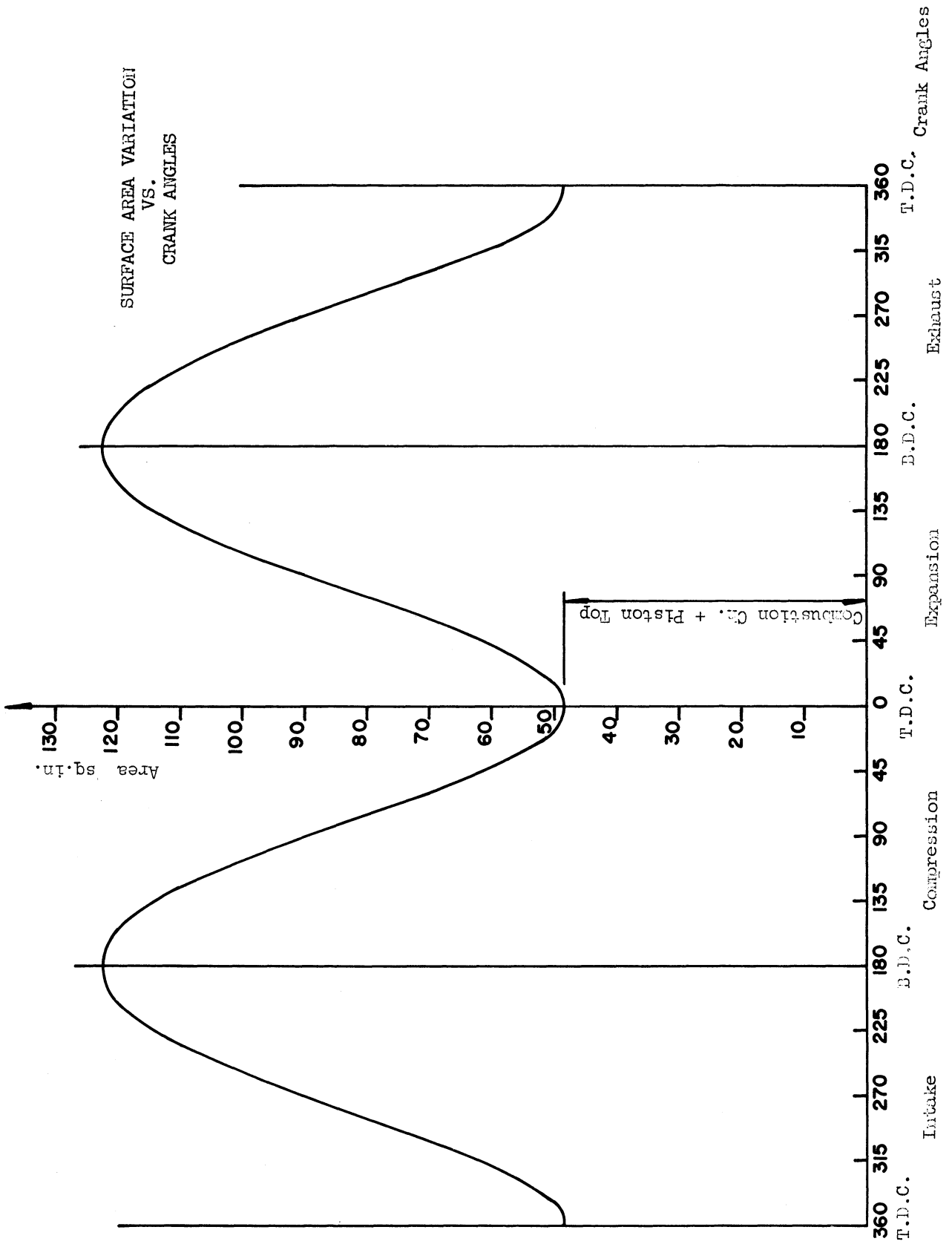


FIG. 54

APPENDIX B

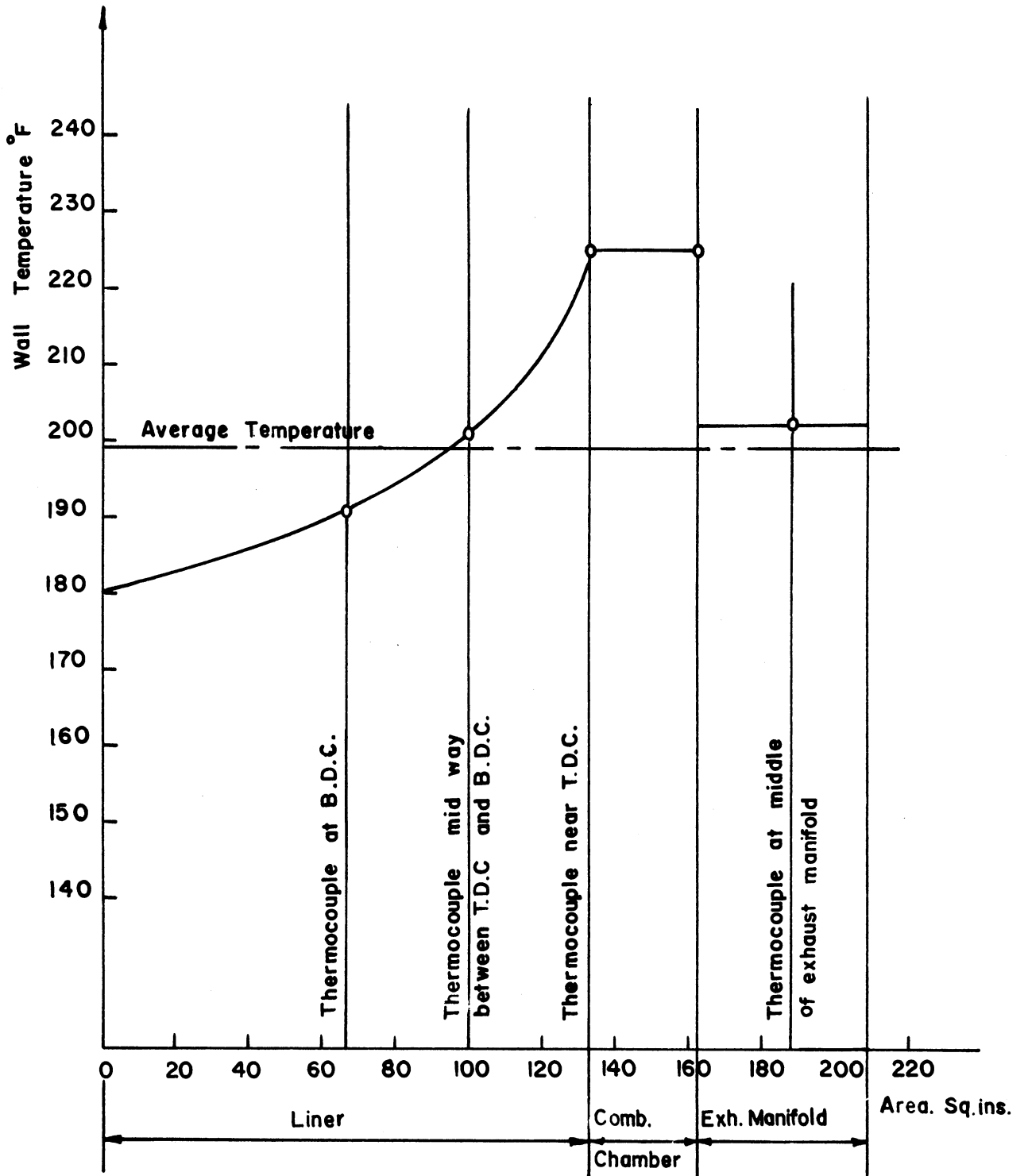
CALCULATION OF CONSTANT "C"
OF EQUATION [2.11]

Run 95:

Area of liner in contact with water	= 133.3 sq. ins.
Area of combustion chamber in contact with water	= 29.0 sq. ins.
Area of exhaust manifold in contact with water	= 46.9 sq. ins.
Total area	= 209.2 sq. ins.
Heat carried by cooling water (table 5)	= 24220 $\frac{\text{B.T.U.}}{\text{hr.}}$
Average wall temperature figure (55)	= 199 °F
Average water temperature	= 168 °F
($T_{\text{wall av.}} - T_{\text{water av.}}$)	= 31 °F
$\alpha_c = \frac{24220 \times 144}{209.2 \times 31}$	= 540 $\frac{\text{B.T.U.}}{\text{hr. sq. ft. °F}}$
μ water at the average temperature	= 0.905 $\frac{\text{lb.}}{\text{ft. sec.}}$
$\left(\frac{c\mu}{k}\right)$ water at the average temperature	= 2.4
$\left(\frac{W_c}{\mu}\right)^{0.6}$	= 115
$\left(\frac{c\mu}{k}\right)^{0.4}$	= 1.42
$\left(\frac{W_c}{\mu}\right)^{0.6} \times \left(\frac{c\mu}{k}\right)^{0.4}$	= 163.2

Similar calculations were made for other runs at various speeds, these are shown in tables (14) and (15). The value of the constant C was calculated from the slope of the line in figure (57) and was found to be equal to 3.15

$$\therefore \alpha_c = 3.15 \left(\frac{W_c}{\mu}\right)^{0.6} \left(\frac{c\mu}{k}\right)^{0.4}$$



CALCULATION OF THE AVERAGE WALL TEMPERATURE

FOR RUN NO. 95

FIG. 55

APPENDIX C

CALCULATION OF THE COMBUSTION CHAMBER
WALL TEMPERATURE FOR RUN NO. 95

1. Using equation [2.14] for the combustion chamber temperature

$$T_{w.g.} = T_{M.E.} \left[\frac{Z}{Z + \frac{k_w}{\alpha_M}} \right] + T_c \left[\frac{Z}{Z + \frac{k_w}{\alpha_M}} \right]$$

where

$$T_{M.E.} = \frac{T_m}{\sqrt[3]{T_m P_m}} \left[\frac{14.71 + 0.233 \text{ I.M.E.P.}}{0.48 + 0.00157 \text{ I.M.E.P.}} \right]$$

$$= 1750 \text{ R} = 1290^\circ\text{F} \quad (\text{Table 16})$$

$$\alpha_M = 32.7 \frac{\text{B.T.U.}}{\text{hr. sq. ft. } ^\circ\text{F}} \quad (\text{Table 16})$$

$$Z = x \frac{A_{w.g.}}{A_m} + \frac{A_{w.g.}}{A_{w.c.}} \cdot \frac{k_w}{\alpha_c}$$

$$x = 0.282 \text{ in.}$$

$$a_m: \frac{A_{w.g.}}{A_m} = 0.877$$

$$a_c: \frac{A_{w.g.}}{A_{w.c.}} = 0.782$$

$$k_w = 27 \frac{\text{B.T.U.}}{\text{hr. sq. ft. } \left(\frac{^\circ\text{F}}{\text{ft}}\right)}$$

$$\alpha_c = 3.15 \left(\frac{W_c}{\mu}\right)^{0.6} \times \left(\frac{c\mu}{k}\right)^{0.4}$$

μ and $\frac{c\mu}{k}$ were evaluated at T_{C_3}

$$\begin{aligned} \therefore \alpha_c &= 3.15 \left(\frac{2435}{0.87}\right)^{0.6} \times (2.3)^{0.4} \\ &= 515 \frac{\text{B.T.U.}}{\text{hr. sq. ft. } ^\circ\text{F}} \end{aligned}$$

$$\therefore Z = 0.738$$

T_c was evaluated at exit from engine = 633°R .

$$\therefore T_{w.g.} = 709.3^\circ\text{R} = 249.3^\circ\text{F}$$

To be compared with $T_{w.g.}$ measured from figure 22, which equals

$$= 243.6^\circ\text{F}$$

$$\% \text{ error} = 2.34 \%$$

To draw figure (56) for the imaginary walls on the gas and coolant sides of the wall, the following was calculated for run number 95:

Effective combustion chamber wall thickness =

$$x \cdot \frac{A_{w.g.}}{A_m} = 0.282 \times 0.877 = 0.247 \text{ in.}$$

Thickness of the imaginary wall on the gas side =

$$\frac{k_w}{\alpha_M} = \frac{27 \times 12}{32.7} = 9.91 \text{ in.}$$

Thickness of the imaginary wall on the cooling water side =

$$\frac{k_w}{\alpha_c} \cdot \frac{A_{w.g.}}{A_{w.c.}} = \frac{27 \times 12}{515} \times 0.782 = 0.491 \text{ in.}$$

2. Piston Crown Maximum Temperature:

Piston crown thickness = 0.75 ins.

k: thermal conductivity = 27 $\frac{\text{B.T.U.}}{\text{hr. sq. ft. } (\frac{^\circ\text{F}}{\text{ft}})}$

$$\alpha_a = 0.0564 \sqrt[3]{S} \sqrt{PT}$$

where P = 14.7

T (oil in crank case) = 164°F = 624°R

S = 11.97 $\frac{\text{ft.}}{\text{sec.}}$

$$\therefore \alpha_a = 12.38 \frac{\text{B.T.U.}}{\text{hr. sq. ft. } ^\circ\text{F}}$$

Thickness of the imaginary wall on the crank case side =

$$\frac{k}{\alpha_a} = \frac{27 \times 12}{12.38} = 26.2 \text{ ins.}$$

Figure (56) drawn with the calculated imaginary walls thickness, shows that the piston-crown maximum temperature equals 990°F compared to 250°F for the combustion chamber walls.

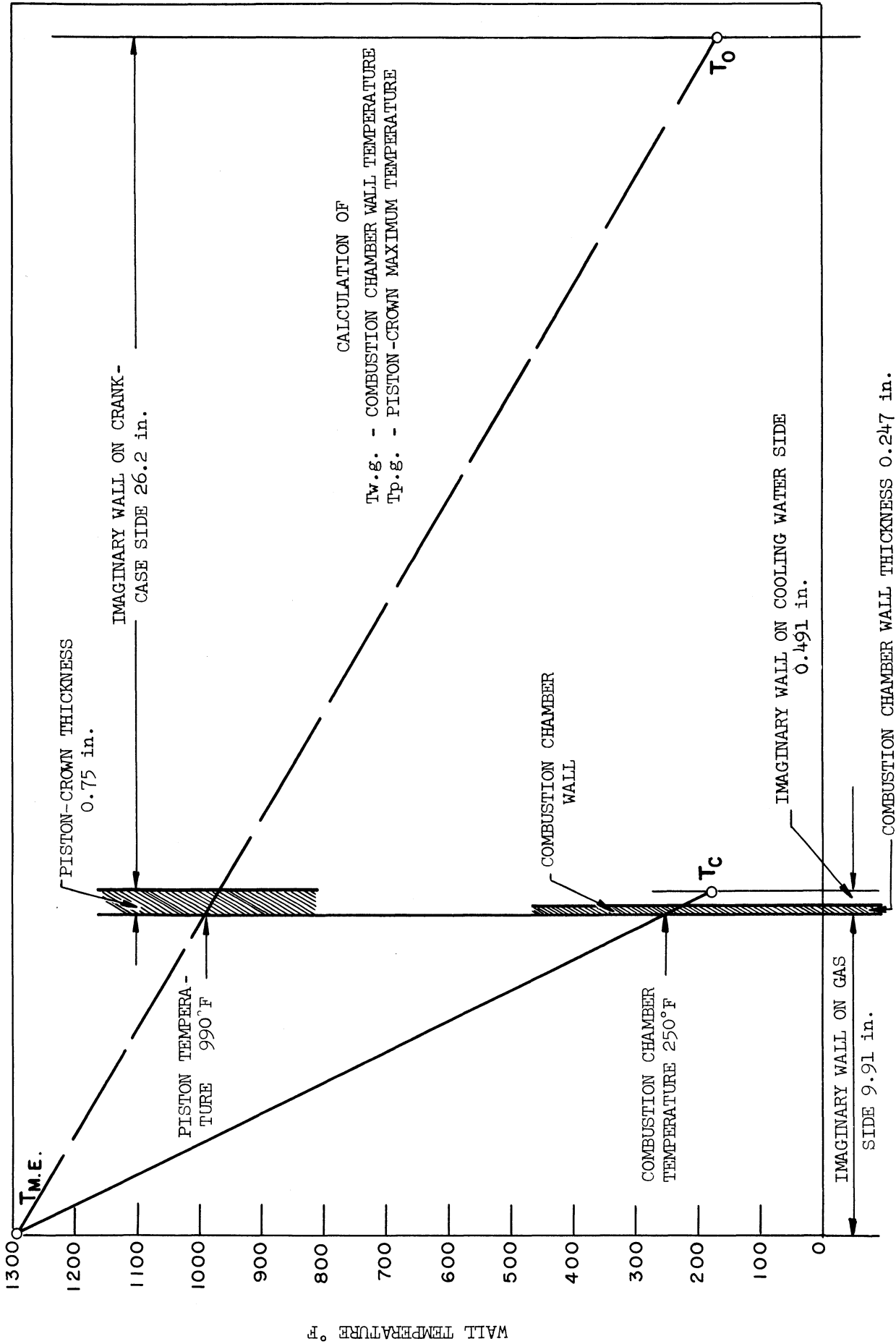


Figure 56

APPENDIX D

CALCULATION OF INTENSITY OF THERMAL LOAD
ON THE COMBUSTION CHAMBER WALLS.

For Run Number 95:

Using equation [2.16]

$$\begin{aligned} \frac{1}{U} &= \frac{1}{\alpha_M} + a_m \times \frac{x}{k_w} + a_c \times \frac{1}{\alpha_c} \\ &= \frac{1}{32.7} + .877 \times \frac{.282}{27 \times 12} + .782 \times \frac{1}{515} \\ &= .0329 \end{aligned}$$

$$U = 30.4 \quad \frac{\text{B.T.U.}}{\text{hr. sq. ft. } ^\circ\text{F}}$$

Substituting in equation [2.15]

$$\begin{aligned} q &= U (T_{M.E.} - T_c) \\ &= 30.4 (1290 - 170) \\ &= 34050 \quad \frac{\text{B.T.U.}}{\text{hr. sq. ft.}} \end{aligned}$$

TABLE III
 Engine Test Results - Series A
 Runs at $P_m \approx 30''$ Hg, $T_m \approx 80^\circ\text{F}$, $N \approx 800$ R.P.M.

Run Number	1	2	3	4	15	85	94	147	148
P_b ins. Hg.	29.15	29.18	28.96	28.96	29.42	29.36	29.52	28.96	28.96
P_m ins. Hg.	28.75	28.78	28.56	28.56	29.02	29.01	29.55	28.56	28.51
T_m °F	83	84	72	72	77.5	82	90	76	76
N R.P.M.	807	800	800	810	854	775	826	803	823
T_o °F	145	149	145	141	143	153	164	146.5	147
$T_{w,exh.}$ °F	171	197	191.5	200	167	187	193	164	157
T_{t1} °F	184	207	201	207	181	206	219	177	169
T_{t2} °F	173	188	186	188	173	192	199	168	171
T_{t3} °F	168	180	178	179	170.5	185	188	165	166
T_8 °F	126	118	115	114	117.5	132	140	124	127
$\Delta T_c = (T_{c3} - T_{c1})$	5.76	7.88	6.845	8.82	5.27	7.4	8.8	4.32	3.78
T_{c2} °F	142.86	-	153.4	-	-	156	162	-	-
T_{c3} °F	146.2	161.7	158	161.6	163	162.7	169	155.5	151
$T_{exh.}$ °F	438	747	658	944	368	603	856	348	307
W_a lbs./hr.	70.6	69.7	69.7	69.3	75.6	69	69.6	71.8	73.8
W_c lbs./hr.	2412	2400	2400	2424	2540	2322	2460	2400	2520
W_f lbs./hr.	1.843	3.22	2.668	3.66	1.471	2.38	3.59	1.363	1.154
F/A Ratio	.0261	.0463	.0383	.0528	.0195	.0345	.0515	.019	.01566
B.H.P.	2.75	6.34	5.14	7.52	1.7	4.29	7.31	1.332	.729
B.M.E.P.	32.35	75.3	61	88	18.9	52.3	84	15.8	8.4
$\eta_{mech.}$ %	52.9	72.5	68.6	75.7	39.2	64.6	74.6	35.1	22.1
I.M.E.P. $\frac{\text{lbs.}}{\text{sq. in.}}$	61.2	101	88.9	116.2	48.3	81	112.5	45	38
B.S.F.C. $\frac{\text{lbs.}}{\text{B.H.P. hr.}}$.671	.508	.52	.487	.867	.555	0.491	1.023	1.584
I.S.F.C. $\frac{\text{lbs.}}{\text{I.H.P. hr.}}$.355	.368	.357	.369	.34	.358	.366	.359	.35
$\eta_{B.Th.}$ %	19.45	25.7	25.1	26.8	15.05	23.52	26.58	12.75	8.24
$\eta_{I.Th.}$ %	36.77	35.5	36.6	35.4	38.4	36.4	35.6	36.4	37.25
$Q_{cooling}$ $\frac{\text{B.T.U.}}{\text{hr.}}$	13900	18900	16410	22400	13400	17200	21650	10370	9520

TABLE IV.

Engine Test Results - Series A
Runs at $P_m \approx 33''$ Hg, $T_m \approx 80^\circ F$, $N \approx 800$ R.P.M.

Run Number	30	32	33	36	37	81	93	95	146	149
P_b ins. Hg.	29.2	29.2	29.2	29.2	29.28	29.39	29.52	29.52	28.96	28.96
P_m ins. Hg.	32.45	32.24	32.7	32.3	31.93	32.84	32.55	32.62	32.01	32.26
T_m °F	73.5	79	75.5	87	77	86	87.5	90	76.5	75
N R.P.M.	793	855	809	790	830	796	832	821	818	816
T_o °F	151	157	157	153	139	150.5	160	164	142	
T_w .exh. °F	174.5	184	187.5	193	206	167	186	202	159.5	155
T_{l1} °F	189	202.5	203	206.5	216	183	208	225	175	168
T_{l2} °F	181	190.5	190	190.5	196	177.5	191	201	168	164
T_{l3} °F	176.5	182	182.5	182.5	184	172	181	191	165	160
T_s °F	120.5	122.5	123	123	111	132	139	141	124	126
$\Delta T_c = (T_{c3} - T_{c1})$	6.74	7.6	8.68	9.0	10.62	6.3	8.75	9.95	4.15	3.78
T_{c2} °F	-	160	162	154.5	156	154	158	167	-	-
T_{c3} °F	163.7	164.6	167.7	163	163	160	166	173	154.2	149.8
$T_{exh.}$ °F	418	592	659	759	962	374	755	875	322	280
W_a $\frac{\text{lbs.}}{\text{hr.}}$	78.5	84.5	81	78.4	80.8	81.6	83.5	82.1	83.3	83.25
W_c $\frac{\text{lbs.}}{\text{hr.}}$	2368	2550	2418	2365	2475	2382	2478	2435	2430	2430
W_{fuel} $\frac{\text{lbs.}}{\text{hr.}}$	1.97	2.982	3.235	3.475	4.41	1.672	3.79	4.19	1.366	1.118
$\frac{F}{A}$ Ratio	.025	.0353	.0399	.0444	.0546	.0205	.0455	.0511	.0164	.01342
B.H.P.	3.26	5.73	6.48	7.52	9.65	2.14	7.64	8.8	1.456	.864
B.M.E.P.	39.05	63.6	76.2	90.5	110.3	25.55	87.1	101.9	16.9	10.12
B.M.E.P. Corr.	37.65	62.5	75.25	89.7	109.8	24	86.3	101.3	15.26	8.39
$\eta_{mech.}$ %	55.8	67	71.2	74.5	78	45.4	73.7	76.7	36.65	25.5
I.M.E.P.	67.5	93.4	105.6	120.4	140.8	52.9	117	132	41.7	32.85
B.S.F.C. $\frac{\text{lbs.}}{\text{B.H.P. hr.}}$.63	.531	.506	.466	.46	.795	.501	.477	1.04	1.564
I.S.F.C. $\frac{\text{lbs.}}{\text{I.H.P. hr.}}$.3515	.356	.3604	.347	.359	.361	.369	.3663	0.381	.399
$\eta_{B.Th.}$ %	20.7	24.6	25.8	28	28.35	16.4	26	27.35	12.56	8.35
$\eta_{I.Th.}$ %	37.15	36.62	36.2	37.6	36.35	36.13	35.35	35.62	32.31	32.7
$Q_{cooling}$ $\frac{\text{B.T.U.}}{\text{hr.}}$	15920	19380	20970	21300	26280	15000	21650	24220	10100	9180

TABLE V.
Engine Test Results - Series A
Runs at $P_m \approx 36''$ Hg, $T_{int} \approx 80^\circ F$, $N \approx 800$ R.P.M.

Run Number	47	48	49	50	51	52	82	87	92	96
P_b ins. Hg.	29.52	29.52	29.52	29.52	29.52	29.52	29.39	29.36	29.52	29.52
P_m ins. Hg.	35.12	35.12	35.27	35.42	35.25	35.17	35.29	36.06	35.52	35.92
T_m °F	73	75	77	79	80.5	81	87	85.5	84	88
N R.P.M.	828	841	829	824	850	847	825	751	823	840
T_o °F	139	149	155	159.5	161	160	156	161	156	166
$T_{w,exh.}$ °F	161	178	185	189	194	207.5	198	178	185	202
T_{i_1} °F	175	194	203	207	217	228.5	177	201	208	223
T_{i_2} °F	170	185	189	192	194	203	169	187	189	202
T_{i_3} °F	166	179	183	184	187	192	165.5	181.5	181	191.5
T_s °F	108	116	118	121	121	123	134.5	139.5	136	143
$\Delta T_c = (T_{c_3} - T_{c_1})$	5.02	7.0	7.65	8.63	9.7	11.0	6.14	7.94	9.2	10.04
T_{c_2} °F	149	156	159	160.5	160.5	161	145	158.5	158	166
T_{c_3} °F	153	162	166	168	169.5	169	149.5	165	163.5	173
$T_{exh.}$ °F	327	473	550	665	780	905	342	466	724	846
W_a lbs. hr.	93.7	92.5	91.7	91.8	90.2	90.3	91.1	85.6	90.8	89.8
W_c lbs. hr.	2478	2508	2478	2460	2538	2526	2460	2250	2434	2508
W_{fuel} lbs. hr.	1.68	2.487	2.943	3.442	3.89	4.685	1.76	2.38	3.65	4.265
$\frac{F}{A}$ Ratio	.0179	.0269	.0321	.0375	.0431	.0519	.0193	.0278	.0403	.0485
B.H.P.	2.265	4.68	6.2	7.65	9.07	10.46	2.507	4.45	8.36	9.93
B.M.E.P.	26.0	52.9	71.1	88.2	101.5	117.3	28.85	55.6	94	114.5
B.M.E.P. Corr.	24.4	51.6	69.9	87.2	100.7	116.7	27.35	54.3	93	113.8
$\eta_{mech.}$ %	47.6	64.6	71.4	75.5	78	80.2	50.4	67.2	76	80
I.M.E.P.	51.3	79.9	98	115.5	129	145.7	54.4	80.8	122.4	142.2
B.S.F.C. $\frac{lbs.}{B.H.P. \cdot hr.}$.79	.545	.484	.455	.431	.45	.742	.554	.441	.433
I.S.F.C. $\frac{lbs.}{I.H.P. \cdot hr.}$.376	.357	.345	.343	.336	.361	.374	.372	.335	.346
$\eta_{b,th.}$ %	16.53	23.95	26.97	28.7	30.3	29	17.6	23.6	29.6	30.17
$\eta_{i,th.}$ %	34.7	37.1	37.8	38	38.85	36.17	34.92	35.1	38.9	37.7
$Q_{cooling}$ $\frac{B.T.U.}{hr.}$	12420	17580	18940	21200	24600	27800	15100	17850	22600	25200

TABLE VI

Engine Test Results - Series A
Runs at $P_m \approx 39''$ Hg, $T_m \approx 80^\circ F$, $N \approx 800$ R.P.M.

Run Number	58	60	61	62	63	64	71	83	91	97
P_b ins. Hg.	29.69	29.69	29.69	29.69	29.69	29.69	29.52	29.39	29.52	29.52
P_m ins. Hg.	38.59	38.59	38.44	39.39	38.99	39.24	39.27	38.54	38.77	38.47
T_m °F	74.5	76	78	79.5	81	32	90	87	80	83
N R.P.M.	840	864	845	817	827	807	789	820	826	814
T_o °F	147.5	155	158	159	159.5	161	159.5	155	157	160
$T_{v,exh.}$ °F	163	178	180.5	186	192.5	199.5	200	174.5	184	198
T_{l_1} °F	177.5	196	200	206	214	220	223	191	208	220
T_{l_2} °F	172	186	188	191.5	196	200.5	200	182	191	202
T_{l_3} °F	168.5	178	181.5	185	187	189.5	189.5	179	184.5	192
T_s °F	124	129.5	134	135.5	138.5	138	138	137	135	140
$\Delta T_c = (T_{c_3} - T_{c_1})$ °F	4.55	7.2	7.99	8.46	10	10.99	12.17	5.02	8.67	9.96
T_{c_2} °F	156	160	161	163	163.5	165.5	161	161	158.6	163.5
T_{c_3} °F	158.6	164.7	166	167.5	169	171.5	170	166	166.5	170
$T_{exh.}$ °F	300	468	521	554	704	792	825.5	328	632	724
W_a lbs./hr.	101.3	103.3	101.2	98	98.7	99	98	99.9	97.4	95.7
W_c lbs./hr.	2502	2574	2490	2442	2472	2412	2364	2448	2460	2430
W_{fuel} lbs./hr.	1.607	2.62	3.013	3.11	3.91	4.2	4.39	1.74	3.29	3.94
F/A Ratio	.01583	.02535	.0298	.0318	.0396	.0424	.0448	.0174	.0338	.0412
B.H.P.	2.4	5.23	6.46	7.06	9.22	10.22	10.4	2.66	7.95	9.09
B.M.E.P.	27.15	57.5	73.5	82	105.6	120.4	123.3	30.8	91.3	106
B.M.E.P. Corr.	25.45	56.1	72.3	80.8	104.6	119.5	122.5	29.2	90.2	105.1
$\eta_{mech.}$ %	49.5	67.8	72.4	75	79.4	81.6	82.3	54.9	76.8	79.5
I.M.E.P.	51.5	82.8	101	107.8	132	146.5	149	53.3	117.5	132.5
B.S.F.C. lbs./H.P. hr.	.714	.514	.4695	.448	.43	.4135	.432	.69	.42	.438
I.S.F.C. lbs./H.P. hr.	.353	.348	.3395	.336	.3412	.337	.355	.379	.3225	.348
η_B Th. %	18.3	25.4	27.8	29.15	30.35	31.6	30.2	18.91	31.1	29.77
η_I Th. %	36.95	37.5	38.45	38.85	38.2	38.7	36.7	34.46	40.5	37.45
$Q_{cooling}$ B.T.U./hr.	11400	18500	19900	20670	24720	26500	28800	12300	21350	24200

TABLE VII.

Engine Test Results - Series A
Runs at $P_m \approx 42''$ Hg, $T_m \approx 80^\circ\text{F}$, $N \approx 800$ R.P.M.

Run Number	66	67	68	69	70	74	84	89	90
P_b ins. Hg.	29.52	29.52	29.52	29.52	29.52	29.52	29.52	29.52	29.52
P_m ins. Hg.	41.47	41.97	41.47	41.72	41.97	41.26	41.71	41.8	41.8
T_m °F	76	82	85	86.5	88.5	86	85	85	72.5
N R.P.M.	827	786	831	805	815	805	775	775	837
T_o °F	149	154	158	158	159	160	159	159	134
T_w exh °F	168	178	181	186	198	164	176	176	182
T_{d1} °F	181.5	195	202	206	220.5	179	200	200	206
T_{d2} °F	175	184	188	190.5	200	172	185.5	185.5	190
T_{d3} °F	172	179.5	180.5	183	190	168	180.5	180.5	181
T_s °F	128	134	136	138	138	135	137	137	126
$\Delta T_c = (T_c - T_{c1})$	5.185	7.9	8.51	9.95	12.83	5.1	7.9	7.9	8.52
T_{c2} °F	157.5	158.5	158	159	159.5	150	158.5	158.5	157
T_{c3} °F	160	162.5	164	165	169	155	164	164	164
T_{exh} °F	303	416	535.5	626	799	305	397	397	610
W_a lbs./hr.	109	106.8	109.8	105.8	106.2	106.5	100.3	100.3	106.2
W_c lbs./hr.	2466	2358	2484	2412	2430	2412	2322	2322	2502
W_{fuel} lbs./hr.	1.674	2.551	3.26	3.7	4.61	1.69	2.485	2.485	3.565
F Ratio	.01535	.0239	.02975	.035	.0434	.0159	.0248	.0248	.0336
B.H.P.	2.84	5.18	7.75	8.75	11	2.89	4.84	4.84	8.08
B.M.E.P.	32.05	62.5	88	102.7	127.2	34.2	59.3	59.3	91.7
B.M.E.P. Corr.	30.35	61.1	86.7	101.6	126.4	32.6	57.9	57.9	90.5
η_{mech} %	55.4	71.2	77	80	83.2	57	69.8	69.8	78
I.M.E.P.	54.8	86	112.6	127	152	57.3	83	83	116
B.S.F.C. $\frac{\text{lbs.}}{\text{B.H.P. hr.}}$.634	.505	.43	.43	.425	.611	.526	.526	.447
I.S.F.C. $\frac{\text{lbs.}}{\text{I.H.P. hr.}}$.351	.3595	.331	.344	.354	.348	.367	.367	.3485
$\eta_{B.Th.}$ %	20.6	25.83	30.4	30.36	30.72	21.38	24.8	24.8	29.2
$\eta_{I.Th.}$ %	37.2	36.3	39.5	37.92	36.9	37.45	35.55	35.55	37.4
$Q_{cooling}$ $\frac{\text{B.T.U.}}{\text{hr.}}$	12800	18600	21170	24000	29550	12300	18350	18350	21200

TABLE VIII.

Engine Test Results - Series A

Runs at $P_m \approx 45''$ Hg, $T_m \approx 80^\circ\text{F}$, $N \approx 800$ R.P.M.

Run Number		72	73	74	75	76
P_b	ins. Hg.	29.45	29.45	29.45	29.45	29.45
P_m	ins. Hg.	44.25	44.25	44.05	44.55	44.7
T_m	$^\circ\text{F}$	83.5	85	88	89.5	90
N	R.P.M.	823	829	832	815	813
T_o	$^\circ\text{F}$	151	154.5	158.5	160	161
$T_{w,exh.}$	$^\circ\text{F}$	159.5	179	178.5	184	193.5
T_{l1}	$^\circ\text{F}$	175	199.5	201	208	216.5
T_{l2}	$^\circ\text{F}$	169	185	187	191	198
T_{l3}	$^\circ\text{F}$	166	181	181	184	189.5
T_s	$^\circ\text{F}$	128.5	133	138	137	138
$\Delta T_c = (T_{c3} - T_{c1})$		5.19	5.4	9.19	9.21	10.5
T_{c2}	$^\circ\text{F}$	146	-	156	160	163
T_{c3}	$^\circ\text{F}$	149	162.5	163	167	170.5
$T_{exh.}$	$^\circ\text{F}$	290.5	386	495	532	668
W_a	$\frac{\text{lbs.}}{\text{hr.}}$	116.3	116	117.2	112.5	110.8
W_c	$\frac{\text{lbs.}}{\text{hr.}}$	2454	2472	2484	2430	2430
W_{fuel}	$\frac{\text{lbs.}}{\text{hr.}}$	1.788	2.427	3.01	3.38	3.96
F Ratio		.01538	.02095	.02565	.0300	.0357
A						
B.H.P.		3.04	4.94	6.78	8.13	9.45
B.M.E.P.		35.1	56.6	77.5	94.6	110.5
B.M.E.P. Corr.		33.4	55.1	76.2	93.4	109.5
$\eta_{mech.}$	%	57.6	68.6	75.2	78.6	81.1
I.M.E.P.		58	80.4	98.6	118.6	135.2
B.S.F.C.	$\frac{\text{lbs.}}{\text{B.H.P. hr.}}$.618	.505	.451	.422	.419
I.S.F.C.	$\frac{\text{lbs.}}{\text{I.H.P. hr.}}$.356	.3465	.339	.3317	.34
$\eta_{B.Th.}$	%	21.12	25.8	28.9	30.92	31.2
$\eta_{I.Th.}$	%	36.65	37.62	38.45	39.3	38.45
$Q_{cooling}$	$\frac{\text{B.T.U.}}{\text{hr.}}$	12720	13350	22800	22400	25500

TABLE IX.
Engine Test Results - Series B
Runs at $P_m \approx 36''$ Hg, $T_m \approx 80^\circ F$, $N \approx 1200$ R.P.M.

Run Number	99	104	121	129	130	134	135	136	137
P_b ins. Hg.	29.25	29.25	29.16	29.03	29.03	29.20	29.20	29.08	29.08
P_m ins. Hg.	35.275	35.45	35.225	35.83	35.53	35.45	35.65	35.48	35.55
T_m °F	82.5	90.5	84	80	87	81	83	82.5	86
N R.P.M.	1240	1197	1210	1208	1190	1227	1216	1223	1212
T_o °F	172.5	177.5	171	167.5	174	159	165	162	169.5
T_w , exh. °F	181	194.5	176	170	192	172	175	177	187
$T_{1/1}$ °F	201	218	197	188	216	194.5	196	200	207
$T_{1/2}$ °F	189.5	200	184	178	190	179	182	179	188
$T_{1/3}$ °F	182	191	178	175	179	173	176	173	179
T_g °F	145	149.5	142	141	146	134	140	136	142
$\Delta T_{c_3} = (T_{c_3} - T_{c_1})$	6.05	8.17	6.26	5.49	9.19	6.35	6.6	7.69	7.72
T_{c_2} °F	160	163	-	-	149.5	-	-	-	153
T_{c_3} °F	165.5	169.5	157	159	158	157	159	155	159
$T_{exh.}$ °F	534	772	578	403	972	588	614	810	838
Exhaust Back Press.	-	-	-	-	-	29.25	34.20	29.23	34.15
V_a ins. Hg.	137	133.75	134.5	135.2	133	135.5	136	135.5	132.8
V_c lbs. hr.	3642	3032	3545	3560	3510	3600	3565	3600	3550
V_{fuel} lbs. hr.	3.39	4.84	3.64	2.51	5.99	3.738	3.808	5.15	5.1
$\frac{F}{A}$ Ratio	.0246	.0362	.02905	.01855	.0451	.02759	.028	.038	.0385
B.H.P.	6.61	11.49	7.92	4.05	14.37	7.93	7.69	11.85	11.6
B.M.E.P.	50.9	91.2	62.3	31.8	114.8	61.4	60.1	92	91
B.M.E.P. Corr.	49.5	90.15	61.05	30.2	114	60.1	58.8	91	90
$\eta_{mech.}$ %	60.8	73.9	65.7	49.5	78.2	65.3	63.15	73.9	72.8
I.M.E.P.	81.5	122	92.9	61	145.9	92.2	93.2	123.1	123.6
B.S.F.C. $\frac{lbs.}{B.H.P. \text{ hr.}}$.528	.426	.4679	.654	.42	.481	.508	.439	.445
I.S.F.C. $\frac{lbs.}{I.H.P. \text{ hr.}}$.3205	.314	.3078	.3238	.3281	.314	.3205	.3242	.3238
$\eta_{B.Th.}$ %	24.8	30.02	27.81	21	18.6	27.15	25.78	29.78	29.4
$\eta_{I.Th.}$ %	40.8	40.7	42.4	42.5	23.8	41.6	40.85	40.39	40.3
$Q_{cooling}$ $\frac{B.T.U.}{hr.}$	22000	24750	22200	19550	32250	22820	23550	27620	27400

TABLE X.

Engine Test Results - Series B.
Runs at $P_m \approx 36''$ Hg, $T_m \approx 140^\circ\text{F}$, $N \approx 1200$ R.P.M.

Run Number		122	126	127	128	131
P_b	ins. Hg.	29.27	29.42	29.42	29.28	29.03
P_m	ins. Hg.	35.63	35.72	35.845	35.78	35.56
T_m	$^\circ\text{F}$	137	142	145	144	141
N	R.P.M.	1201	1216	1216	1204	1204
T_o	$^\circ\text{F}$	176	173	175	173	178
$T_{w, \text{exh.}}$	$^\circ\text{F}$	182	183	184	175	199
T_{l1}	$^\circ\text{F}$	208	208	211	199	224
T_{l2}	$^\circ\text{F}$	191	192	188	187	200
T_{l3}	$^\circ\text{F}$	186	184	178	180	190
T_s	$^\circ\text{F}$	145	144	145	144	148
$\Delta T_c = (T_{c3} - T_{c1})$		6.64	7.05	8.52	6.35	9.08
T_{c2}	$^\circ\text{F}$	-	158	-	156	160
T_{c3}	$^\circ\text{F}$	166	164	157	162	168
$T_{\text{exh.}}$	$^\circ\text{F}$	640	697	865	514	920
W_a	$\frac{\text{lbs.}}{\text{hr.}}$	125.1	126.7	125.2	126.2	122.4
W_c	$\frac{\text{lbs.}}{\text{hr.}}$	3535	3585	3585	3550	3550
W_{fuel}	$\frac{\text{lbs.}}{\text{hr.}}$	3.76	3.94	4.97	3.01	5.735
$\frac{F}{A}$ Ratio		.0301	.0311	.0397	.0239	.0468
B.H.P.		7.78	8.54	11.55	5.125	12.58
B.M.E.P.		61.6	66.75	90.4	40.4	99.2
B.M.E.P. Corr.		60.4	65.55	89.45	55.9	75.9
$\eta_{\text{mech.}}$	%	65.6	67.8	74	55.9	75.9
I.M.E.P.		92	96.7	120.8	70	129.8
B.S.F.C.	$\frac{\text{lbs.}}{\text{B.H.P. hr.}}$.493	.471	.4372	.6075	.459
I.S.F.C.	$\frac{\text{lbs.}}{\text{I.H.P. hr.}}$.3232	.319	.3215	.339	.348
$\eta_{\text{B.Th.}}$	%	26.5	27.75	30	21.5	15.57
$\eta_{\text{I.Th.}}$	%	40.4	40.9	40.6	38.5	20.55
Q_{cooling}	$\frac{\text{B.T.U.}}{\text{hr.}}$	23450	25300	30580	22550	32200

TABLE XI.

Engine Test Results - Series B
 Runs at $P_m \approx 36''$ Hg, $T_m \approx 200^\circ\text{F}$, $N \approx 1200$ R.P.M.

Run Number		123	124	125	132	133
P_b	ins. Hg.	29.27	29.27	29.27	29.12	29.12
P_m	ins. Hg.	35.65	35.49	35.70	35.75	35.62
T_m	$^\circ\text{F}$	193	198	198	197	204
N	R.P.M.	1212	1231	1212	1211	1214
T_o	$^\circ\text{F}$	177	176	175	178	178
$T_{w. \text{ exh.}}$	$^\circ\text{F}$	186	200	187	174	184
T_{l_1}	$^\circ\text{F}$	214	230	213	199	213
T_{l_2}	$^\circ\text{F}$	195	206	196	186	190
T_{l_3}	$^\circ\text{F}$	188	195	187	180	180
T_s	$^\circ\text{F}$	148	148	146	148	150
$\Delta T_c = (T_{c_3} - T_{c_1})$		7.13	9.02	7.25	6.19	7.97
T_{c_2}	$^\circ\text{F}$	-	-	-	-	154
T_{c_3}	$^\circ\text{F}$	168	173	165.5	163	159.5
$T_{\text{exh.}}$	$^\circ\text{F}$	688	949	700	475	807
W_a	$\frac{\text{lbs.}}{\text{hr.}}$	110	109	109.2	119.9	118.5
W_c	$\frac{\text{lbs.}}{\text{hr.}}$	3565	3617	3565	3558	3580
W_{fuel}	$\frac{\text{lbs.}}{\text{hr.}}$	3.675	4.98	3.69	2.555	4.355
$\frac{F}{A}$ Ratio		.0334	.0457	.0338	.0213	.0367
B.H.P.		7.68	11.62	7.83	3.755	9.76
B.M.E.P.		60.2	89.6	61.25	29.42	76.25
B.M.E.P. Corr.		59.1	88.8	60.15	27.92	75.25
$\eta_{\text{mech.}}$	%	64.7	73.5	65.2	47.2	69.8
I.M.E.P.		91.4	119.4	92.3	59.2	107.8
B.S.F.C.	$\frac{\text{lbs.}}{\text{B.H.P. hr.}}$.487	.432	.488	.7124	.4521
I.S.F.C.	$\frac{\text{lbs.}}{\text{I.H.P. hr.}}$.315	.3178	.318	.336	.3152
$\eta_{\text{B.Th.}}$	%	26.8	30.2	27.23	18.2	28.9
$\eta_{\text{I.Th.}}$	%	41.5	41.1	41.87	38.6	41.4
Q_{cooling}	$\frac{\text{B.T.U.}}{\text{hr.}}$	25420	32600	25850	22000	28520

TABLE XII.
Engine Test Results
Runs at $P_m \approx 36''$ Hg, $T_m \approx 80^\circ\text{F}$, Variable Speeds

Run Number	98	99	101	105	106	110	113	114	115	120
P_b	ins. Hg. 29.25	29.25	29.25	29.25	29.25	29.58	29.53	29.53	29.53	29.16
P_m	ins. Hg. 35.5	35.25	34.97	35.25	35.33	35.61	35.66	35.76	35.38	35.04
T_m	$^\circ\text{F}$ 78	82.5	86	88.5	89.5	76	82	83	86	79.8
N	R.P.M. 993	1240	1555	1421	1001	1315	1257	1362	1769	1270
T_o	$^\circ\text{F}$ 155	172.5	186	185.5	176	172	173	178	193	177
T_w , exh.	$^\circ\text{F}$ 170	181	182	191	204	169	186	183	190	182
T_{l1}	$^\circ\text{F}$ 188	201	205.5	215	231	181.5	209	208	214	207
T_{l2}	$^\circ\text{F}$ 178	189.5	190	193	205	178	192	190	196	189
T_{l3}	$^\circ\text{F}$ 174	182	182	183	191.5	174.1	185	183	186	182
T_s	$^\circ\text{F}$ 132	145	153	154	148	144	146	148	158	146
$\Delta T_c = (T_c - T_{c1})$	6.07	6.05	6.15	7.64	10.75	3.99	6.8	6.96	6.26	7
T_{o2}	$^\circ\text{F}$ 154	160	157	-	162	154	-	-	152	-
T_{c3}	$^\circ\text{F}$ 158	165.5	162	160.5	170	157	168	174	158	162
$T_{exh.}$	$^\circ\text{F}$ 427	534	674	850	947	405	676	685	832	717
W_a	$\frac{\text{lbs.}}{\text{hr.}}$ 111	137	174	159.2	111	149.2	138.5	156	199	140.2
W_c	$\frac{\text{lbs.}}{\text{hr.}}$ 2940	3642	4542	4170	2968	3660	3690	3990	5220	3720
W_{fuel}	$\frac{\text{lbs.}}{\text{hr.}}$ 2.41	3.39	4.98	6.05	5.365	2.461	4.54	4.79	6.28	4.71
F Ratio	.0217	.0246	.0287	.0379	.0483	.0165	.0328	.0307	.0316	.0336
B.H.P.	4.55	6.61	9.41	13.43	12.39	3.13	9.5	10.17	11.4	10.35
B.M.E.P.	43.55	50.9	57.5	89.7	117.4	22.6	75.7	71	61.3	77.5
B.M.E.P. Corr.	42.05	49.5	56.2	88.7	116.7	21	74.55	69.8	60.1	76.4
$\eta_{\text{mech.}}$ %	59.7	60.8	59.85	71.7	79.4	39.9	68.4	67	58.2	69.9
I.M.E.P.	70.5	81.5	93.9	123.8	147	52.7	109	104.2	103.3	109.2
B.S.F.C. $\frac{\text{lbs.}}{\text{H.P. hr.}}$.548	.528	.542	.4562	.436	.848	.485	.479	.562	.461
I.S.F.C. $\frac{\text{lbs.}}{\text{I.H.P. hr.}}$.3265	.3205	.324	.3262	.346	.338	.3315	.321	.3265	.322
$\eta_{B.Th.}$ %	23.78	24.8	24.05	28.62	30	15.44	26.9	27.2	23.25	28.3
$\eta_{I.Th.}$ %	39.8	40.8	40.25	40	37.8	38.72	39.39	40.63	40	40.55
Q_{cooling} $\frac{\text{B.T.U.}}{\text{hr.}}$	17850	22000	27870	31810	31900	15400	25100	27790	32600	26020

TABLE XIII.
 Engine Test Results
 Extra Runs Referred To In The Calculations

Run Number		10	53	57	102
P_b	ins. Hg.	29.34	29.52	29.68	29.25
P_m	ins. Hg.	27.34	36.12	34.38	35.4
T_m	°F	72	81	77	88
N	R.P.M.	1740	566	656	1760
T_o	°F	184	153.5	148	194
T_w exh.	°F	194	184	168	184
T_{l_1}	°F	201	199.5	178	206
T_{l_2}	°F	183	189	173	189.5
T_{l_3}	°F	175	182	170	181
T_s	°F	119.5	117.5	126	159
$\Delta T_c = (T_{c_3} - T_{c_1})$		5.76	8.86	4.62	6.115
T_{c_2}	°F	-	158	157	-
T_{c_3}	°F	162	165.9	159.6	158.1
$T_{exh.}$	°F	842	509	318	746
W_a	$\frac{\text{lbs.}}{\text{hr.}}$	137.1	63.9	71.5	197.5
W_c	$\frac{\text{lbs.}}{\text{hr.}}$	5140	1730	1980	5232
W_{fuel}	$\frac{\text{lbs.}}{\text{hr.}}$	5.46	2.16	1.217	5.72
$\frac{E}{A}$ Ratio		.0398	.0338	.01701	.0289
B.H.P.		6.46	4.2	1.615	9.71
B.M.E.P.		35.3	70.5	23.6	52.5
B.M.E.P. Corr.		-	69.4	22	51.2
$\eta_{mech.}$	%	46.4	73.5	46.5	54.5
I.M.E.P.		76.2	94.4	47.4	94
B.S.F.C.	$\frac{\text{lbs.}}{\text{B.H.P. hr.}}$.845	.522	.802	.604
I.S.F.C.	$\frac{\text{lbs.}}{\text{I.H.P. hr.}}$.392	.384	.372	.3295
$\eta_{B.Th.}$	%	15.45	25	16.3	21.6
$\eta_{I.Th.}$	%	33.3	34	35	39.7
$Q_{cooling}$	$\frac{\text{B.T.U.}}{\text{hr.}}$	29600	15340	9150	32000

TABLE XIV.

Calculation of the Constant "C" in the Equation [2.11].

Run Number	53	57	62	74	89	95	96	97
Average water temperature °F.	161.47	157.3	163.27	158.4	160.05	168	168	165
Average wall temperature °F.	185.2	171.5	191	187.8	184.2	199	200	198.5
($T_{\text{wall aver.}} - T_{\text{water aver.}}$) °F	23.73	14.2	27.77	29.39	24.15	31	32	33.5
$Q_{\text{cooling}} \frac{\text{B.T.U.}}{\text{hr.}}$	15340	9150	20670	22800	18350	24220	25200	24200
$\alpha_c \frac{\text{B.T.U.}}{\text{sq. ft. hr. °F}}$	445	444	514	534	524	540	544	497
μ at $T_{\text{water average}}$	0.958	0.99	0.945	0.975	0.965	0.905	0.905	0.93
$\frac{W_c}{k}$	1807	2000	2586	2550	2410	2705	2770	2617
$\frac{H}{(\frac{W_c}{k})^{0.6}}$	90	95.8	111	110	107	115	116	113
$\frac{CU}{k}$ at average temperature	2.535	2.62	2.5	2.57	2.55	2.4	2.4	2.46
$(\frac{CU}{k})^{0.4}$	1.45	1.47	1.443	1.459	1.454	1.42	1.42	1.434
$(\frac{W_c}{k})^{0.6} (\frac{CU}{k})^{0.4}$	130.5	142.2	160.3	160.5	155.8	163.2	164.7	162

TABLE XV.

Calculation of the Constant "C" in the Equation [2.11].

Run Number	10	98	101	102	131	133
Average water temp. °F	159.1	155	158.9	155.1	163.5	155.5
Average wall temp. °F	185	179.2	186.5	186.5	198.5	187.5
($T_{\text{wall aver.}} - T_{\text{water aver.}}$) °F	25.9	24.2	27.6	31.4	35	32
Q_{cooling} B.T.U./hr.	29600	17850	27870	32000	32200	28520
α_c B.T.U./sq.ft.°F.hr.	788	510	698	702	633	614
μ at $T_{\text{water average}}$	0.97	1.01	0.98	1.01	0.95	1.0
$\frac{Wc}{\mu}$	5300	2910	4635	5170	3740	3580
$(\frac{Wc}{\mu})^{0.6}$	171.5	120	159	170	139	135
$\frac{c\mu}{k}$ at average temp.	2.58	2.67	2.59	2.68	2.51	2.65
$(\frac{c\mu}{k})^{0.4}$	1.461	1.481	1.464	1.484	1.445	1.475
$(\frac{Wc}{\mu})^{0.6} (\frac{c\mu}{k})^{0.4}$	250.3	177.8	233	252	201	199

CALCULATION OF "C" IN EQUATION [2.11]

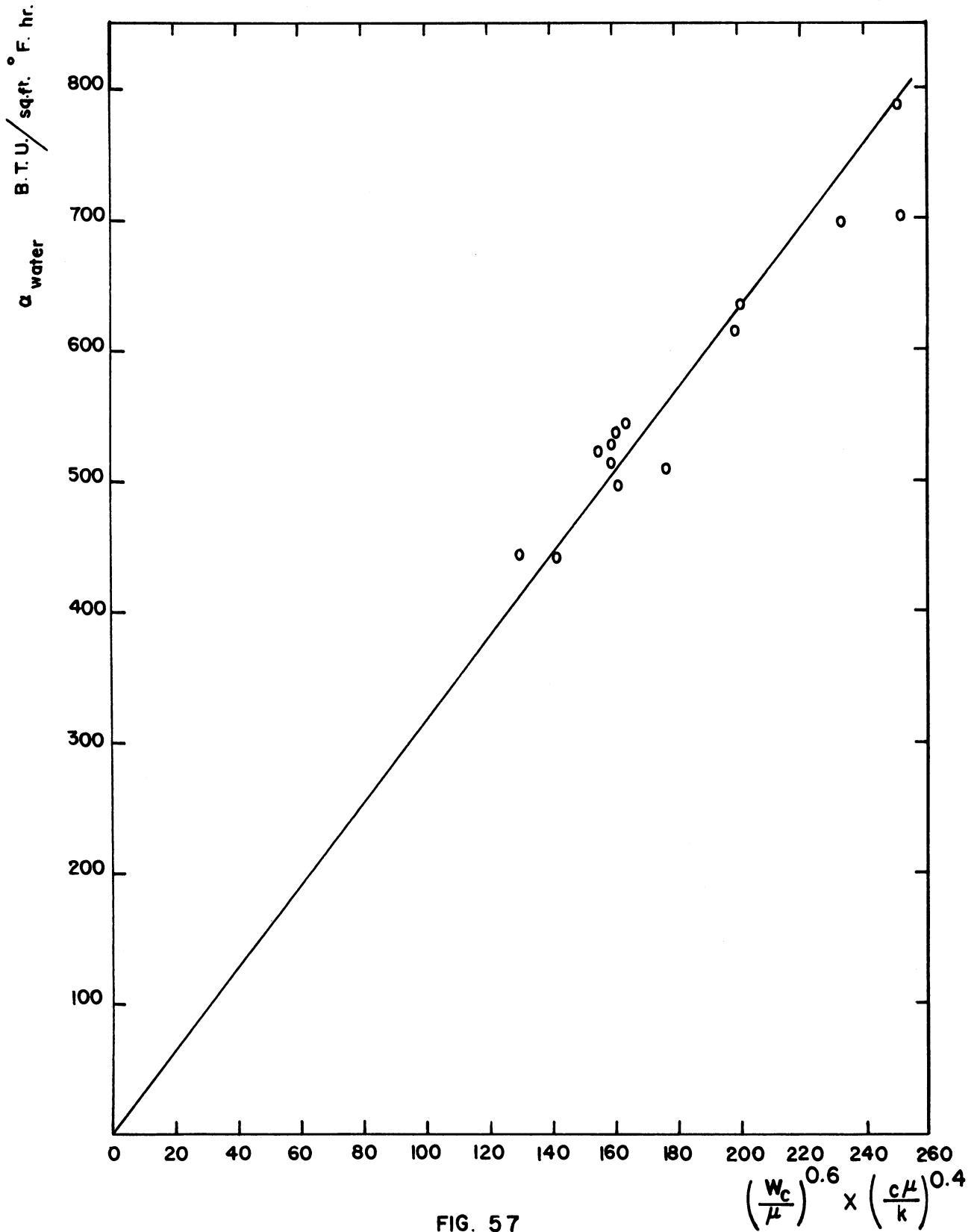


FIG. 57

APPENDIX E

CALCULATION OF THE MEAN WALL-TEMPERATURES
FOR RUN NO. 95

1. Wall temperature over the whole cycle.
2. Wall temperature at any crank angle.
3. Mean wall temperature during the intake stroke.

1. Wall Temperature Over The Whole Cycle:

The areas enclosing the gas consist mainly of the combustion chamber and the cylinder liner areas.

- a. The combustion chamber area equals 48.4 sq. ins. and its mean temperature was calculated from figure (22)
= 243.6 F
- b. The cylinder liner area equals 74.2 sq. ins. and its temperature at T.D.C. equals that of the combustion chamber and changes to lower values toward the B.D.C. This change was calculated from the readings of the three thermocouples measuring the liner outside surface temperature, and the temperature drop ΔT through the liner walls.

$$\Delta T = \frac{Q_{ln} \frac{D_2}{D_1}}{2\pi k_w L}$$

where

$$\begin{aligned} Q &= \text{heat gained by water in the engine barrel} \\ &= W_c \times \text{sp. ht.} \times (T_{c_2} - T_{c_1}) \\ &= 2435 \times 4 &= 9740 \frac{\text{B.T.U.}}{\text{hr.}} \\ D_2 &= 5.063 \text{ ins.} \\ D_1 &= 4.5 \text{ ins.} \end{aligned}$$

$$\begin{aligned} k_w: & \text{ thermal conductivity of the wall} = 27 \\ L & = \text{stroke} = 5.25 \text{ ins.} \\ \therefore \Delta T & = \frac{9740 \ln \frac{5.063}{4.5} \times 12}{2\pi \times 27 \times 5.25} = 15.6 \text{ }^\circ\text{F} \end{aligned}$$

This temperature drop was added to the reading of the thermocouple midway between the T.D.C. and the B.D.C., and the curve a b c d, figure (58), representing the liner inside wall temperature was drawn.

2. Wall Temperature At Any Crank Angle:

The curve a b c d, figure (58) representing the liner temperature was extended to point e which represents the liner temperature at a point beyond the first piston-ring, and this temperature was assumed constant. At any crank angle, the temperature of the wall could be found by drawing a curve between point e and the temperature of the combustion chamber at the same angle.

3. Mean Wall Temperature During The Intake Stroke:

The wall temperature during the intake stroke was found by using the method under item No. 2. The mean combustion chamber temperature during the suction stroke = 238°F.

The mean temperature of the combustion chamber and liner,
(figure 58) = 224°F.

The mean area of the combustion chamber and liner,
(figure 54) = 122.6 sq. in.

During the intake stroke the air is in contact with the intake manifold, whose area equals 34.3 sq. ins., and at a temperature of 170°F, assumed equal to that of the cooling water in the cylinder head.

∴ Mean temperature of the walls during the intake stroke =

$$\frac{224 \times 122.6 + 34.3 \times 170}{122.6 + 34.3} = 212 \text{ }^\circ\text{F}$$

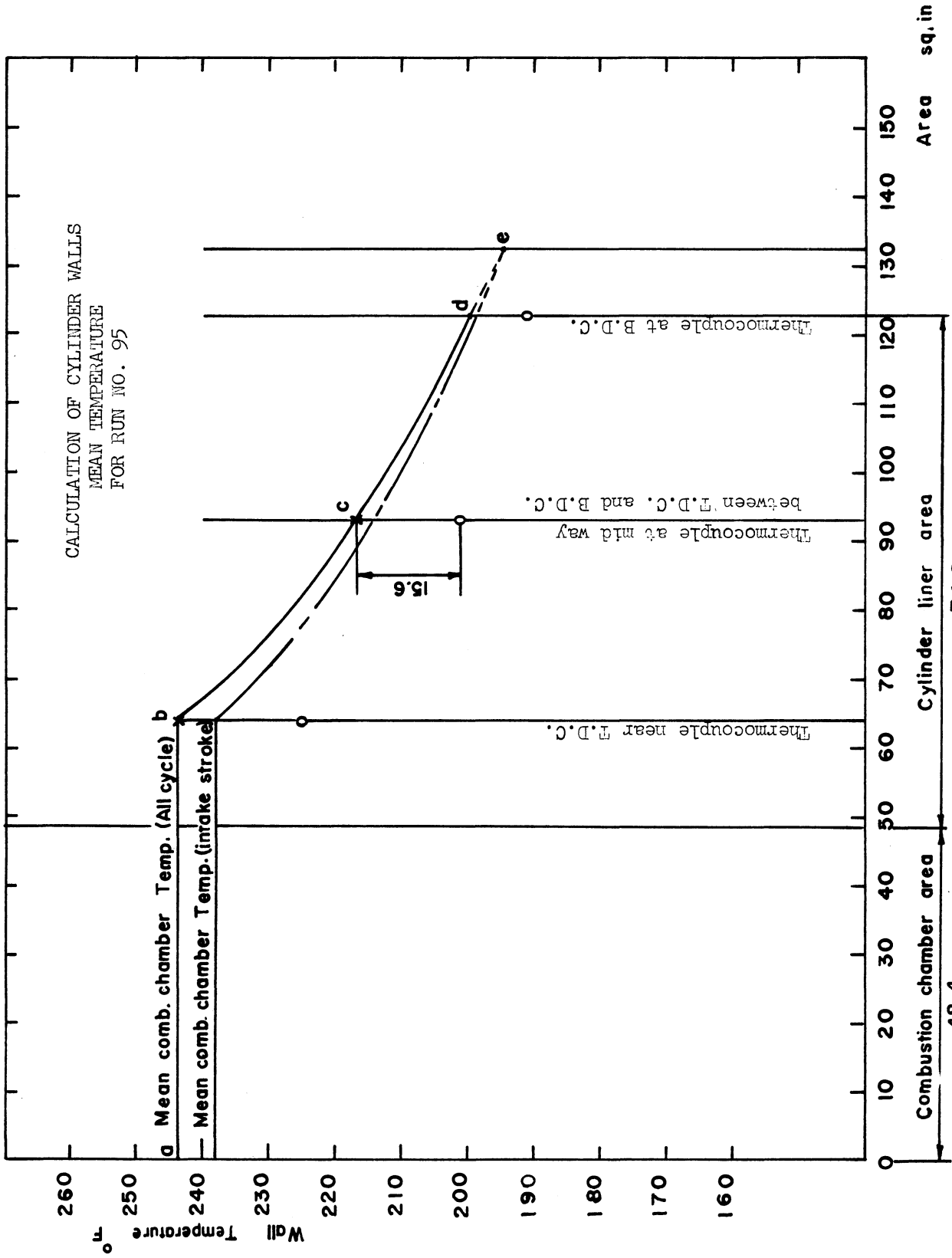


FIG. 58 74.2

TABLE XVI

α_M = Mean Coefficients of Heat Transfer and
 $T_{M.E.}$ = Mean Effective Temperatures

Run Number	1	94	30	95	96	62	97	70	
$P_m \frac{\text{lbs.}}{\text{sq. in.}}$	14.08	14.48	15.82	16.02	17.59	19.30	18.86	20.56	
T_m °R	543	550	533.5	550	548	539.5	543	548.5	
N R.P.M.	807	826	793	821	840	817	814	815	
$S \frac{\text{Ft.}}{\text{sec.}}$	11.77	12.03	11.55	11.97	12.23	11.9	11.87	11.88	
C_M	Intake	11.42	11.8	12.3	12.02	13.13	13.58	12.72	14.28
	Compression	26.2	28	28.15	26.55	33.3	31.6	32.6	32.8
	Expansion	51.8	68.1	52.7	70.3	76.4	69.4	77.4	79.6
	Exhaust	16.1	18.6	14.9	18.56	18.95	16.9	17.37	17.85
	Total Cycle	26.38	31.63	27.01	31.86	35.45	32.87	35.02	36.13
$(C_M^{T.M.E.}) \times 10^{-4}$	Intake	.688	.74	.767	.796	.811	.821	.797	.895
	Compression	2.3	2.85	2.67	2.415	3.4	3.14	3.38	3.23
	Expansion	8.97	15.4	9.74	15.5	18.18	14.88	17.86	17.78
	Exhaust	1.535	2.415	1.32	2.48	2.48	1.641	2.12	2.27
	Total Cycle	3.373	5.351	3.624	5.298	6.218	5.121	6.04	6.044
$T_{M.E.}$ °R	1278	1690	1342	1660	1755	1557	1722	1670	
C_M Calculated	25.85	30.2	27.22	32.7	34.8	32.6	34.30	36.95	
$T_{M.E.}$ °R Calculated	1380	1718	1381	1750	1738	1504	1646	1700	
I.M.E.P $\frac{\text{lbs.}}{\text{sq. in.}}$	61.2	112.5	70.0	132	142.2	107.8	132.5	152	

TABLE XVII

α_M = Mean Coefficients of Heat Transfer and

$T_{M.E.}$ = Mean Effective Temperatures

Run Number	84	89	72	74	127	131	124	133	
P_m $\frac{\text{lbs.}}{\text{sq. in.}}$	20.24	20.5	21.68	21.6	17.58	17.42	17.4	17.46	
T_m $^{\circ}\text{R}$	546	545	543.5	548	605	601	657	664	
N R.P.M.	805	775	823	832	1216	1204	1231	1214	
S $\frac{\text{Ft.}}{\text{sec.}}$	11.72	11.3	12	12.12	17.72	17.58	17.97	17.71	
α_M	Intake	14.18	13.97	14.58	13.97	15.33	15.22	15.9	15.7
	Compression	36.6	34.3	35.28	33.5	36	34.9	34	34.8
	Expansion	54.6	60	57	68.4	83.1	87.7	81.7	78.4
	Exhaust	14	14.42	14	16	21.35	21.57	22.18	20.55
	Total Cycle	29.85	30.67	30.215	32.97	38.95	39.85	38.45	37.35
$(\alpha_M^{T_{M.E.}}) \times 10^{-4}$	Intake	.902	.87	.893	.912	.975	1.0	1.085	1.083
	Compression	3.5	3.31	3.48	3.25	3.882	3.725	3.615	3.79
	Expansion	9.0	11.35	8.94	13.43	19.4	22.0	19.6	18.15
	Exhaust	1.082	1.30	1.068	1.503	2.88	2.96	3.13	2.64
	Total Cycle	3.621	4.21	3.595	4.774	6.784	7.421	6.856	6.416
$T_{M.E.}$ $^{\circ}\text{R}$	1212	1372	1190	1448	1740	1862	1782	1720	
α_M Calculated	29	30.75	29.82	33.32	38.60	39.20	39.63	38.57	
$T_{M.E.}$ $^{\circ}\text{R}$ Calculated	1202	1352	1178	1422	1757	1792	1852	1790	
I.M.E.P. $\frac{\text{lbs.}}{\text{sq. in.}}$	57.3	83	58	98.6	120.8	129.8	119.4	107.8	

TABLE XVIII
 COMBUSTION CHAMBER WALL TEMPERATURES
 CALCULATED AND MEASURED

Run No.	P _m inches Hg absolute	T _m °F	N R.P.M.	F/A Ratio	I.M.E.P. lbs. per sq. in.	T _{w.g.} calculated °F	T _{w.g.} measured °F	Error °F	% Error
Constant Speed 800 R.P.M. and Constant T _m									
P _m = 30 ins. Hg.									
1	28.75	83	807	.0261	61.2	192.5	212.8	20.3	9.5
2	28.78	84	800	.0463	101	225.2	231.9	6.7	2.9
94	29.55	90	826	.0515	112.5	273.8	245	-28.8	-11.7
4	28.56	72	810	.0528	116.2	251	258.3	7.3	2.8
P _m = 33									
81	32.84	86	796	.0205	55.4	198.5	219	20.5	9.4
93	32.55	87.5	832	.0455	118.2	261.8	237.9	-23.9	-10
36	32.3	87	790	.0444	121.5	237.2	231.6	-5.6	-2.4
95	32.62	90	821	.0511	132	249.3	243.6	5.7	2.34
37	31.93	77	830	.0546	141.6	242.7	241.6	-1.1	-0.5
P _m = 35									
47	35.12	73	828	.0179	51.3	188.2	200.4	12.2	6.1
51	35.25	80.5	850	.0431	129	240.8	227.2	-13.6	-6
52	35.17	81	847	.0519	145.7	250.8	229.7	-21.1	-9.2
P _m = 39									
83	38.54	87	820	.0174	53.3	200.4	208.5	8.1	3.9
97	38.47	83	814	.0412	132.5	250.1	237.9	-12.2	-5.1
64	39.24	82	807	.0424	146.5	241.8	246.2	4.4	1.8
71	39.27	90	789	.0448	149	255.2	260.7	5.5	2.1
P _m = 42									
66	41.47	76	827	.0154	54.8	193.1	206.7	13.6	6.6
90	41.8	72.5	837	.0336	116	234.3	245	10.7	4.4
69	41.72	86.5	805	.035	127	240.5	252.2	11.7	4.6
70	41.97	88.5	815	.0434	152	262.5	260.4	-2.1	-0.8
P _m = 45									
72	44.25	83.5	823	.0154	58	186.6	211.1	24.5	11.6
74	44.05	88	832	.0257	98.6	220.2	244.9	24.7	10.1
75	44.55	89.5	815	.030	118.6	234.2	254.6	20.4	8
76	44.70	90	815	.0357	135.2	237.7	250.4	12.7	5

TABLE XIX
 COMBUSTION CHAMBER WALL TEMPERATURES
 CALCULATED AND MEASURED

Run No.	P _m inches Hg absolute	T _m OF	N R.P.M	F/A Ratio	I.M.E.P. lbs. per sq. in.	T _{w.g.} calcu- lated OF	T _{w.g.} measured OF	Error OF	% Error										
P _m = 35" Hg, T _m = 80°F, Variable R.P.M. and F/A ratio										98	35.5	78	993	.0217	70.5	203.2	232.8	29.6	12.7
										106	35.33	89.5	1001	.0483	147	255	259.6	4.6	1.8
										99	35.25	82.5	1240	.0246	81.5	215.7	235.4	19.7	8.4
										113	35.66	82	1257	.0328	109	229.8	236.9	7.1	3
										120	35.04	79.8	1270	.0336	109.2	225.2	255.5	31.3	12.2
										110	35.61	76	1315	.0165	52.7	190.9	187.9	-3	-1.6
										114	35.76	83	1362	.0307	104.2	232.8	245	12.2	5
										105	35.25	88.5	1421	.0379	123.8	233	257.2	24.2	9.4
										101	34.97	86	1555	.0287	93.9	220.2	243	22.8	9.4
										115	35.38	86	1769	.0316	103.3	218.7	248	29.8	11.8
T _m = 80°F										104	35.45	90.5	1197	.0362	122	243.8	260.5	16.7	6.4
										136	35.48	82.5	1223	.038	123.1	226.6	264	27.4	10.4
										130	35.83	80	1190	.0451	145.9	240.8	246.2	5.4	2.2
P _m = 36" Hg, R.P.M. = 1200 T _m = 140°F										128	35.78	144	1204	.0239	70	215.4	223	7.6	3.4
										126	35.72	141	1216	.0311	96.7	230.2	240.9	10.7	4.4
										127	35.85	145	1216	.0397	120.8	239.4	242.7	3.3	1.4
										131	35.56	141	1204	.0468	129.8	251.8	247.5	-4.3	-1.7
										123	35.64	193	1212	.0334	91.4	238.4	241.5	3.1	1.3
P _m = 36" Hg, R.P.M. = 1950 T _m = 195°F										125	35.71	198	1212	.0338	92.3	238.8	248	9.2	3.7
										133	35.62	204	1214	.0367	107.8	242.7	228.5	-14.2	-6.2

TABLE XX

CALCULATED THERMAL LOADINGS AND MEASURED HEAT LOSSES TO COOLING WATER

Run No.	U B.T.U. hr. sq.ft. °F	Q Calculated B.T.U. hr.	Q Measured B.T.U. hr.	Error B.T.U. hr.	% Error		
Constant Speed 800 R.P.M., Constant T_m	$P_m = 30''$ Hg.	1	24.36	13350	13900	350	2.52
		2	26.4	19100	18900	-200	-1.06
		94	28.1	21270	21650	380	1.75
		4	27.6	21250	22400	1150	5.15
	$P_m = 33$	81	24.65	11720	15000	3280	21.85
		93	29.4	21900	21650	-250	-1.15
		36	29	22200	21300	-900	-4.23
		95	30.4	23900	24220	320	1.32
		37	30.4	25050	26280	1230	4.68
	$P_m = 36$	47	25.3	10670	12420	1750	14.1
		51	31.4	22700	24600	1900	7.73
		52	31.95	25600	27800	2200	7.9
$P_m = 39$	83	26.3	10770	12300	1530	12.4	
	97	31.63	22860	24200	1340	5.55	
	64	32.7	24500	26500	1900	7.16	
	71	32.7	25370	28800	3430	11.9	
$P_m = 42$	66	26.9	10470	12800	2330	18.2	
	90	31.38	19650	21200	1550	7.3	
	69	31.95	21900	24000	2100	8.75	
	70	33.9	25750	29550	3800	12.87	
$P_m = 45$	72	27.8	11200	12720	1520	11.94	
	74	30.93	17520	22800	5280	23.2	
	75	32.4	20400	22400	2000	8.95	
	76	33.5	22900	25500	2600	10.2	

TABLE XXI

CALCULATED THERMAL LOADINGS AND MEASURED HEAT LOSSES TO COOLING WATER

	Run No.	U B.T.U. hr. sq.ft. °F	Q Calculated B.T.U. hr.	Q Measured B.T.U. hr.	Error B.T.U. hr.	% Error	
P _m = 36" Hg, T _m = 80°F and Variable R.P.M.	98	28.5	14680	17850	3170	17.75	
	106	34.1	27800	31900	4100	12.85	
	99	31.6	17800	22000	4200	19.1	
	113	33.9	23100	25100	2000	7.97	
	120	33.86	22830	26020	3190	12.25	
	110	29.95	12670	15400	2730	17.72	
	114	34.4	22200	27790	5590	20.1	
	105	36.45	26900	31810	4910	15.45	
	101	35.1	21880	27870	5990	21.45	
	115	37.45	24770	32600	7830	24	
P _m = 36" Hg., R.P.M. = 1200	T _m = 80°F	104	34.37	24850	24750	100	0.4
	136	34.56	25300	27620	2320	8.4	
	130	36	28750	32250	3500	10.85	
P _m = 36" Hg., R.P.M. = 1200	T _m = 140°F	128	31.6	18250	22550	4300	19.1
	126	33.7	23500	25300	1800	7.1	
	127	35.62	28500	30580	2080	6.8	
	131	36.4	29650	32200	2550	7.92	
P _m = 36" Hg., R.P.M. = 1200	T _m = 195°F	123	34.15	25000	25420	420	1.65
	125	34.23	25500	25850	350	1.35	
	133	35.6	29300	28520	-780	-2.74	

APPENDIX F

SCAVENGING AIR FLOW-RATE

For the engine used in experimental work, the opening of the inlet valve and the closing of the exhaust valve allowed a period of overlap of 36 crank angles.

Air flowing during this period through the exhaust valve does not take part in the combustion process. For the purpose of comparison between the operating conditions studied it was assumed that the air flow rate is function only of the square root of the difference in pressure head between the inlet and exhaust manifolds.

While the engine was at rest the air pressure in the intake surge tank was kept constant at 6" Hg above the atmospheric, while the back pressure was atmospheric, the air flow rate was measured for different crank angles over the scavenging period. The results are shown in the following table and in figure (59).

Crank angles before T.D.C.	6.5	5.5	4	3.7	2.7	0.9
Flow rate $\frac{\text{lbs.}}{\text{sec.}}$.00495	.0071	.01005	.0112	.0127	.0185

Crank angles after T.D.C.	0.6	2.4	3	6.8	8.2	9.7	11.3
Flow rate $\frac{\text{lbs.}}{\text{sec.}}$.0224	.0256	.0258	.0196	.0049	.00115	.00075

From figure (59) the average flow rate of the scavenging air,

(at $\Delta P = 6''$ Hg. and $T_m = 77^\circ\text{F}$) = 0.764×10^{-2} lbs. per sec.

For any run with the air at P_m and T_m the average flow rate during the scavenging period was calculated from

$$W_a = 0.764 \times 10^{-2} \sqrt{\frac{(P_m - 30)}{6}} \times \frac{537}{T_m} \text{ lbs. per sec.}$$

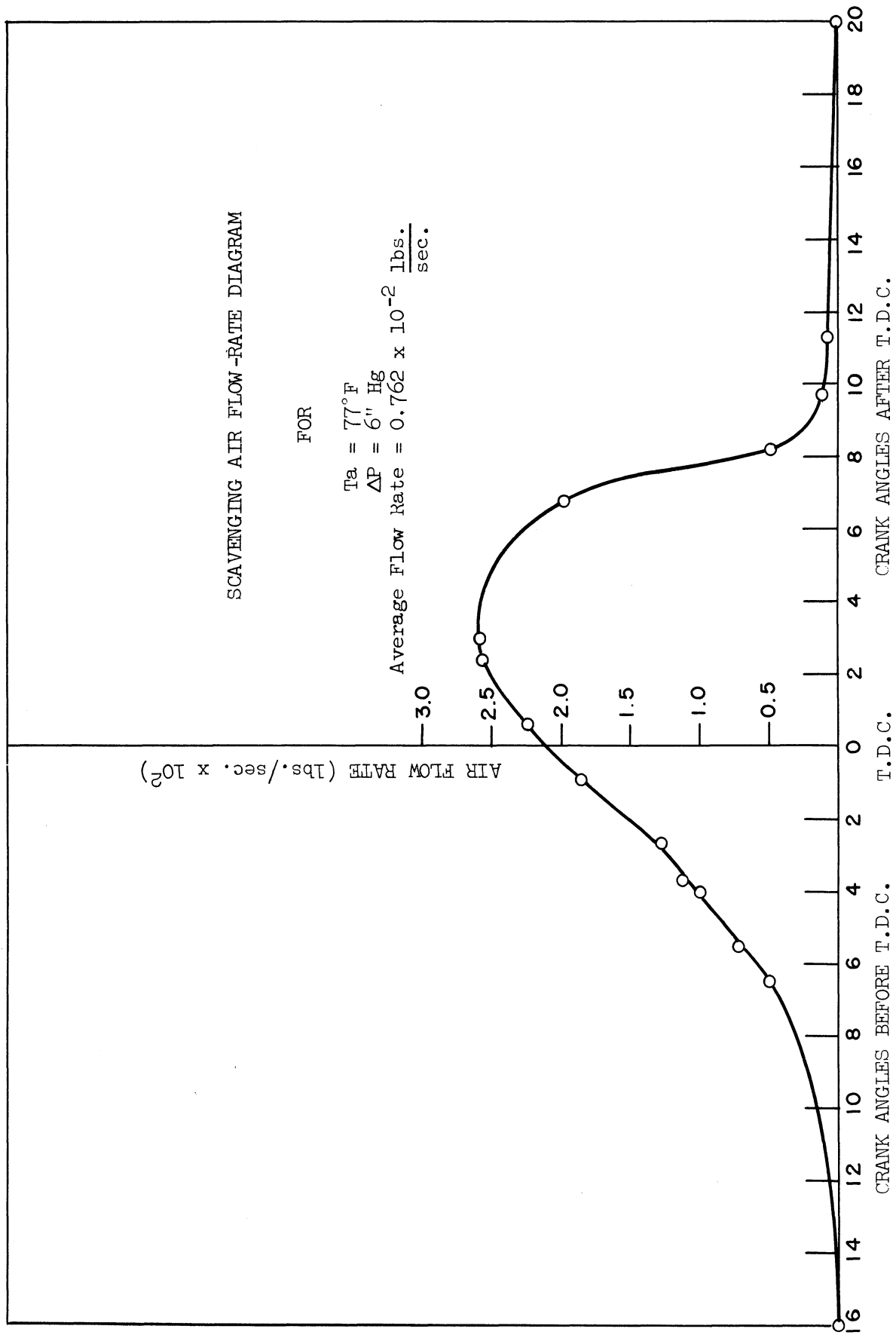


FIGURE 59

APPENDIX G

SAMPLE CALCULATIONS FOR THE EFFECT OF AFTERCOOLING

Assumed Operating Conditions:

Aftercooler effectiveness, ϵ	=	50%
Air pressure at the intake manifold	=	45 ins. Hg.
Pressure drop between compressor and engine	=	0.5 $\frac{\text{lb.}}{\text{sq.in.}}$
P_2 : Pressure at compressor outlet	=	$45 \times 0.49 + 0.5 = 22.5 \frac{\text{lb.}}{\text{sq.in.}}$
P_1 : Pressure at compressor inlet	=	$14.7 \frac{\text{lb.}}{\text{sq. in.}}$
T_1 : Temperature at compressor inlet	=	540°R
η_c : Compressor efficiency	=	80%

Calculations:

h_1^*	=	129.1 $\frac{\text{B.T.U.}}{\text{lb.}}$
P_{r1}	=	1.386
$P_{r2} = 1.386 \times \frac{22.5}{14.7}$	=	2.12
h_2'	=	145.8 $\frac{\text{B.T.U.}}{\text{lb.}}$
Δh isentropic = $h_2' - h_1 = 145.8 - 129.1$	=	16.7 $\frac{\text{B.T.U.}}{\text{lb.}}$
$h_2 - h_1 = \frac{h_2' - h_1}{\eta_c}$	=	20.86
h_2	=	149.96 $\frac{\text{B.T.U.}}{\text{lb.}}$
T_2	=	627 %
ϵ : Aftercooling effectiveness = $\frac{T_2 - T_m}{T_2 - T_1}$	=	50 %
$\therefore T_m$	=	583.5 °R
Correction factor for the I.M.E.P., $\frac{T_m}{T_1}$	=	0.925

* Keenan and Kaye Tables, Reference No. 20.

The power output of the turbocharged engine was calculated from the I.M.E.P. values of 45 ins. Hg. of figure (25), and the correction factor 0.925. The calculations will be continued for an output of 140 lbs. per sq. in.

$$\begin{aligned}
 T_{M.E.} \text{ calculated from equation [7.1]} &= 1682 \text{ } ^\circ\text{R} \\
 \alpha_M \text{ calculated from equation [7.2]} &= 37.3 \frac{\text{B.T.U.}}{\text{hr. sq. ft. } ^\circ\text{F}} \\
 k_w &= 27 \frac{\text{B.T.U.}}{\text{hr. sq. ft. } \left(\frac{^\circ\text{F}}{\text{ft.}}\right)}
 \end{aligned}$$

Equating in equation [2.21] we get

$$T_{p.g.} : \text{Piston-Top maximum temperature} = 965 \text{ } ^\circ\text{F}$$

For the calculations of the intensity of thermal loads the following conditions were considered:

$$\begin{aligned}
 T_c : \text{cooling water temperature} &= 160 \text{ } ^\circ\text{F} \\
 W_c : \text{cooling water flow rate} &= 2400 \frac{\text{lbs.}}{\text{hr.}} \\
 \text{Substituting in equations [2.11], we get } \alpha_c &= 500 \frac{\text{B.T.U.}}{\text{hr. sq. ft. } ^\circ\text{F}} \\
 a_m, \text{ from equation [7.5]} &= 0.877 \\
 a_c, \text{ from equation [7.6]} &= 0.782 \\
 x, \text{ from equation [7.7]} &= .282 \text{ in.} \\
 \text{By substitution in equation [2.15], the} & \\
 \text{intensity of thermal load} &= 36490 \frac{\text{B.T.U.}}{\text{hr. sq. ft.}}
 \end{aligned}$$

TABLE XXII
 PISTON-CROWN TEMPERATURES, AND INTENSITY OF THERMAL LOADS

$\epsilon = 0\%$

I.M.E.P. lbs. sq.in.	P_m ins. Hg.	T_m OR	Piston-Crown Maximum Temperatures OF					Intensity of Thermal Loads B.T.U. sq.ft. hr.						
			60	80	100	120	140	150	60	80	100	120	140	150
30	540		662	769	867	958	1040	1081	17985	22500	26890	31300	35720	37950
33	565		669	777	873	965	1051	1092	18770	23570	28050	32790	37350	39650
36	581		666	775	870	961	1046	1085	19100	23970	28650	33330	38050	40460
39	597.5		664	771	867	958	1045	1085	19480	24420	29240	34050	39010	41390
42	613.5		661	768	865	995	1042	1083	19770	24870	29780	34670	39690	42160
45	627		658	764	861	953	1038	1076	20060	25210	30230	35230	40350	42830

TABLE XXIII
 PISTON-CROWN TEMPERATURES, AND INTENSITY OF THERMAL LOADS

$\epsilon = 50\%$

I.M.E.P. lbs. sq.in.	P_m ins. Hr.	T_m OR	Piston-Crown Maximum Temperatures OF						Intensity of Thermal Loads $\frac{\text{B.T.U.}}{\text{sq.ft. hr.}}$					
			60	80	100	120	140	150	60	80	100	120	140	150
30	540		662	769	864	954	1040	1081	17985	22500	26890	31300	35720	37950
33	552.5		654	759	854	945	1029	1069	18090	22700	27140	31700	36260	38440
36	560.6		642	746	840	929	1012	1052	18050	22700	27250	31720	36390	38580
39	568.8		631	733	825	913	995	1035	18000	22640	27220	31780	36420	38670
42	576.8		619	722	813	900	982	1020	17940	22660	27270	31890	36490	38770
45	583.5		608	709	799	885	965	1003	17820	22550	27140	31810	36490	38940

TABLE XXIV
 PISTON-CROWN TEMPERATURES, AND INTENSITY OF THERMAL LOADS

$\epsilon = 100\%$

I.M.E.P. lbs. sq.in.	P_m ins. Hg.	T_m °R	Piston-Crown Maximum Temperatures OF					Intensity of Thermal Loads $\frac{\text{B.T.U.}}{\text{sq. ft. hr.}}$						
			60	80	100	120	140	150	60	80	100	120	140	150
	30	540	662	769	864	954	1040	1081	17985	22500	26890	31300	35720	37950
	33	540	638	742	835	924	1006	1046	17470	21995	26320	30760	35080	37330
	36	540	617	718	809	895	976	1014	16990	21480	25820	30180	34500	36740
	39	540	597	696	784	869	948	986	16530	20980	25250	29600	33850	36080
	42	540	578	675	762	844	921	959	16050	20490	24740	29030	33380	35480
	45	540	563	657	743	823	899	937	15710	20090	24360	28530	32880	35020

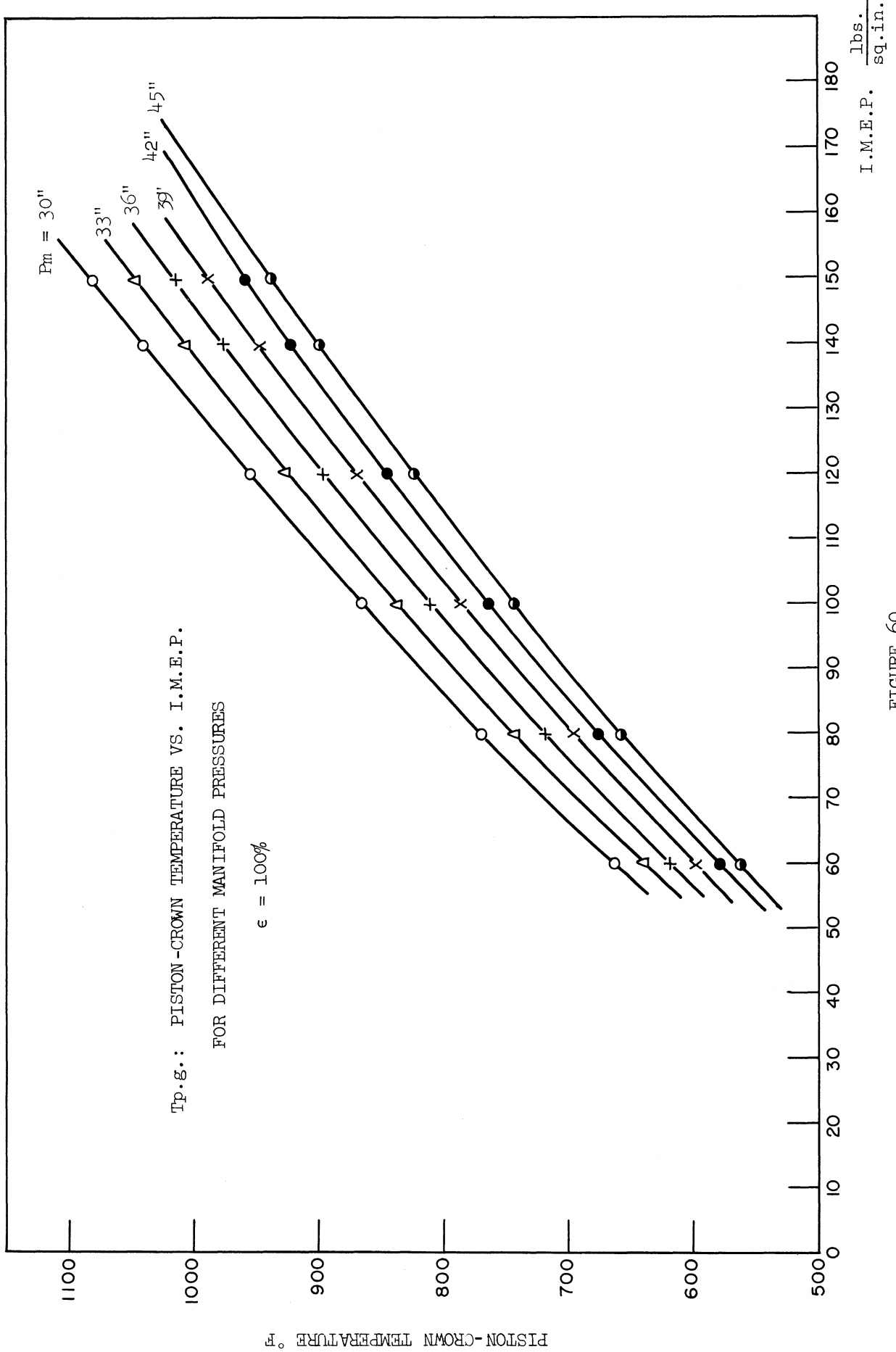


FIGURE 60

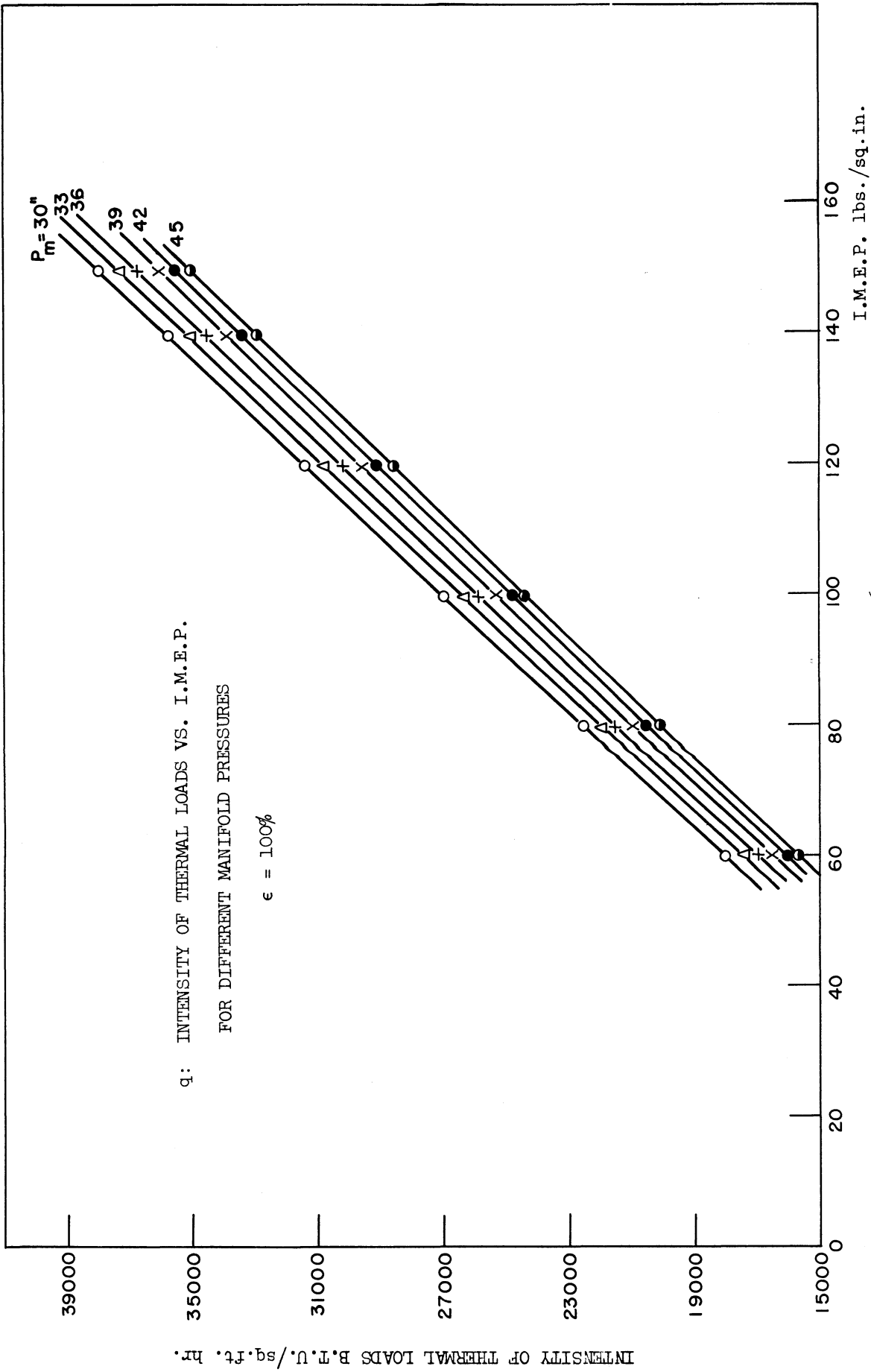


FIGURE 61

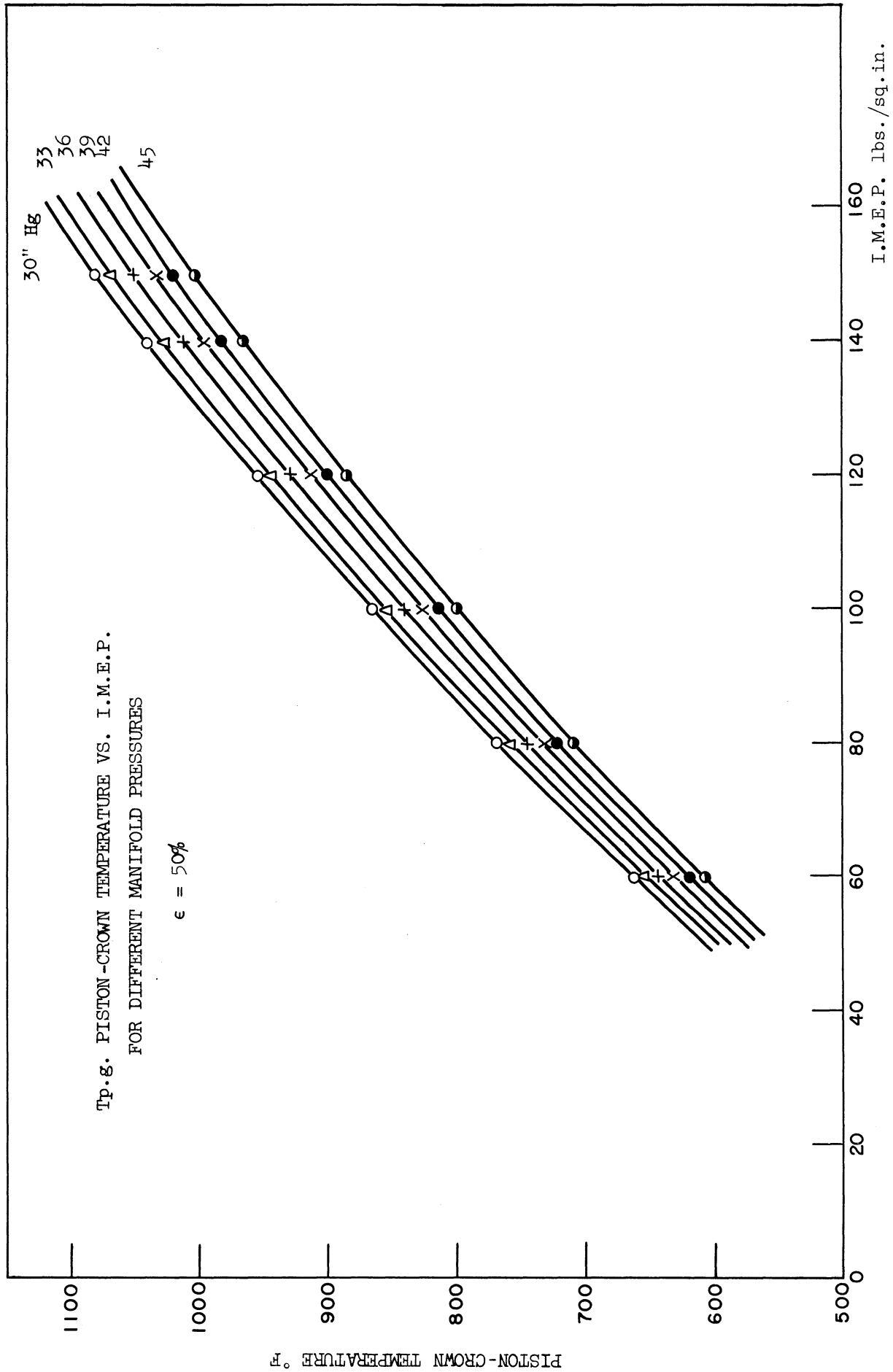


FIGURE 62

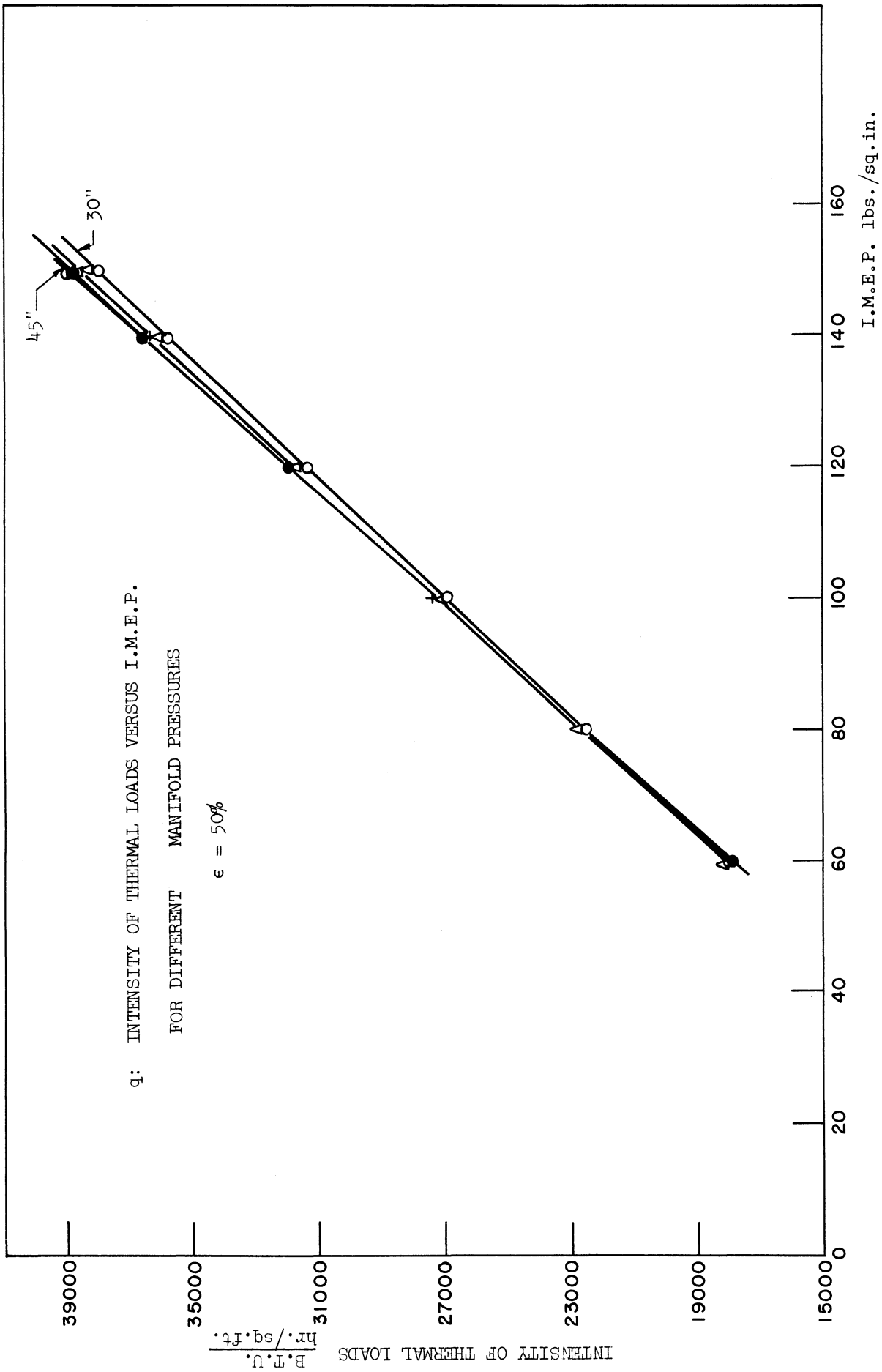


FIGURE 63

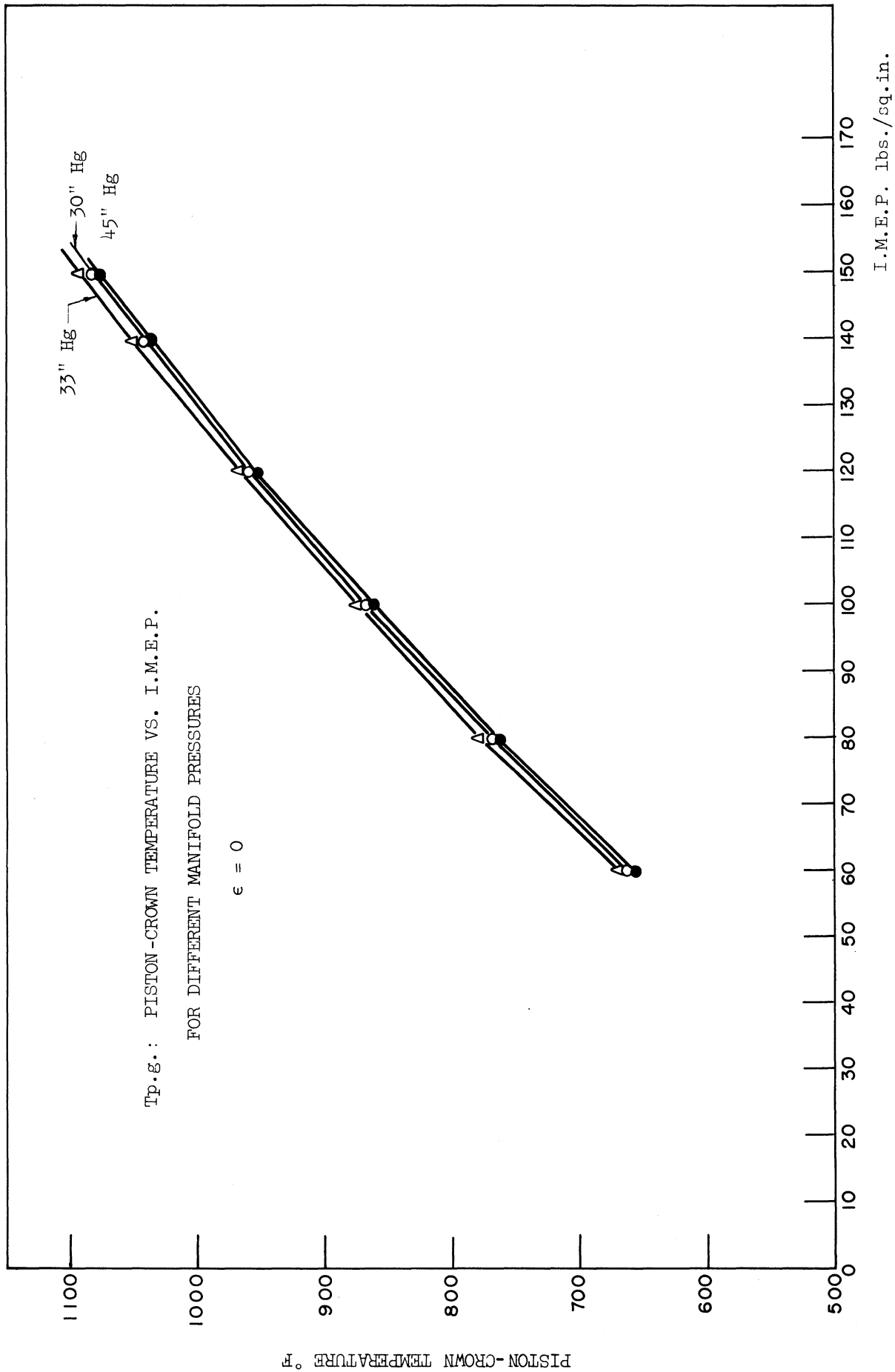


FIGURE 64

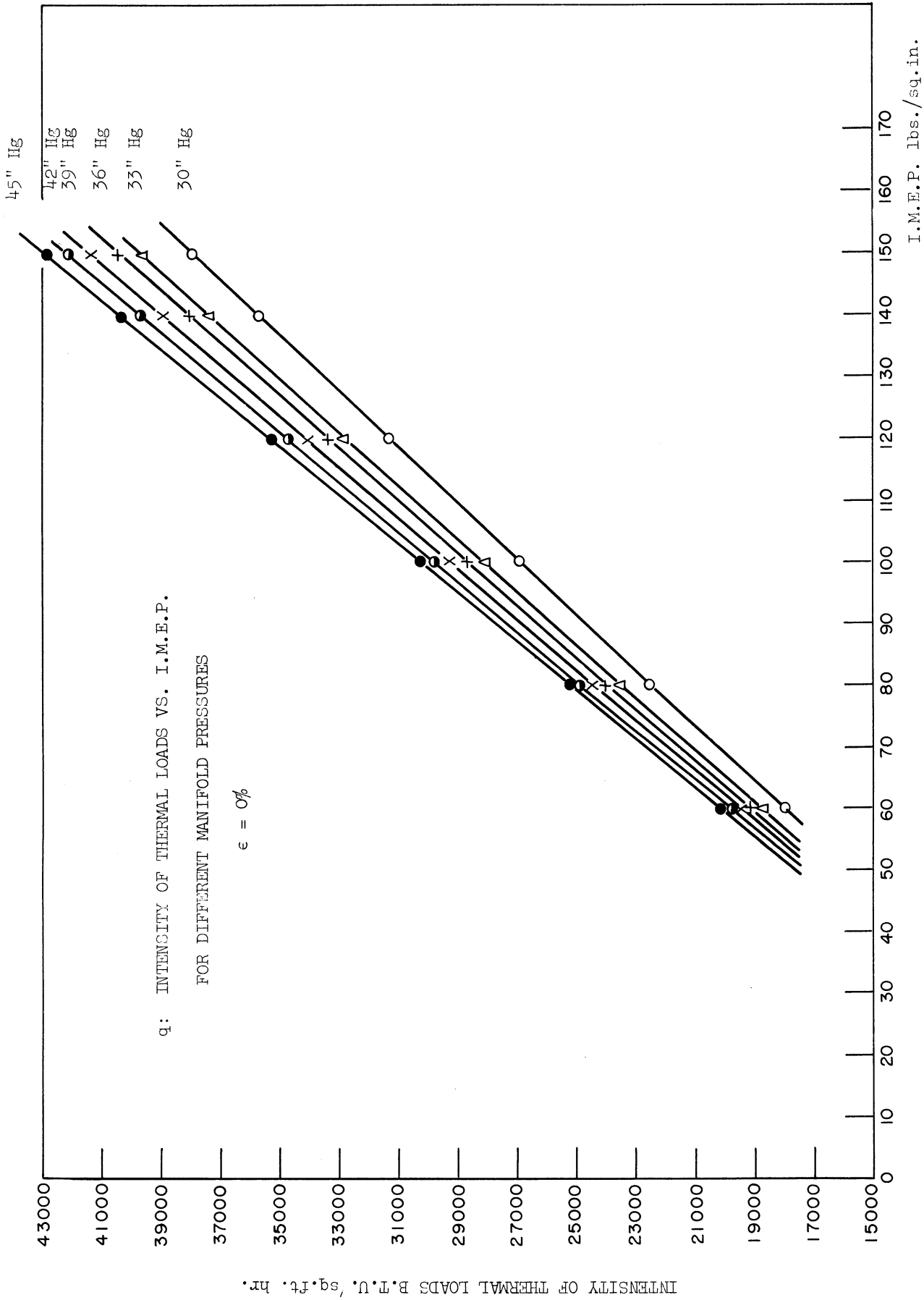


FIGURE 65

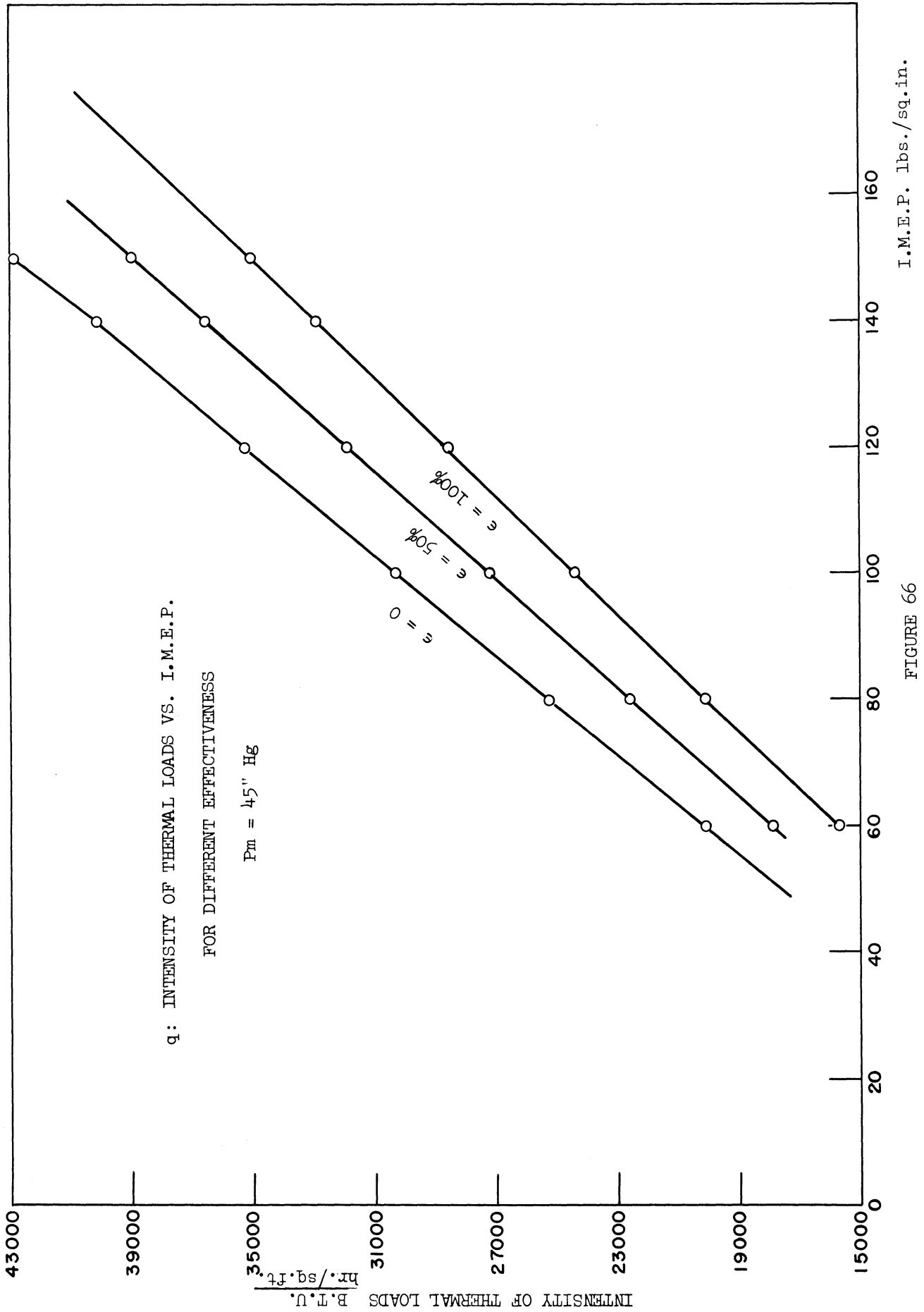


FIGURE 66

APPENDIX H

CORRECTION FACTOR FOR THE B.M.E.P.

The effect of the back pressure on the B.M.E.P. was not fully investigated. Some tests were made at different back pressures, and the B.M.E.P. was not affected until the back pressure was boosted to valves near the inlet manifold pressure. This indicated that the friction load, on the single cylinder engine used for the tests, was not very sensitive to the increase in the back pressure and the drop in the power output was rather due to the poor scavenging efficiency at these conditions.

The scavenging efficiency⁽⁵⁾ is function on the ratio $\frac{P_m - P_{exh.}}{P_m}$. To get the drop in the B.M.E.P. due to increase in the back pressure for an equal scavenging efficiency, a value of, 0.04, was used for the above ratio. This low value was chosen, because of the relatively low supercharging pressures reached in the tests. Few runs were made at an average intake manifold pressure of 35.6" Hg. The back pressure was changed from atmospheric to 34.2, with the $\frac{F}{A}$ constant, (Table 9). The drop in B.M.E.P. is shown in figure (67).

CORRECTION FACTOR FOR THE B.M.E.P.

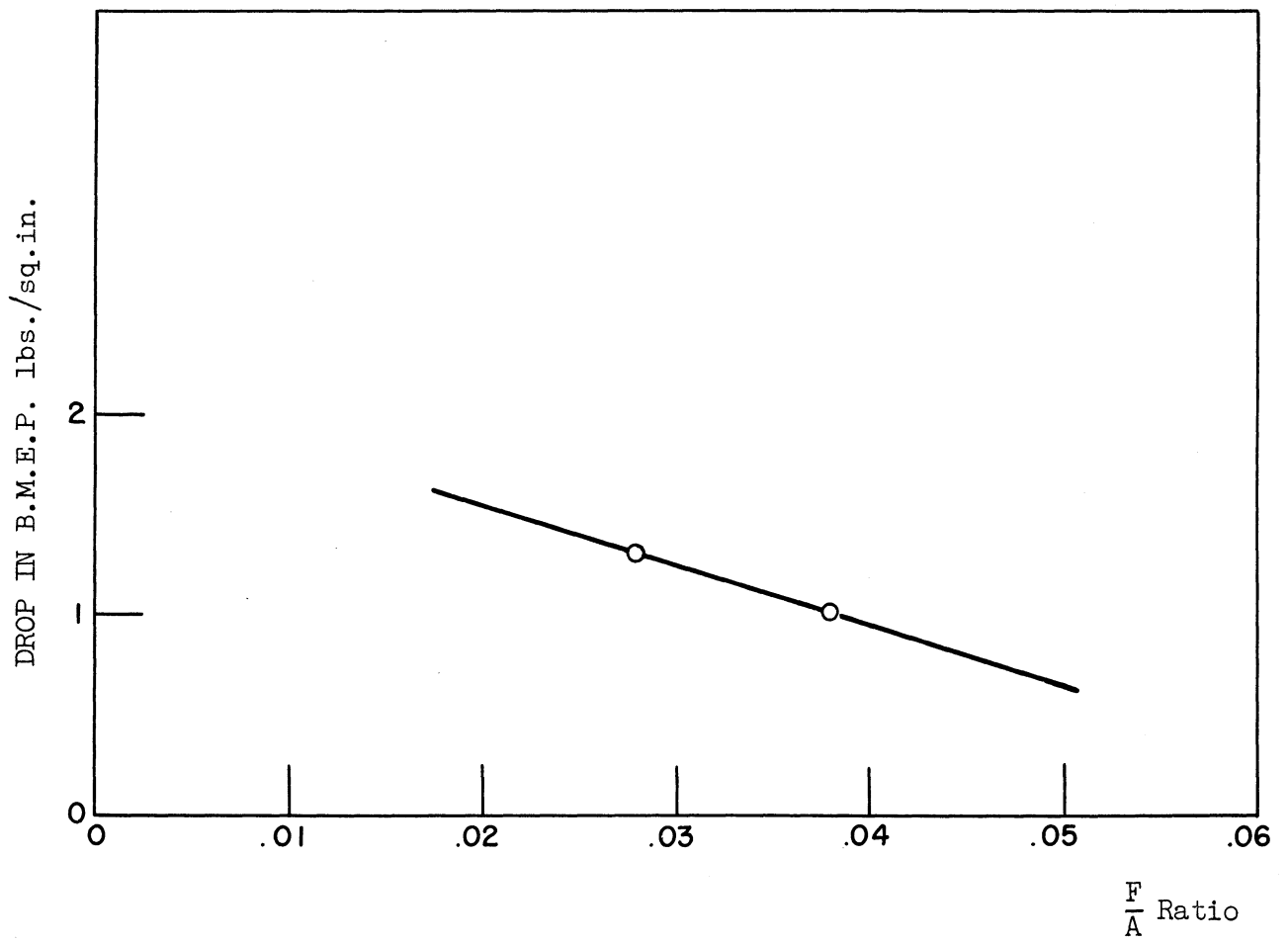


FIGURE 67

APPENDIX I

ENGINE SPECIFICATIONS

Manufacturer: Nordberg Mfg. Co., Milwaukee, Wisconsin, U.S.A.

Number of cylinders: 1

Cycle: 4 strokes per cycle

Compression ratio: 14.5

Bore: 4 1/2 inches

Stroke: 5 1/4 inches

Piston Displacement: 83.48 cubic inches.

Combustion Chamber Type: Energy Cell

Engine Timing, Crank Degrees

Fuel pump port closing: 30° before T.D.C.

Injection begins (approximately): 19° before T.D.C.

Exhaust valve opens: 45° before B.D.C.

Exhaust valve closes: 20° after T.D.C.

Intake valve opens: 16° before T.D.C.

Intake valve closes: 38° after B.D.C.

BIBLIOGRAPHY

1. A.S.M.E. Special Research Committee on Fluid Meters, "Fluid Meters - their theory and application," Part I. 4th ed., 1937.
2. A.S.M.E. Power Test Codes, Supplement on Instruments and Apparatus, Part 5: Measurement of quantity of materials, 1949.
3. Baker, H. Dean, Ryder, E. A. and Baker, N. H. Temperature measurement in engineering. New York: Wiley, 1953.
4. Bendersky, David. "A Special Thermocouple for Measuring Transient Temperatures," Mechanical Engineering, 75, 1953, 117.
5. Birrmann, R. "A Look at Turbocharging," Diesel Power, Vol. 32, No. 1, 1954, p. 80-87.
6. Birrmann, R. "New Developments in Turbocharging," S.A.E. Reprint No. 250, 1954.
7. Birrmann, R. "Aerothermodynamic Considerations Involved in Turbocharging Four-And Two-Cycle Diesel Engines," A.S.M.E., 78, 1956, 171.
8. Dicksee, C. B. "Supercharging the Compression-Ignition Engine," Proc. Institute of Automobile Engineers, 36, (1941-42), 1-27.
9. Eichelberg, G. "Some New Investigations on Old Combustion-Engine Problems," Engineering, 148 (July-December, 1939), 463-466, 547-550, 603-606, 683-686; 149, 296-299.
10. Giedt, W. H. "The Determination of Transient Temperatures and Heat Transfer at a Gas-Metal interface Applied to a 40-mm. Gun Barrel" Jet Propulsion, April, 1955.
11. Goldberg, A. and Goldstein, S. B. "An Analysis of Direct Heat Losses in an Internal Combustion Engine," Thesis, M.I.T. Library, 1933.
12. Heldt, P. M. High-Speed Combustion Engines. Philadelphia, Chilton Co. 1956.
13. Høegh, Carl, The Cylinder Wear in Diesel Engines with a Special View to Large Marine Units, 1st American ed., Brooklyn, Chemical Pub. Co., 1949.
14. Ibrahim Abdelfattah, A. I. "Piston Temperatures," Automobile Engineer, 44, 1954, 335-339.

15. Janeway, R. N. "Quantitative Analysis of Heat Transfer in Engines," S.A.E. Trans. 33, 1938, 371.
16. Johnson, L. "Supercharged Diesel Performance versus Intake and Exhaust Conditions," S.A.E. Trans., 61, 1953, 34-43.
17. Judge, A.W. Automobile and Aircraft Engines. 4th ed., New York, Pitman, 1947.
18. Judge, A.W. Aircraft Engines. 2nd ed., London, Chapman & Hall Ltd., 1947.
19. Judge, A.W. The Testing of High Speed Internal Combustion Engines. 4th ed., London, Chapman & Hall, 1955.
20. Keenan, J. H. and Kaye J. Gas Tables. New York: John Wiley & Sons, Inc. 1950.
21. Ku, P. M. "Factors Affecting Heat Transfer in the Internal-Combustion Engine," N.A.C.A., T.N. No. 737, 1940.
22. Lichty, L. C. Internal Combustion Engines. 6th ed., New York: McGraw-Hill Book Co. Inc. 1951.
23. Maleev, V. L. Diesel Engine Operation and Maintenance. New York, McGraw-Hill, 1954.
24. McAdams, W. H. Heat Transmission, 3rd ed. New York: McGraw-Hill Book Co., 1954.
25. Miller, R. "Rating Supercharged Engines on the Basis of the Mean Temperature of the Cycle," A.S.M.E., 65, 1943, 685.
26. Morgan, W. "Note on the Estimation of Suction and Compression Temperatures in Internal Combustion Engines," Proc. Inst. of Automobile Engineers, April 1923, 314-336.
27. Moore, C. S. and Foster, H. H. "Boosted Performance of a Compression-Ignition Engine with a Displacer Piston," N.A.C.A., T.N. 569, 1936.
28. Moore, C. S. and Collins, J. H. Jr. "Compression Ignition Engine Performance at Altitudes and at Various Air Pressures and Temperatures," N.A.C.A., T.N. 619.

29. Nutt, H. V., Landen, E. W. and Edgar, J. A. "Effect of Surface Temperature on Wear of Diesel-Engine Cylinders and Piston Rings," S.A.E. Trans., 63, 1955, 694-703.
30. Obert, E. F. Internal Combustion Engines. 2nd ed., Scranton, Penn.: International Testbook Co., 1953.
31. Pinkel, B., Manganiello, E. J. and Bernardo, E. "Heat-Transfer Processes in Liquid-Cooled Engine Cylinders," N.A.C.A. (E-131), ARR No. E5J31, 1945.
32. Pounder, C. C. Diesel Engine Principles and Practice. New York: Philosophical Library, 1955.
33. Purday, H. F. P. Diesel Engine Design. 5th ed. London: Constable & Co., 1948.
34. Pye, D. R. The Internal Combustion Engine, vol. II. London: Oxford University Press, 1934.
35. Pyles, Russell "Diesel Supercharging - Its Effect on Design and Performance," S.A.E. Transactions, 1938, 215-224.
36. Ricardo, Sir Harry Ralph. The High-Speed Internal-Combustion Engine, 4th ed., London: Blackie, 1953.
37. Schneider, H. "Heat Problem Seen as Block to Power Increase in Diesels," Diesel Progress, December 1955.
38. Taylor, C. F. "Effect of Engine Exhaust Pressure on Performance of Compressor - Engine - Turbine Units," S.A.E. Transactions, Vol. 54, No. 2. February 1946.
39. Taylor, C. F. "Heat Transmission in Internal-Combustion Engines," Proceedings of the general discussion on heat transfer, September 1951, arranged by I.M.E. and A.S.M.E. London: 1951.
40. Tryhorn, D. W. "An Approach to the Problem of Pressure Charging the Compression-Ignition Engine," The Chartered Mechanical Engineer, Vol. 4, No. 3, I.M.E., London, 1957.
41. Vincent, E. T. Supercharging the Internal Combustion Engine 1st ed. New York, McGraw-Hill Company, 1948.
42. Whitney, E. G. and Foster, H. H. "The Diesel as a High-Output Engine for Aircraft," S.A.E. Transactions, Vol. 33, 1933, 161-169.

UNIVERSITY OF MICHIGAN



3 9015 03026 6384